DEVELOPMENT AND CHARACTERIZATION OF AN IRIDIUM-MODIFIED ELECTROCHEMICAL BIOSENSOR FOR POTENTIAL DIABETIC PATIENT MANAGEMENT

by

LEI FANG

Submitted in partial fulfillment of the requirements

For the degree of Doctor of Philosophy

Dissertation Advisor: Dr. Chung-Chiun Liu

Department of Chemical Engineering

CASE WESTERN RESERVE UNIVERSITY

January, 2009

Print out two copies of this form, as it will accompany your thesis or dissertation. (This notice will not show up on printouts).

CASE WESTERN RESERVE UNIVERSITY

SCHOOL OF GRADUATE STUDIES

We hereby approve the thesis/dissertation of

Lei Fang

candidate for the Ph.D degree *.

(signed) Dr. Chung-Chiun Liu
(chair of the committee)

Dr. Vernon Anderson

Dr. Heidi B. Martin

Dr. Harihara Baskaran

(date) 07/03/2008

*We also certify that written approval has been obtained for any proprietary material contained therein.

Table of Contents

List of Tables

List of Figures

Acknowledgements

The completion of this dissertation would not be possible without supervision, guidance, assistance, support, and encouragement from the following people whom I wish I could say thank you enough for what they have given me.

Dr. Chung-Chiun Liu for always being supportive throughout my Ph.D research. His wisdom and experience enlightened my study and research, and greatly facilitated the completion of my doctoral research.

Dr. Heidi Martin and Dr. Vernon Anderson for serving as my committee members. Dr. Harihara Baskaran for providing bovine serum samples and using the equipment for the spectrophotometric studies undertaken during my experiment, him giving me useful suggestions for the simulation of the reaction kinetics, and serving as my committee member.

Dr. Aaron Jennings from the Civil Engineering Department for providing the needed laboratory space for my experiment.

Dr. Shih-Han Wang from Taiwan for her helpful advice and discussion.

The staff of the Electronics Design Center, especially Laurie Dudik for the fabrication of the sensor prototypes as well as for providing technical information, and Meijun Shao for helpful discussion.

Friends and family in the P.R.China and the US for their encouragement and support.

Special thanks to my wife Yan and my son Allan, my mother Yansu and my sister Kun, for the joys, love and support from them, in this seemingly long period of time to complete my doctoral study.

Development and Characterization of an Iridium-Modified Electrochemical Biosensor for Potential Diabetic Patient Management

Abstract

by

LEI FANG

The goal of this research was to apply thick-film screen printing technology to produce a single-use, disposable, cost-effective electrochemical biosensor prototype in large scale. Iridium nanoparticles supported by carbon were selected to modify the electrode of the biosensor for its excellent catalytic effect towards the commonly detected electrochemical active species, *i.e.*, hydrogen peroxide, nicotinamide adenine dinucleotide (reduced form, NADH), and nicotinamide adenine dinucleotide (oxidized form, NAD^+).

The development of this electrochemical biosensor prototype can establish a platform technology for various analytes of clinical importance. This study focused on the biosensing of the following analytes related to diabetes, *i.e.*, 3-hydroxybutyrate (3HB), fructosyl valine, and the HbA_{1c}, providing an analytical tool for diabetic patient management.

The first part of this study discusses the importance of developing a point-of-care amperometric biosensor to detect 3-hydroxybutyrate (3HB) for diabetic patient management. Current electrochemical detection methods for 3HB require at least two stepwise reactions or a mediator. The detection method in this study only requires a

single reaction step without any mediator, which can potentially also be more accurate, sensitive, cost-effective and stable over the long term. In this detection method, the enzyme D-3-hydroxybutyrate dehydrogenase (3HBDH, EC 1.1.1.30) was immobilized on the iridium–modified sensor prototypes which detect the NADH produced by the reaction of 3HB with NAD^+ in the presence of 3HBDH. This microelectrode quantified the NADH electrochemically, which produced an electrical current that would then be used to quantify the concentration of 3HB. The interferences from uric acid, NAD^+, and serum were measured. It was concluded that the level of 3HB could still be quantified well in the presence of these interfering species. Spectrometric measurements of NADH and 3HB were performed in both PBS and bovine serum and correlated very well with the electrochemical measurements of 3HB, using our biosensor prototype.

The relationship between the sensing performance of this 3HB biosensor and the element properties in fabrication and the characterization parameters were assessed. As a result, the value for the element properties in fabrication and the parameters in the characterization were determined based on the experimental results together with the requirements for practical applications. Finally, inkjet printing technology was applied for the enzyme ink deposition for the mass-production of this biosensor. The biosensors from inkjet printing were characterized in both PBS and bovine serum.

In the next part of this study, this biosensor prototype was used for the detection of NAD^+, in order to quantify the interference from AcAc on the 3HB detection, and to quantify numerous biomarkers related to NAD^+. This biosensor operated in the

reduction mode at a relatively low electrochemical potential (-0.4V vs Ag/AgCl reference electrode) in both buffer solution and bovine serum. The biosensor outputs showed high sensitivity, high linearity, and high reproducibility. The temperature effect and the interference from NADH were also assessed.

As a separate study, the measurement of glycosylated hemoglobin (HbA_{1c}) was considered to be most important for the long-term management of diabetic patients. Electrochemical detection of HbA_{1c} was proposed involving multi-step decomposition of HbA_{1c} to small molecules proportional to the concentration of $HbA_{1c,}$ then detection of the produced molecules amperometricly. This biosensor prototype was used for the detection of both HbA_{1c}, and fructosyl valine (FV), one of the produced small molecules as a model compound for the HbA_{1c} detection.

Consequently, electrochemical biosensors for the detection of FV and HbA_{1c} were developed. Quantifications of FV and HbA_{1c} were carried out at a relatively low electrochemical potential (+0.25V vs Ag/AgCl) at an ambient temperature to detect the enzymatically produced H_2O_2. The enzymes, *e.g.*, fructosyl amine oxidase (E.C. 1.5.3.x, FAO) and the lysis buffer were then co-immobilized onto the iridium-modified disposable sensor for HbA_{1c} detection in whole human blood. This reagent-free electrochemical biosensor detected HbA_{1c} in the physiological range with practical sensitivity and good linearity.

Finally, a diffusion-reaction model was developed for the electrochemical detection of 3HB in solution which achieved reasonable agreement with the experimental results.

Chapter 1 Introduction

The aim of this research is to develop a single use, disposable, cost-effective, thick-film printed electrochemical biosensor as a platform technology, and to demonstrate the application of this platform technology in several important biosensors for diabetic patient management. Specifically, this biosensor platform technology can be applied for the detection and quantification of ketone body 3-hydroxybutyrate (3HB), nicotinamide adenine dinucleotide (oxidized form, NAD^+), fructosyl valine (FV) and glycosylated hemoglobin (HbA_{1c}). In this chapter, the general knowledge of biosensors, the applications of biosensors in health care, electrochemical based biosensors, microfabrication technologies to produce the biosensors, the importance of a 3HB biosensor, the importance of a NAD^+ biosensor, the importance of a FV biosensor and a HbA_{1c} biosensor, as well as the motivation and significance of this research will be discussed.

1.1 Biosensors

Biosensors are analytical devices composed of a recognition element of biological origin and a physico-chemical transducer [1]. The first biosensor was invented by Professor L.Clark of the Children's Hospital in Cincinnati, Ohio in 1962 based on the famous "Clark-type electrode" [2]. This biosensor had enzyme immobilized onto the working electrode and was often referred to as the "enzyme electrode". Since then, the designs and applications of biosensors in analytical chemistry have developed rapidly for the last thirty years. The operational principle of a biosensor is that the

biological element interacts with the analyte and produces a physical or chemical change, which can then be sensed by the transducer or the detector, producing a signal proportional to the concentration of this analyte as shown in **Figure 1. 1**.

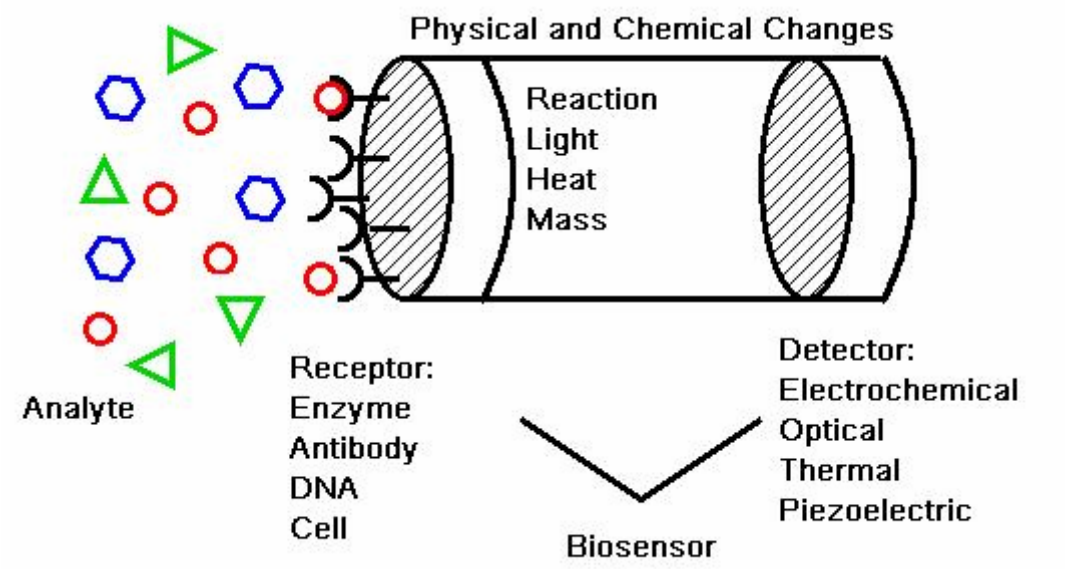

Figure 1. 1 Principles of a biosensor

1.2 Applications of biosensors

Biosensors have important applications in various fields: medical applications, defense applications, food safety, environmental monitoring and pharmaceutical research [3]. Compared with the traditional laboratory-based clinical chemistry methods, medical biosensors can be more cost-effective, faster, more portable, smaller, more user-friendly, selective and sensitive by nature. Therefore, the use of medical biosensors in clinical chemistry has grown fast and become the most important application among these fields [4].

The most successful example of medical biosensors was the one developed for diabetic patient management, *i.e.*, the personal glucose meter [5]. Biosensors for other analytes of clinical importance have also been developed, *e.g.,* cholesterol, urea, ascorbic acid, uric acid, and creatinine [6]. Other important and emerging biosensors are DNA biosensors [7-9] for genetic disease detection, immunosensors as an alternative for immunoassays [10, 11], and living-cell based biosensors [12-14]. These examples demonstrate the potential scientific, clinical and commercial significance of biosensor technology.

1.3 Electrochemical based biosensors

Biosensors can be divided into several subcategories based on the sensing mechanism, *e.g.*, electrochemical, optical, piezoelectric, and others. Electrochemical biosensors are cost-effective, suitable for turbid testing media, have fast response times and can be manufactured in large scale [15].

Amperometric biosensors [16] are one type of electrochemical biosensor. Amperometric biosensors require relatively simple electrochemical sensing platform which is ideal for the point-of-care applications. Amperometric biosensors are also compatible with existing blood gas sensors [17, 18]. Therefore, amperometric biosensors are the most important and promising sensor type for medical biosensors. The amperomtric sensing mode also provides the possibility of simultaneous detecting multiple analytes from a physiological sample [19, 20]. It is based on these assessments that electrochemical based biosensors, particularly amperometric based biosensors will be the focus of this study.

1.4 Microfabrication technologies for the biosensors

Biosensors can be made manually in a laboratory scale in limited quantity and quality. The growing market for electrochemical biosensor, especially the large number of diabetic patients worldwide, requires that biosensors be manufactured in large quantity at a relatively low cost and with good quality control. Microfabrication technologies, including thick film screen printing and ink-jet printing, are ideal for the mass-production of single use, disposable biosensors. A main advantage of the microfabrication technologies is small sensor size, therefore enabling use of small sample volume, high reproducibility, easy integration between different sensors, low cost and a large number produced at per batch [21].

1.4.1 Thick film screen printing

Thick film screen printing is one the most widely applied mircofabrication technologies for mass production of commercial biosensors [22]. The use of thick film technology in biosensor production has provided the possibility of producing cost-effective biosensors. This thick film screen printing technology has been previously developed for the electronic industries to produce miniature and robust electronics circuits in a cost-effective manner, as this technology is massive and automated. This technology can produce well-defined, highly reproducible structures, and these characteristics are very desirable for biosensor applications as shown in **Figure 1. 2**.

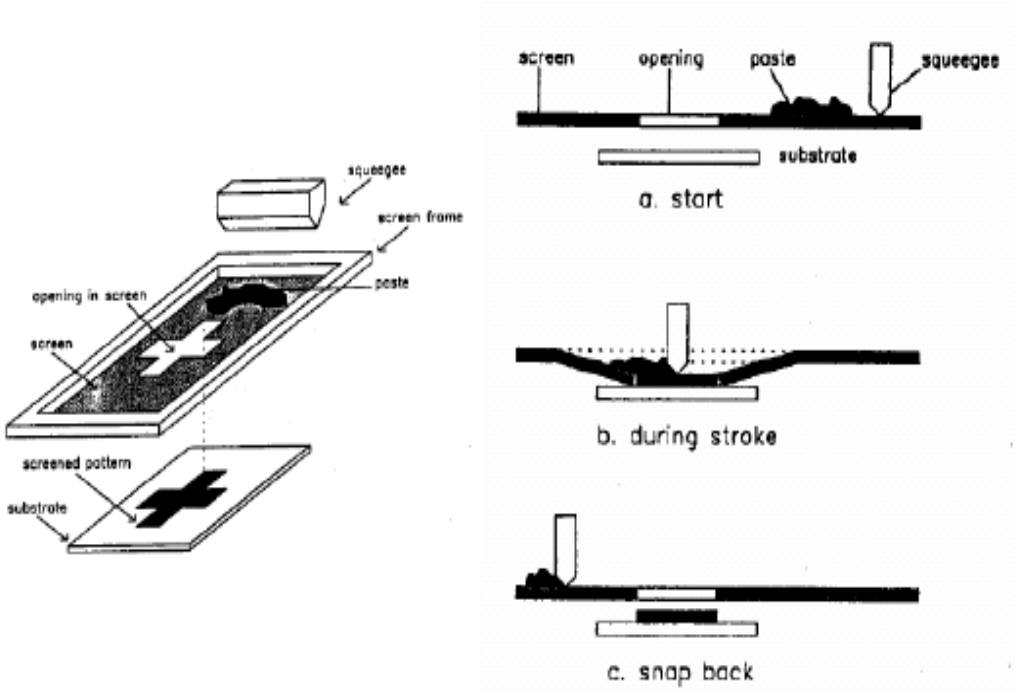

Figure 1. 2 Thick film screen printing component and process [22]

The working principle of thick film screen printing can be described as follows [22]. An ink is firstly pressed onto the substrate by a mechanical squeegee through the openings of a screen. The pattern from the screen is then transferred onto the substrate.

The thick film screen printing ink is a paste-like material normally composed of a solvent, a binder and the material of interest. The binder can be an organic or inorganic salt, which binds the material of interest, *e.g.*, the metallic particles, onto the substrate after the firing process. The solvent serves as a vehicle to provide a homogeneous mixture of the ink for the printing.

The screen consists of a finely woven mesh of stainless steel, nylon or polyester, mounted under tension on a metal frame. During printing, the substrate is held at a distance from one side of the screen, while the ink is placed on the opposite side of the screen and a

squeegee traverses the screen under pressure. The screen is thereby brought into contact with the substrate and also the ink is forced through the open area of the mesh. The required device pattern from the screen is thus left on the substrate.

The next step is to dry the substrate removing the solvent, most likely an organic component but possibly water from the paste. After drying, the film is relatively mechanically stable and the substrates can be handled. In order to remove the nonvolatile portion of the solvent, firing under high temperature is required. Further screen printing layers may be added after firing if necessary.

1.4.2 Ink jet printing

Ink jet printing provides another choice to pattern ink solution on a substrate by a drop delivery system [22]. It is mainly developed for BioMEMS applications to provide fast and cost-effective delivery, as this technology is large-scale and automated. This technology can deliver ink with well-defined volume and shape in a reproducible manner, highly desirable for biosensor applications.

In the ink jet printing technology, an ink-jet nozzle is concerted to a container filled with ink to be delivered with a computer-controlled x-y stage. The two common ink jet mechanisms are thermal and piezoelectric.

In the thermal mechanism, a bubble is formed by superheated ink which collapses and drops onto the substrate. This process is then repeated in a very fast and reproducible manner on different positions over the substrate controlled by the computer in the x-y dimensions. In the piezoelectric mechanism, the ink jet head consists of a reservoir of ink and a nozzle [22]. A thin diaphragm with an attached piezoelectric crystal is the

reservoir wall. This diaphragm is in contact with a voltage applied to the crystal, and ejects a small drop of ink from the nozzle. In this piezoelectric mechanism, enzyme ink can be delivered without losing enzymatic activity. With more than one nozzle, inks containing different reagents can be delivered, forming biosensors arrays. The flexibility of this approach is the main advantage of ink jet printing compared with thick film screen printing.

In summary, electrochemical biosensors, specifically amperometric biosensors, address important issues in the medical field. In other words, the application of amperometric biosensors to detect analytes of clinical importance can provide a faster, more portable, accurate and cost-effective assay when compared to traditional clinical analytical methods. Biosensors can be manufactured in large scale at relatively low cost with the microfabrication methods described previously in a reproducible and flexible manner. These advantages provide the rationale for employing thick film screen and ink jet printing technologies in the fabrication of the biosensor prototypes in this study.

1.5 Status of diabetes, the importance of ketone, nicotinamide adenine dinucleotide, FV and HbA_{1c} biosensors

Diabetes remains a serious challenge after decades of research and study. Currently, the most effective method for diabetic patient management is glycemic control by self monitoring of analytes of importance. Other than glucose, the related analytes are ketone, HbA_{1c} (glycosylated hemoglobin) and NAD^+. Therefore, biosensors for the

relevant analytes are important and meaningful for the point-of-care application in diabetic patient management.

1.5.1 Status of diabetes

An important application of electrochemical biosensors in the medical field is diabetic patient management. Approximately 171 million people world wide (2000) suffer from diabetes, and this number is expected to double in 30 years [23]. Therefore, diabetes is a very critical public health concern.

Diabetes occurs when the human body becomes unable to use glucose effectively. Glucose is the main fuel source for the human body and insulin is the hormone that assists the glucose to leave the blood and enter the body cells where it provides energy for the body. The normal blood glucose concentration of an individual is less than 6.11mM (110 mg/dL) [24]. Diabetes happens when the pancreas (the organ responsible for producing insulin) is either unable to produce sufficient insulin or the insulin produced is not able to transfer glucose into the body cells effectively. Therefore, in the blood of a diabetic patient, the glucose concentration is higher than normal [25-27]. The relevant blood glucose concentration range for *in vitro* diagnosis is 3-12 mM (54-216 mg/dL) [24].

1.5.2 The importance of a ketone 3-hydroxybutyrate biosensor

When glucose cannot provide the energy for the body cells, fat as the alternative energy source is oxidized directly, which produces ketone bodies [28, 29]. Therefore, in the blood of a diabetic patient, the concentrations of ketone bodies are also higher than normal [30]. Ketone bodies refer to 3-hydroxybutyrate (3HB), acetoacetate

(AcAc) and acetone, of which 3HB represents approximately 90% of the ketone bodies in diabetic patients [28-30]. As a result, the measurement of 3HB is important and representative for diabetic patient management application.

The commonly involved reaction of 3HB and NAD^+ (Nicotinamide adenine dinucleotide, oxidized form) is catalyzed by enzyme 3-hydroxybutyrate dehydrogenase (3HBDH, EC 1.1.1.30), producing AcAc and NADH as shown in reaction (1.1) [31]. Consequently, the detection of NADH produced can then be used to quantify the present 3HB.

$$\text{3-hydroxybutyrate} + NAD^+ \xrightleftharpoons{\text{3HBDH}} \text{AcAc} + \text{NADH} + H^+ \qquad (1.1)$$

1.5.3 The importance of a NAD^+ biosensor

NAD^+ is an important co-factor which is involved in several hundred enzymatic reactions, especially in the catabolic reactions [32-42]. These reactions are important in drug development, molecular diagnostics, assay development and bioreactors. Therefore, the measurement of NAD^+ is meaningful in the quantification of numerous important biomarkers involved in the above applications, for example, the pyruvate fermentation to lactate as shown in reaction (1.2) [33, 34]. The level of pyruvate is of clinical importance, which can be quantified through the detection of NAD^+.

$$\text{pyruvate} + \text{NADH} + H^+ \xrightarrow[\text{EC 1.1.1.28}]{\text{lactate dehydrogenase}} \text{lactate} + NAD^+ \qquad (1.2)$$

Due to the significant number of enzymatic reactions [32-42] involved with NAD^+, the detection of NAD^+ provides a platform technology for the quantification of the biomarkers shown in these enzymatic reactions.

Furthermore, interference from AcAc exists for the ketone body 3HB quantification based on NADH detection. The presence of AcAc suppresses the production of NADH in the reversible reaction (1.1). As a result, the successful detection of NAD^+ can be applied to quantify this interference.

Briefly stated, the electrochemical detection of NAD^+ forms the basis for the development of various biosensors involving reactions of NAD^+; the electrochemical detection of NAD^+ can also be used to quantify the interference from AcAc in 3HB detection for diabetic patient management, which is directly related to the main purpose of this study.

1.5.4 The importance of a HbA_{1c} biosensor

Glucose reacts with the N-terminal group of the β-chain of HbA_0 in blood forming the glycosylated hemoglobin (HbA_{1c}) [43-45]. High levels of glucose in diabetic patients will result in high levels of HbA_{1c}. Therefore, the HbA_{1c} level is considered to be a useful diagnostic marker for diabetic patients in addition to the measurement of glucose level. Since the life time of hemoglobin in blood is about 2-3 months, the HbA_{1c} level indicates the glucose level over the time period of the past 2-3 months. Consequently, the measurement of HbA_{1c} is very important for the long-term control of the glycemic state in diabetic patients [46].

An enzymatic assay of HbA_{1c} consists of the following steps as shown in reaction (1.3): firstly HbA_{1c} proteolysis produces glycated hexapeptides; secondly, glycated hexapeptides is further decomposed to fructosyl amine such as fructosyl valine **(**FV); finally, FV oxidation is catalyzed by the enzyme FAO to produce hydrogen peroxide

[47]. Consequently, the electrochemical detection of hydrogen peroxide can then be used to quantify the present HbA_{1c}. This provides an excellent indication of the level of HbA_{1c} as described above.

$$HbA_{1c} \xrightarrow{\text{endoproteinase Glu-C}} \underset{\text{Fru-Val-His-Leu-Thr-Pro-Glu}}{\text{glycated hexapeptides}} \xrightarrow{\text{proteinase}} FV \xrightarrow{FAO} H_2O_2 \qquad (1.3)$$

1.5.5 The importance of FV biosensor

Fructosyl valine (FV) is an intermediate in the enzymatic assay for HbA_{1c} [47] as shown in reaction (1.3). Since the FV detection does not involve the first two steps in reaction (1.3), the development of a FV biosensor is less challenging than the development of an HbA_{1c} biosensor. The development of a FV biosensor will demonstrate the feasibility of the HbA_{1c} biosensor development. Therefore, the measurement of FV is meaningful and serves as a pilot study for a HbA_{1c} biosensor. Enzymatic assay of FV consists of the following step as shown in reaction (1.4):

$$\text{Fructosyl Valine(FV)} \xrightarrow{FAO} H_2O_2 \qquad (1.4)$$

The electrochemical detection of hydrogen peroxide can then be used to quantify the present FV.

In summary, diabetic patient management is a very important application of electrochemical biosensors. The relevant biomarkers for diabetes are ketone bodies 3HB, NAD^+, FV and HbA_{1c}, other than thoroughly studied glucose.

1.6 Motivation and scope of this study

Biosensors technology is important for medical applications because of its numerous advantages over traditional analytical methods. Among medical applications of biosensors, diabetic patient management is one of the most important applications. Glucose biosensors have been thoroughly studied and are available commercially for diabetic patient management. However, other important biomarkers for diabetes exist and remain to be studied and developed for the benefit of diabetic patients. Therefore, the aims of this study are to develop biosensor prototypes for self-testing of other essential diabetes biomarkers, *e.g.*, 3HB, NAD^+, FV and HbA_{1c}. These biosensors can be produced with cost-effective microfabrication technologies, namely thick film screen printing and ink jet printing. The methods to produce the biosensor substrate and to dissipate the enzymatic ink must be fully automated and reproducible in order to be manufactured on an industrial scale. Ideally, the methods developed for the substrate fabrication and enzyme ink dissipation should be suitable for other analytes of importance, generating a platform technology which has broader application for biosensors.

In order to demonstrate the flexibility of this platform technology for different types of analytes, the same biosensor substrate and the same base ink formula are used for detection of different analytes throughout this study. The enzyme ink has different active ingredients based on the analytes of interest. Experiments are carried out initially in buffer solution and finally in a physiological fluid, *i.e.*, bovine serum and whole blood samples from patients, for potential practical application. The biosensors

are optimized in terms of both fabrication conditions and characterization conditions. Potential interferences are also assessed to investigate if other electrochemically active species interfere with analyte detection.

1.7 Significance of this study

This study will contribute to the development of electrochemical biosensors, especially for diabetic patient management. Specifically, ketone body 3-hydroxybutyrate (3HB) biosensor, NAD^+ biosensor, FV biosensor and HbA_{1c} biosensor will be developed.

The electrochemical detection of 3HB is based on the detection of NADH. On the other hand, the electrochemical detection of FV and HbA_{1c} is based on the detection hydrogen peroxide (H_2O_2). NADH, NAD^+ and H_2O_2 are common products and reactants in a significant number of enzymatic reactions [32-42]. Therefore, this biosensor substrate will serve as the platform technology for various enzymatic reactions that involve NADH, NAD^+ and H_2O_2. The ink for the biosensor and the method to dissipate the ink onto the biosensor substrate will also serve as the platform technology for different analytes of interest.

This platform technology will also greatly facilitate the development of sensor arrays for multiple analytes. The substrate, the ink dissipation method and the electrochemical sensing methods are easily integrated for sensor array application. The sensor array will enable accurate diagnosis and monitoring of a specific disease by assessing multiple analytes of significance.

Reference List

1. Thevenot DR, Toth K, Durst RA, Wilson GS. Electrochemical biosensors: recommended definitions and classification. Biosensors & Bioelectronics 2001; 16 (1-2):121-131

2. Clark LC, Lyons C. Electrode systems for continuous monitoring in cardiovascular surgery. Annals of the New York Academy of Sciences 1962; 102 (1):29-45

3. Mehrvar M, Abdi M. Recent developments, characteristics, and potential applications of electrochemical biosensors. Analytical Sciences 2004; 20 (8):1113-1126

4. D'Orazio P. Biosensors in clinical chemistry. Clinica Chimica Acta 2003; 334 (1-2):41-69

5. Wang J. Glucose biosensors: 40 years of advances and challenges. Electroanalysis 2001; 13 (12):983-988

6. Malhotra BD, Chaubey A. Biosensors for clinical diagnostics industry. Sensors and Actuators B-Chemical 2003; 91 (1-3):117-127

7. Odenthal KJ, Gooding JJ. An introduction to electrochemical DNA biosensors. Analyst 2007; 132 (7):603-610

8. He PA, Xu Y, Fang YZ. A review: Electrochemical DNA biosensors for sequence recognition. Analytical Letters 2005; 38 (15):2597-2623

9. Rivas GA, Pedano ML, Ferreyra NF. Electrochemical biosensors for sequence-specific DNA detection. Analytical Letters 2005; 38 (15):2653-2703

10. Wang K, Jiang DC, Liu BH, Zhang S, Lu TP, Kong JL. Label-free immunosensors-principles and applications. Chinese Journal of Analytical Chemistry 2005; 33 (3):411-416

11. Lin JH, Ju HX. Electrochemical and chemiluminescent immunosensors for tumor markers. Biosensors & Bioelectronics 2005; 20 (8):1461-1470

12. Lim DV, Simpson JM, Kearns EA, Kramer MF. Current and developing technologies for monitoring agents of bioterrorism and biowarfare. Clinical Microbiology Reviews 2005; 18 (4):583

13. Wang P, Xu GX, Qin LF, Xu Y, Li Y, Li R. Cell-based biosensors and its application in biomedicine. Sensors and Actuators B-Chemical 2005; 108 (1-2):576-584

14. Wolf B, Kraus M, Brischwein M, Ehret R, Baumann W, Lehmann M. Biofunctional hybrid structures - cell-silicon hybrids for applications in biomedicine and bioinformatics. Bioelectrochemistry and Bioenergetics 1998; 46 (2):215-225

15. Shah J, Wilkins E. Electrochemical biosensors for detection of biological warfare agents. Electroanalysis 2003; 15 (3):157-167

16. Murphy L. Biosensors and bioelectrochemistry. Current Opinion in Chemical Biology 2006; 10 (2):177-184

17. Li CM, Dong H, Cao XD, Luong JHT, Zhang XJ. Implantable electrochemical sensors for biomedical and clinical applications: Progress, problems, and future possibilities. Current Medicinal Chemistry 2007; 14 (8):937-951

18. Hahn CEW. Electrochemical analysis of clinical blood-gases, gases and vapours. Analyst 1998; 123 (6):57R-86R

19. Plegge V, Slama M, Suselbeck B, Wienke D, Spener F, Knoll M, Zaborosch C. Analysis of ternary mixtures with a single dynamic microbial sensor and chemometrics using a nonlinear multivariate calibration. Analytical Chemistry 2000; 72 (13):2937-2942

20. Diamond D. Progress in Sensor Array Research. Electroanalysis 1993; 5 (9-10):795-802

21. Suzuki H. Advances in the microfabrication of electrochemical sensors and systems. Electroanalysis 2000; 12 (9):703-715

22. Marc J.Madou. Fundamentals of Microfabrication: The Science of Miniaturization, 2002

23. Wild S, Roglic G, Green A, Sicree R, King H. Global prevalence of diabetes - Estimates for the year 2000 and projections for 2030. Diabetes Care 2004; 27 (5):1047-1053

24. Bais R. Clinical Chemistry: Principles, Procedures, Correlations, 5th ed. Michael L. Bishop, Edward P. Fody, and Larry Schoeff. Baltimore, MD: Lippincott Williams & Wilkins, 2005, 756 pp., $76.95, hardcover. ISBN 0-7817-4611-6. Clin Chem 2005; 51 (8):1567

25. Coursin DB, Connery LE, Ketzler JT. Perioperative diabetic and hyperglycemic management issues. Critical Care Medicine 2004; 32 (4):S116-S125

26. Koschinsky T, Heinemann L. Sensors for glucose monitoring: technical and clinical aspects. Diabetes-Metabolism Research and Reviews 2001; 17 (2):113-123

27. Macleod KM, Gold AE, Frier BM. Frequency, Severity and Symptomatology of Hypoglycemia - A Comparative Trial of Human and Porcine Insulins in Type-1 Diabetic-Patients. Diabetic Medicine 1995; 12 (2):134-141

28. Charfen MA, Fernandez-Frackelton M. Diabetic Ketoacidosis. Emergency Medicine Clinics of North America 2005; 23 (3):609-628

29. Umpierrez GE, Murphy MB, Kitabchi AE. Diabetic Ketoacidosis and Hyperglycemic Hyperosmolar Syndrome. Diabetes Spectr 2002; 15 (1):28-36

30. Laffel L. Ketone bodies: a review of physiology, pathophysiology and application of monitoring to diabetes. Diabetes/Metabolism Research and Reviews 1999; 15 (6):412-426

31. Williamson DH. Enzymic Determination of D(-)-Beta-Hydroxybutyric Acid and Acetoacetic Acid in Blood. Current Contents/Life Sciences 1983; (22):19

32. Scherf U, Sohling B, Gottschalk G, Linder D, Buckel W. Succinate-Ethanol Fermentation in Clostridium-Kluyveri - Purification and Characterization of 4-Hydroxybutyryl-CoA Dehydratase/Vinylacetyl -CoA Delta(3)-Delta(2)-Isomerase. Archives of Microbiology 1994; 161 (3):239-245

33. Zapatabacri AM, Burstein C. Enzyme electrode composed of the pyruvate oxidase from pediococcus species coupled to an oxygen-electrode for measurements of pyruvate in biological media. Biosensors 1987; 3 (4):227-237

34. Hetzel M, Brock M, Selmer T, Pierik AJ, Golding BT, Buckel W. Acryloyl-CoA reductase from Clostridium propionicumi - An enzyme complex of propionyl-CoA dehydrogenase and electron-transferring flavoprotein. European Journal of Biochemistry 2003; 270 (5):902-910

35. Filonov AE, Akhmetov LI, Puntus IF, Esikova TZ, Gafarov AB, Izmalkova TY, Sokolov SL, Kosheleva IA, Boronin AM. The construction and monitoring of genetically tagged, plasmid-containing, naphthalene-degrading strains in soil. Microbiology 2005; 74 (4):453-458

36. Connors MA, Barnsley EA. Naphthalene plasmids in Pseudomonads. Journal of Bacteriology 1982; 149 (3):1096-1101

37. Bartlett ATM, White PJ. Species of Bacillus That Make A Vegetative Peptidoglycan Containing Lysine Lack Diaminopimelate Epimerase But Have Diaminopimelate Dehydrogenase. Journal of General Microbiology 1985; 131 (SEP):2145-2152

38. Maaheimo H, Fiaux J, Cakar ZP, Bailey JE, Sauer U, Szyperski T. Central carbon metabolism of Saccharomyces cerevisiae explored by biosynthetic fractional C-13 labeling of common amino acids. European Journal of Biochemistry 2001; 268 (8):2464-2479

39. Avendano A, Deluna A, Olivera H, Valenzuela L, Gonzalez A. GDH3 encodes a glutamate dehydrogenase isozyme, a previously unrecognized route for glutamate biosynthesis in Saccharomyces cerevisiae. Journal of Bacteriology 1997; 179 (17):5594-5597

40. Culbertson CW, Zehnder AJB, Oremland RS. Anaerobic Oxidation of Acetylene by Estuarine Sediments and Enrichment Cultures. Applied and Environmental Microbiology 1981; 41 (2):396-403

41. Junior LR, Neto GD, Fernandes JR, Kubota LT. Determination of salicylate in blood serum using an amperometric biosensor based on salicylate hydroxylase immobilized in a polypyrrole-glutaraldehyde matrix. Talanta 2000; 51 (3):547-557

42. Rahni MAN, Guilbault GG, Deoliveira GN. Immobilized Enzyme Electrode for the Determination of Salicylate in Blood-Serum. Analytica Chimica Acta 1986; 181:219-225

43. Goldstein DE, Little RR, Lorenz RA, Malone JI, Nathan D, Peterson CM, Sacks DB. Tests of glycemia in diabetes. Diabetes Care 2004; 27 (7):1761-1773

44. John WG. Haemoglobin A1c reference method. Scandinavian Journal Of Clinical And Laboratory Investigation 2006; 66 (1):1-4

45. Kilpatrick ES. HbA1c measurement. J Clin Pathol 2004; 57 (4):344-345

46. Jeppsson. Approved IFCC Reference Method for the Measurement of HbA. Clinical Chemistry and Laboratory Medicine 2002; 40 (1):78

47. Nanjo Y, Hayashi R, Yao T. An enzymatic method for the rapid measurement of the hemoglobin A(1c) by a flow-injection system comprised of an electrochemical detector with a specific enzyme-reactor and a spectrophotometer. Analytica Chimica Acta 2007; 583 (1):45-54

Chapter 2 Study of a 3-hydroxybutyrate Biosensor for the Potential Management of Diabetic Patients

2.1 Introduction

The American Diabetes Association advises that blood ketone testing methods which quantify 3-hydroxybutyrate (3HB) will be desirable for the diagnosis and monitoring of ketoacidosis for the management of diabetic patients [1]. Blood ketone refers to 3-hydroxybutyrate (3HB), acetoacetate (AcAc) and acetone [2-4].These three ketone bodies are produced by the liver and used as an energy source when glucose can not sufficiently provide the energy for the body cells. 3HB and AcAc are the major ketone compounds in a human subject and acetone is in a relatively low concentration level in blood. For a normal individual, the ratio between 3HB and AcAc is approximately 1:1, whereas under DKA (diabetic ketoacidosis, a vital symptom associated with diabetes), this ratio could become as high as 10:1 [1, 2, 5].Therefore, the detection of 3HB is suggested for the management of DKA [1], reflecting the total ketone in a diabetic patient.

2.1.1 Current measurement technique

Various methods have been developed to detect the 3HB concentration in urine, serum and blood samples. The commonly involved reaction of 3HB and NAD^+ (Nicotinamide adenine dinucleotide, oxidized form) is catalyzed by the enzyme 3-hydroxybutyrate dehydrogenase (3HBDH, EC 1.1.1.30), producing AcAc (Acetone acetate) and NADH (Nicotinamide adenine dinucleotide, reduced form) as shown in

reaction (2.1). Consequently, NADH detection can then be used to quantify the presence of 3HB. This will provide an excellent indication of the level of ketones as described above.

$$\text{3-hydroxybutyrate} + NAD^+ \xrightarrow{\text{3HBDH}} \text{AcAc} + \text{NADH} + H^+ \qquad (2.1)$$

3HB has been detected using enzymatic reaction shown in equation (2.1), through NADH detection with a spectrophotometer [6].Based on the same principle, a flow injection system with immobilized enzymes on beads has been developed employing chemiluminescence detection [7].Furthermore, gas-chromatographic measurement has also been coupled with an enzymatic system in order to determine the 3HB concentrations [8]. However, these methods are either time-consuming or require expensive apparatus, *e.g*., gas-chromatography, and they will not be suitable for the point-of-care detection of 3HB.

Amperometric biosensors based on enzymatic reactions have raised increasing attention recently due to the high selectivity, sensitivity and convenience of these biosensors. These properties are desirable for a point-of-care device. However, only a limited number of biosensors for rapid 3HB detection have been reported [9-11].

In 2005, Forrow *et al.* reported a commercial amperometric biosensor for 3HB [9].This biosensor required two stepwise chemical reactions involving first reaction (2.1) which produced NADH, and a second reaction of the oxidation of NADH by a redox mediator (1, 10-phenanthroline quinine) as shown in reaction (2.2).

$$\text{1,10-phenanthroline quinine}_{(ox)} + \text{NADH} \longrightarrow \text{1,10-phenanthroline quinine}_{(red)} + NAD^+ \qquad (2.2)$$

This biosensor quantified the 3HB concentration through the oxidation current of the reduced form of the mediator (1,10-phenanthroline quinine) produced in reaction(2.2). Evaluations [12-14] of this biosensor showed that the interference from AcAc was possible. The biosensor constructed by Forrow [9] also lost its accuracy over time [9], which could be caused by the mediator (1, 10-phenanthroline quinine) decreasing the activity of the enzyme 3HBDH [11]. In 2005, Li *et al.* [10] developed an amperometric biosensor similar to the one constructed by Forrow [9], and the mediator employed in the second reaction was potassium ferricyanide as shown in reaction (2.3).

$$[Fe(CN)_6]^{3-} + NADH \longrightarrow [Fe(CN)_6]^{4-} + NAD^+ + H^+ \qquad (2.3)$$

In 2006, Kwan *et al.* [11] reported that an amperometric biosensor using a bienzyme system, which used reaction (2.1) and detected the NADH by reacting NADH with salicylate hydroxylase (SHL,E.C. 1.14.13.1) as shown in reaction (2.4).

$$\text{Salicylate} + NADH + O_2 \xrightarrow{SHL} \text{Catechol} + NAD^+ + CO_2 \qquad (2.4)$$

All of these amperometric biosensor technologies quantified the 3HB concentration by detecting NADH, the product of the enzymatic reaction (2.1). However, none of these approaches detected NADH directly, instead relying on a mediator reaction or through the product of another enzymatic reaction. Indirect detection of 3HB increased the complexity and cost of the sensing system, and it could introduce interference and may cause sensitivity loss over time. Therefore, there are considerable potential advantages if an amperometric biosensor could be developed to

quantify the 3HB concentration by a single direct detection of NADH as shown in reaction (2.1).

2.2 Experiment

The development of an amperometric biosensor involved the following steps. First, the sensor prototype would have to be fabricated. Second, electrochemical measurements, *e.g.*, amperometry, would be undertaken of the sensors in different testing media, including 3HB in buffer solution, and bovine serum. Potential interference by other species in the physiological sample would also be assessed.

2.2.1 Fabrication of the enzyme sensor

This sensor consisted of an Ir-Carbon modified working electrode with the immobilized enzyme 3HBDH, a Ag/AgCl reference electrode, and an Ir-Carbon modified counter electrode. The surface area of the working electrode was approximately 7.85 $*10^{-3}cm^2$. These electrodes were screen-printed on a polyester substrate as shown in **Figure 2. 1**. The detailed fabrication procedure of this three-electrode configuration enzyme sensor is described as follows:

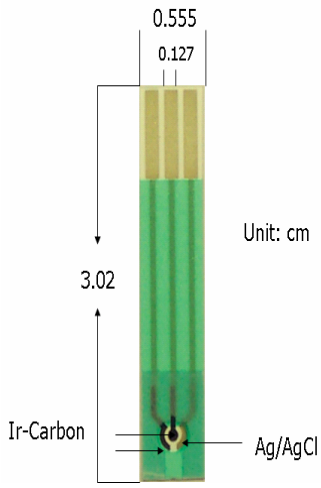

Figure 2. 1 The configuration of the thick-film sensor

a. Preparation of the ink based solution:

The ink based solution for the printing of the working and the counter electrodes was prepared by mixing the phosphate buffer, an enzyme immobilizing agent and a thickening polymer. Typically a 10 ml, pH 7.0 phosphate buffer (PBS, Fisher Chemicals, Cat. No. SB107-500) was mixed with the enzyme immobilizing agent, 1.36 mL polyethylenimine (Aldrich, Cat. No. 482595), and the thickening polymer, 0.34 g 2-hydroxyethyl cellulose (Aldrich, Cat. No. 30863-3). Mixing should be complete when a clear, homogeneous solution was obtained.

b. Preparation of the Ir-Carbon ink:

A quantity of 0.9 g Ir-Carbon (5% Ir, E-TEK^{SM}) was added to 5 mL of the ink based solution from step (a), and mixing and homogenization (for approximately 5 minutes) were carried out resulting in the Ir-Carbon ink for the printing of both working and counter electrodes.

c. Fabrication of the working electrode and the counter electrode for the sensor prototype:

This three-electrode configuration sensor was prepared by screen-printing on a polyester substrate. The electrical contacts of these three-electrodes were silver, and the three electrodes were first printed with the silver ink. Both the working and the counter electrodes of this three-electrode configuration sensor prototype were prepared by screen-printing the electrodes using the Ir-Carbon ink prepared from step (b) on the two silver based electrode contacts on the polyester substrate.

d. Preparation of the Ag/AgCl reference electrode:

For the reference electrode, a AgCl thick film ink was used and printed over the silver based electrode, serving as the Ag/AgCl reference electrode.

e. Preparation of the enzyme 3HBDH ink:

Enzyme 3HBDH ink was prepared in the following manner and applied to the sensor prototype. 1mL of the ink from step (b) was mixed with 125 units of enzyme 3HBDH (EC 1.1.1.30, Wako Chemicals USA, Cat. No. 086-05441), 150 mg NAD^+, and 5.0 mg bovine serum albumin. Mixing of these components was carried out until a clear solution was obtained.

f. Fabrication of the micro-biosensor prototype:

The enzyme ink from step (e) was then hand-dipped on the Ir-Carbon working electrode of a sensor prototype from step (c), forming the working electrode of this micro-biosensor prototype. This sensor prototype was stored at 4ºC prior to any electrochemical measurement.

2.2.2 Electrochemical measurements of the sensor

The performance of the fabricated sensor prototypes was evaluated using electrochemical measuring techniques. This included cyclic voltammetry and amperometry. The cyclic voltammetric and the amperometric experiments were conducted using a CH Instrument 660B electrochemical workstation (CH Instrument, Inc, Austin, TX, USA). These experiments were performed using a 4mL test medium, which was prepared by mixing PBS, supporting electrolyte 0.03mM potassium

chloride (KCl, Fisher, Cat. No. P217-500), and NADH (Sigma-Aldrich, Cat. No. N6785-10VL) or 3HB (Sigma-Aldrich, Cat. No.H6501-5G). This test medium was adjusted to pH 7.2 by adding potassium hydroxide (KOH, Fisher, Cat. No. P251-500). Uric acid (Sigma, Cat. No.U0881) and NAD^+ were added into the test medium to assess the possible interference on 3HB. Amperometric measurement was also performed in undiluted bovine serum (Invitrogen, Cat. No.16170-086). The solution temperature was well controlled during the measurement using a water bath (Fisher Scientific ISOTEMP 202). For the experiments without temperature control, the temperature was ambient temperature, which fluctuated between 22.0 ºC to 26.2 ºC. All potentials reported were referenced to the Ag/AgCl electrode. The working potential for all the amperometric experiments was fixed at +0.2 V versus the reference electrode, and the time of recording was 120s in order to reach a steady-state.

2.2.3 Spectrometric measurement

Spectrometric measurements of 3HB and NADH served as an independent gold standard quantification of these components and were carried out in order to further validate the electrochemical measurements by this biosensor. The spectrometric measurement was carried out in both PBS and undiluted bovine serum using a spectrophotometer (SpectraMaxM2, Molecular Devices) according to Sigma's Protocol.

2.3 Results and discussion

In this study, we investigated (1) the feasibility of direct measurement of NADH using this iridium-modified sensor prototype, (2) the feasibility of using the NADH measurement to quantify 3HB as shown in reaction (2.1). We also defined an optimal testing condition for this sensor prototype for 3HB detection and investigated any potential interference by other biological species. The sensor evaluation for the 3HB detection in serum was meaningful in the development of this biosensor prototype.

The following sections describe further the research undertaken in this study.

2.3.1 NADH detection

The feasibility of direct NADH measurement using the iridium modified sensor prototype was studied using cyclic voltammetry and amperometry [15].

2.3.1.1 Cyclic voltammograms

The reactions at the working electrode surface of this sensor prototype could be described in the following two steps: firstly reaction (2.1) was catalyzed by the enzyme 3HBDH producing NADH; then secondly the NADH was electrochemically oxidized to NAD^+ producing an oxidation current. Thus, the measurement of the NADH oxidation current in the second step could be used to quantify the 3HB present in the test medium. Therefore, it would be necessary and important to experimentally demonstrate a proof that NADH could be oxidized at a selected applied potential using the fabricated sensor prototype. **Figure 2. 2** compares the cyclic voltammograms obtained at ambient temperature (22.0 ^oC) in the presence and the absence of NADH. The test medium was a 4mL PBS solution with 0.03 M KCl,

adjusted to approximately pH 7.2 by KOH. In this cyclic voltammetric study, the applied potential range was -0.1 V to +0.6V vs Ag/AgCl and the linear potential scan rate was 2mV/second. For evaluation purpose, a solution of 0.4 mM NADH was used in this preliminary study along with the test medium without any NADH.

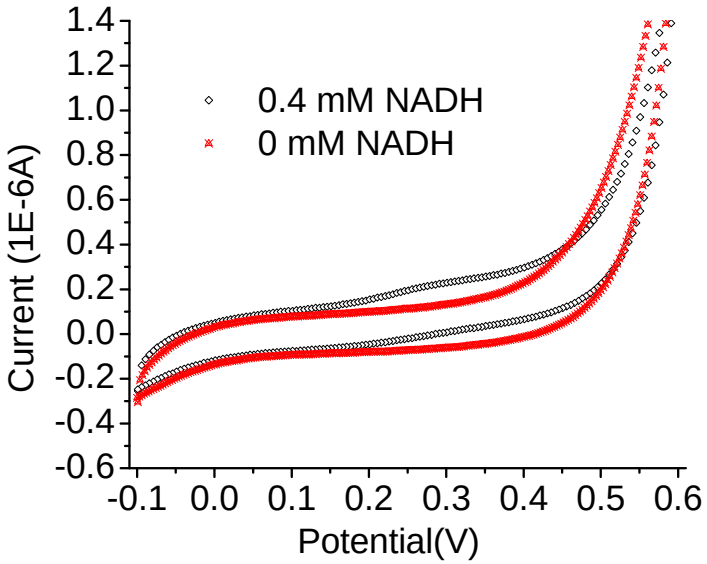

Figure 2. 2 Cyclic voltammograms of the sensor prototype in a 0.4mM NADH solution and a 0mM NADH solution.

Figure 2. 2 shows the voltammograms obtained in these test media. The NADH oxidation could be observed at a potential range from +0.18 to +0.44 V vs Ag/AgCl, as shown. Consequently, the selection of the applied potential to oxidize NADH in this sensor development could be made based on the results in **Figure 2. 2**. It should be recognized that at a higher oxidation potential, the possibility of oxidizing other electrochemically active species, such as ascorbic acid, would be possible. Thus, a relatively low applied potential of +0.2 V vs Ag/AgCl for NADH oxidation was

chosen in this study minimizing the potential interference from the potential oxidation of other species in the test medium.

2.3.1.2 Quantification of NADH by chrono-amperometry

Our research objective was to quantify the 3HB concentrations by measuring the NADH produced according to reaction (2.1). The measurements of the concentration of NADH could then be used to quantify the 3HB in the test medium. Amperometric study of NADH in the phosphate buffer solution (PBS) was then carried out. **Figure 2. 3** shows the amperometry for NADH from 0 mM to 0.4 mM in the test medium which contained the PBS and 0.03 M KCl supporting electrolyte. The concentration range studied was determined by the normal physiological 3HB concentration, 0 to 10mM, and the equilibrium constant [16] of reaction (2.1), 1.42 nM. An applied potential of +0.2 V vs Ag/AgCl was chosen, as suggested by the cyclic voltammograms in **Figure 2. 2**. Our experimental results showed that this sensor system reached steady-state at 120 seconds, and this incubation time was then chosen for our study. The experimental temperature for the test medium could affect the current of the amperometry, thus, two different temperatures, ambient temperature (26.2 ºC) and 37.5 ºC, the normal temperature of a human, were selected to demonstrate the possible temperature effect on detecting NADH.

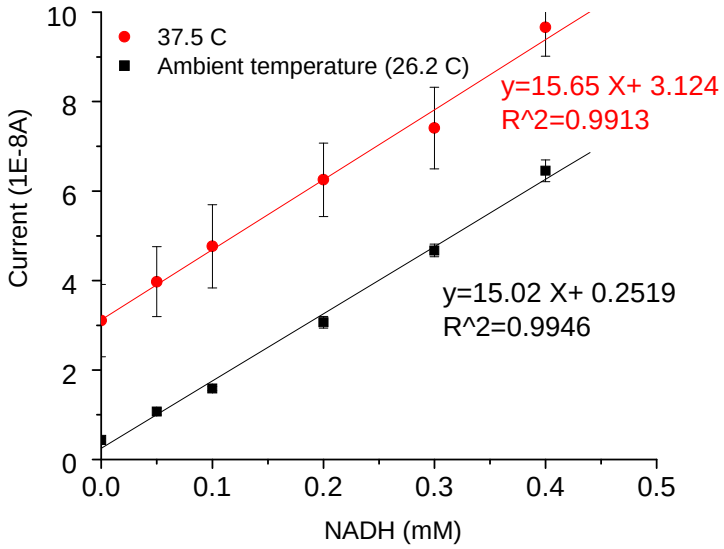

Figure 2. 3 Amperometry of NADH under ambient temperature (26.2 ºC) and 37.5 ºC

Figure 2. 3. shows the amperometry of different concentrations of NADH at an ambient temperature (26.2 ºC) and at 37.5 ºC. The amperometric current increased with the NADH concentration, at both temperatures. The amperometry showed good linearity and sensitivity at both temperatures. At 37.5 ºC, the amperometry showed a larger background current (the current corresponds to 0.0 mM of NADH solution), and a larger error at each NADH concentration, compared to the amperometry at ambient temperature (26.2 ºC). This result was reasonable and expected since the kinetics of the electrochemical reaction increased at a higher temperature, which produced a larger oxidation current from reaction (2.1) as well as a larger error. **Figure 2. 3** shows that the amperometric current could be used to quantify the concentrations of NADH solutions from 0 to 0.4 mM, at both temperatures, 26.2 ºC and 37.5 ºC. However, further experiments would be needed in order to optimize the

sensor operating temperature. The planned experiments in this study were described as follows.

2.3.2 Detection of 3HB with 3HBDH and NAD^+ in test medium

The feasibility of using the measurement of NADH to quantify 3HB was assessed in this study, and the optimal value of the parameters of this detection, *e.g.*, the concentration of NAD^+ and the operating temperature, were investigated.

2.3.2.1 NAD^+ effect

Previous experimental results showed that NADH could be quantified by the amperometric technique. Thus, it would be meaningful to assess 3HB through reaction (2.1) by detecting NADH in the test medium. There were two reactants in reaction (2.1), ketone body 3HB and NAD^+. Literature indicated general agreement that the normal serum levels of ketone bodies could be less than 0.5 mM; hyperketonemia could be defined at a level in excess of 1.0 mM, and ketoacidosis could be defined at a level in excess of 3.0 mM [2]. Patients under hyperketonemia were suggested to have different medical care from patients under ketoacidosis [17]. Therefore, a sensor or a testing assay range for the 3HB should extend well beyond 3.0 mM, *i.e.*, up to 5 or 6mM [9]. Hence, this range of 3HB was further increased to 10 mM for evaluation purpose.

The concentration of the other reactant in reaction (2.1), NAD^+, should be sufficiently high in the test medium ensuring that it would not be the rate limiting factor in reaction (2.1). On the other hand, excess NAD^+ will increase the biosensor cost. So in

the development of this ketone sensor, the effects of the NAD^+ concentration were evaluated experimentally in order to obtain the optimal required NAD^+ concentration. **Figure 2. 4** shows the effects of NAD^+ concentrations on the amperometric detection of reaction (2.1). In these studies, a fixed enzyme concentration in a solution of 25 units/mL 3HBDH was used, and a fixed temperature of 37.5 ºC was chosen. Thus, the NAD^+ concentrations, 1.48g/L, 3.40g/L and 7.60g/L, were used in a test medium of PBS with 0.03M KCl supporting electrolyte.

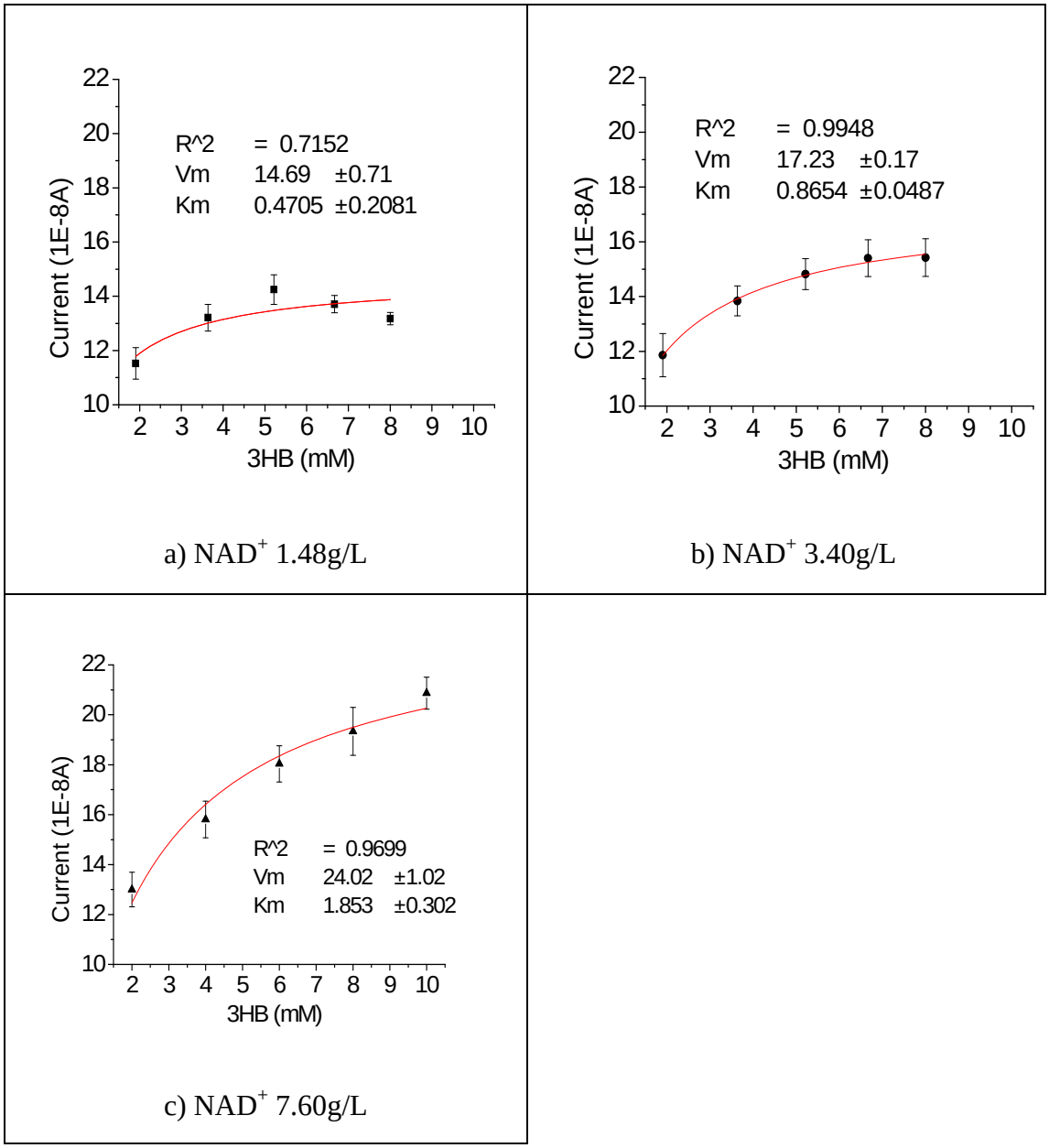

Figure 2. 4 Amperometry of 3HB with 3HBDH and different concentrations of NAD^+ at 37.5 ºC, a) NAD^+ 1.48g/L, b) NAD^+ 3.40g/L, c) NAD^+ 7.60g/L.

As shown in **Figure 2. 4**.(a), at a relatively low NAD^+ concentration of 1.48g/L, the experimental data showed a poor fit for the Michaelis-Menten equation at high 3HB concentration, namely at 6.3 mM and above. This indicated that at the 6.3 mM or higher 3HB concentration, the NAD^+ at a concentration of 1.48g/L became the rate limiting factor. On the other hand, at NAD^+ concentrations of 3.40g/L and 7.60g/L,

the experimental results showed an excellent fit of the Michaelis-Menten mechanism indicating that NAD^+ at these concentration levels would not be the rate limiting factor. Furthermore, the experimental results clearly showed that the concentrations of 3HB can be quantified by the measurements of the NADH concentration as postulated. Based on the results shown in **Figure 2. 4**.(b) and (c), a NAD^+ concentration of 7.6 g/L was chosen in our study ensuring that NAD^+ would not be a rate limiting factor in this sensor development.

2.3.2.2 Temperature effect

The effects of the operating temperature on the sensor performance were assessed experimentally. A fixed enzyme concentration of 25 units/mL was used and the NAD^+ concentration of 7.6 g/L was selected based on the results obtained above. A concentration range of 0 to 10 mM 3HB was used in the test medium of PBS with a 0.03 M KCl solution as the supporting electrolyte. Evaluations of the operating temperature effects on the sensor performance were carried out at four temperatures, namely, 25.8 ºC, 33.0 ºC, 37.5 ºC and 42.0 ºC, covering the range of ambient temperature to the maximum temperature which allowed the enzyme to retain its activity.

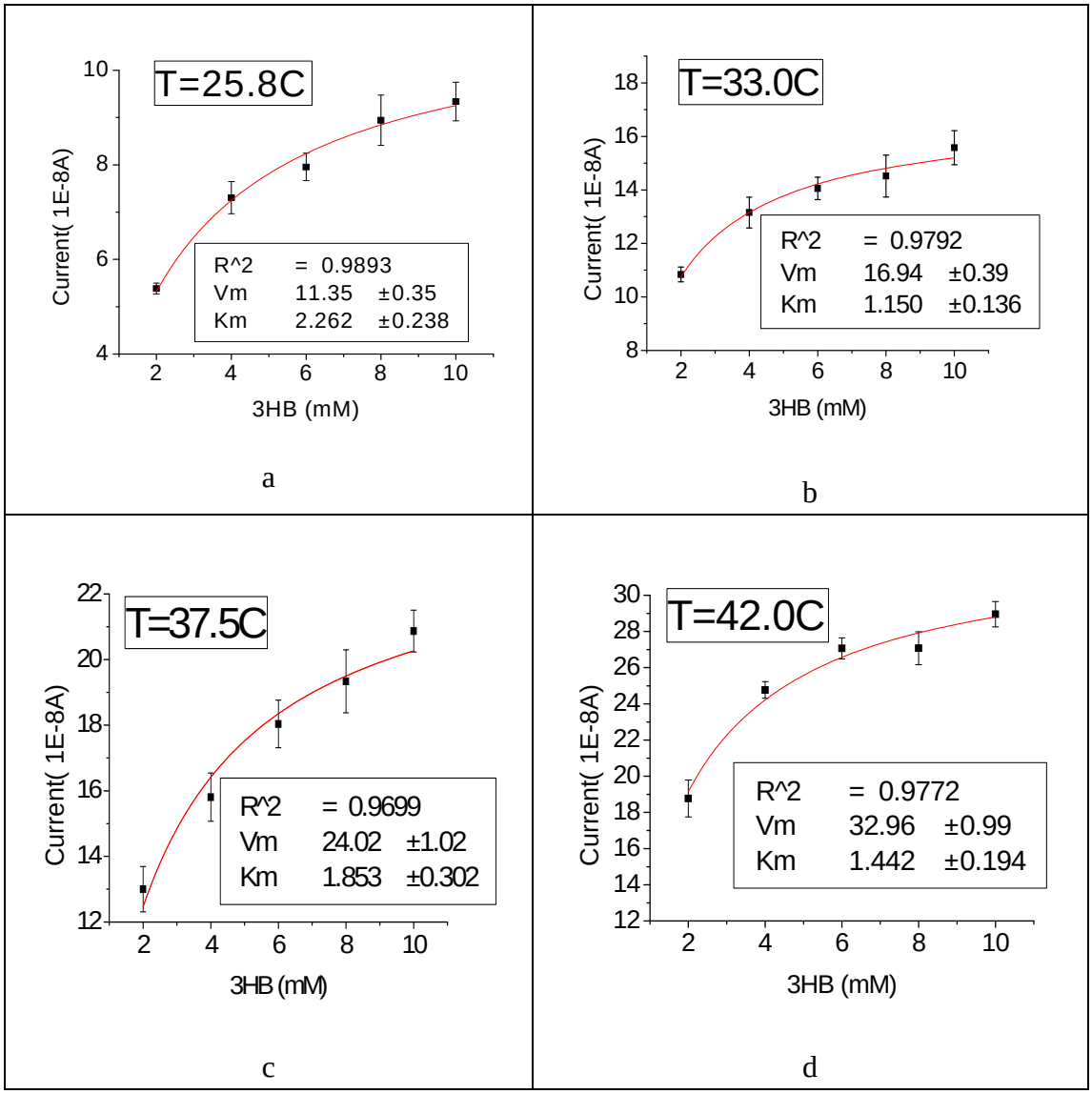

Figure 2. 5 Amperometry of 3HB with 3HBDH and NAD^+ under different temperatures, a) 25.8 ºC, b) 33.0 ºC, c) 37.5 ºC, d) 42.0 ºC.

Figure 2. 5 shows the amperometric studies of the temperature effects on 3HB detection under the designated experimental conditions described. Over the temperature range of 25.8 ºC to 42.0 ºC, the sensor outputs in current showed a Michaelis-Menten relationship to the analyte 3HB concentrations, consistent with an enzymatic based reaction. The higher operating temperature yielded a higher

amperometric current indicating a higher sensitivity of the sensor at higher operating temperature. However, the difference between the currents obtained at 37.5 ºC, and 42.0 ºC was relatively small; in order to minimize the denaturation of enzyme at higher temperature, the sensor operating temperature at 37.5 ºC was then chosen.

2.3.3 Detection of 3HB with 3HBDH and NAD^+ immobilized on sensor

In the last section of discussion, the sensor prototype was experimentally assessed to quantify 3HB with the enzyme 3HBDH and free NAD^+ in the test medium. In order to develop a practical micro-biosensor, the enzyme 3HBDH and the co-reactant NAD^+ were both immobilized on the iridium-modified microelectrode surface. The details of the immobilization of enzyme 3HBDH and NAD^+ had been given primarily in section 2.2.1. The sensing property of this micro-biosensor was evaluated in this study. **Figure 2. 6** shows the amperometry from this micro-biosensor with 3HB in the test medium of PBS and 0.03 M KCl supporting electrolyte under an operating temperature of 37.5 ºC. Sensors fabricated without enzyme 3HBDH were also compared under identical.

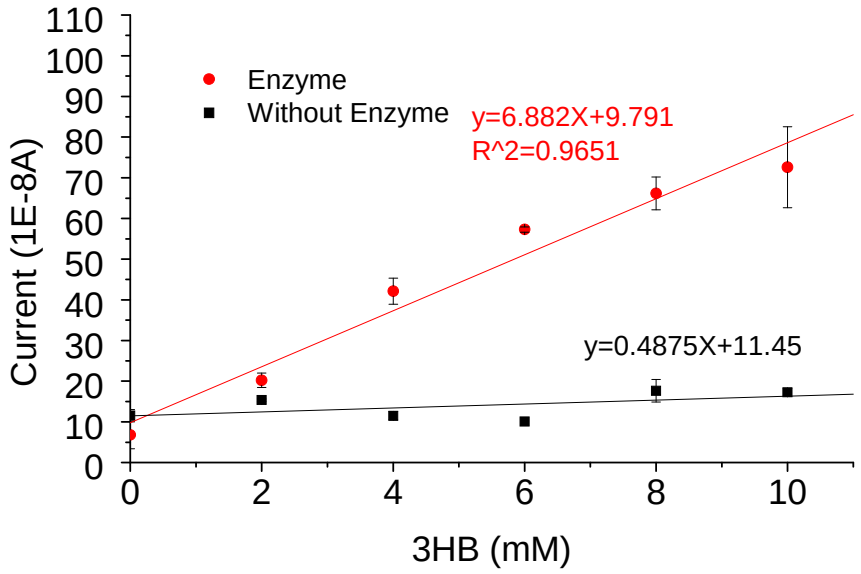

Figure 2. 6 Amperometry of 3HB tested by micro-biosensor at 37.5 ºC in the presence and absence of enzyme 3HBDH.

Figure 2. 6 shows the difference between the presence and the absence of enzyme 3HBDH immobilized on the micro-biosensor. For the sensor without the immobilized enzyme, the amperometric responses for different 3HB concentrations were almost identical, with a baseline oxidation current value of approximately $15*10^{-8}$ A. On the other hand, the sensor with the immobilized enzyme 3HBDH showed a linearly increasing amperometric response with respect to 3HB concentration. This demonstrated that the concentration of 3HB can be quantified only with both the enzyme 3HBDH and the NAD^+ present, in this case immobilized on the micro-sensor surface as shown in **Figure 2. 1**. This micro-biosensor with 3HBDH immobilized also showed high sensitivity, approximately 5 times more sensitive to 3HB than when 3HBDH was in solution(**Figure 2. 5** (c)). The higher sensitivity was most likely due to the high concentration of enzyme 3HBDH on the working electrode, producing a

high concentration of NADH near the vicinity of the working electrode for the subsequent NADH detection.

2.3.4 Evaluation of the interference from uric acid

The micro-biosensor showed that it could be used to detect 3HB in a PBS test medium with a supporting electrolyte of 0.03 M KCl. In a real and practical application, this micro-biosensor would be used in a test medium of serum or other physiological fluids. Consequently, potential interference by the possible biological species would require careful assessment. Ascorbic acid and uric acid were two common bio-components in the physiological fluids which might produce potential interference in this biosensor application. Therefore, ascorbic acid and uric acid were assessed under the same electrochemical oxidation process as the 3HB measurement, +0.2 V vs Ag/AgCl, within the physiological range separately for their potential interference on this micro-biosensor for 3HB measurements.

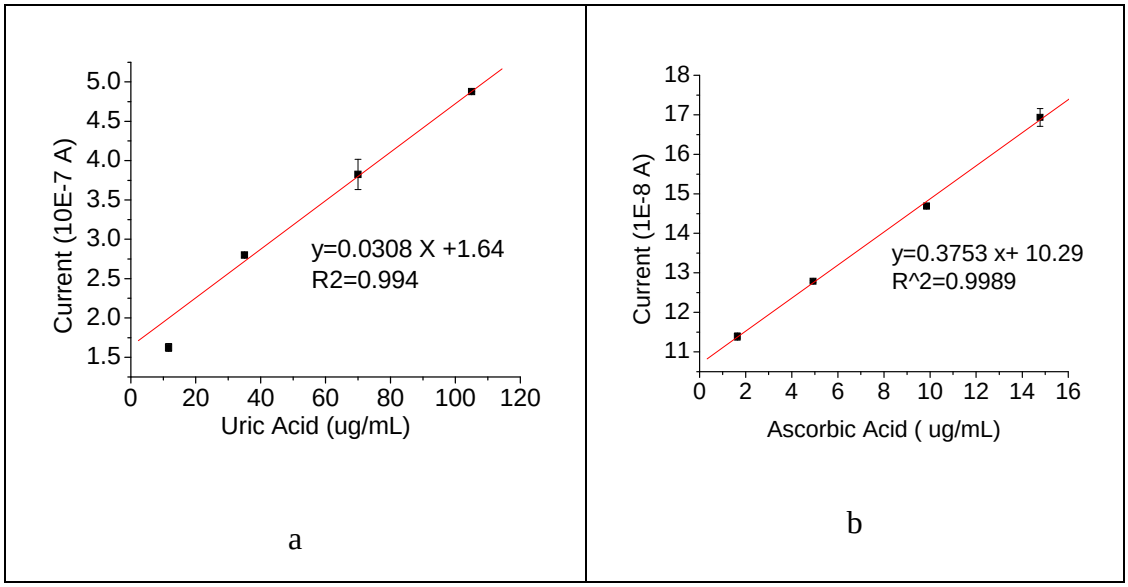

Figure 2. 7 Amperometry of a) uric acid, and b) ascorbic acid under 37.5 ºC and +0.2V vs Ag/AgCl

The experimental results shown in **Figure 2. 7** indicated that the interference from uric acid was more significant than the ascorbic acid due to the high concentration range, 21.8-77ug/mL [18]for uric acid as compared to 15 to 20 ug/mL for ascorbic acid [19]. Therefore, the further interference study focused on uric acid, specifically, uric acid in the concentration range of 22ug/mL to 77ug/mL was used. Four uric acid concentrations, 20ug/ml, 40ug/ml, 60ug/mL and 77ug/mL were used, adding into the 3HB testing solutions with a concentration range of 0 to 10mM 3HB. Sensors fabricated without enzyme 3HBDH were also tested under identical condition for comparison purpose.

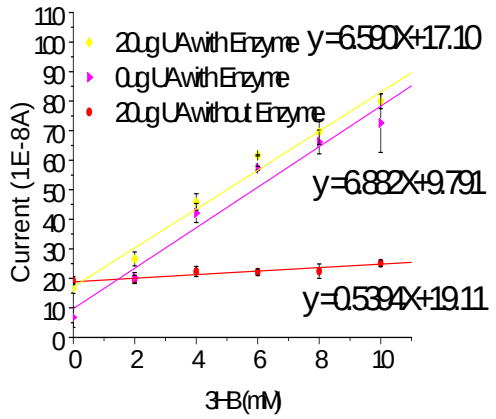

a

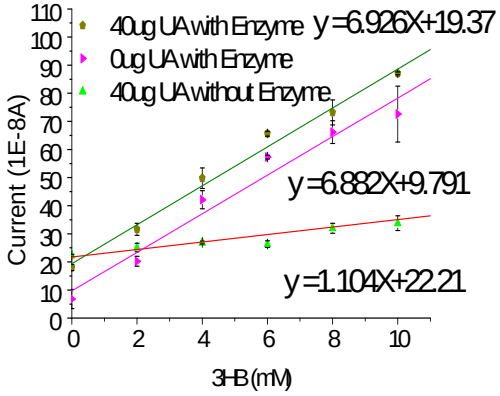

b

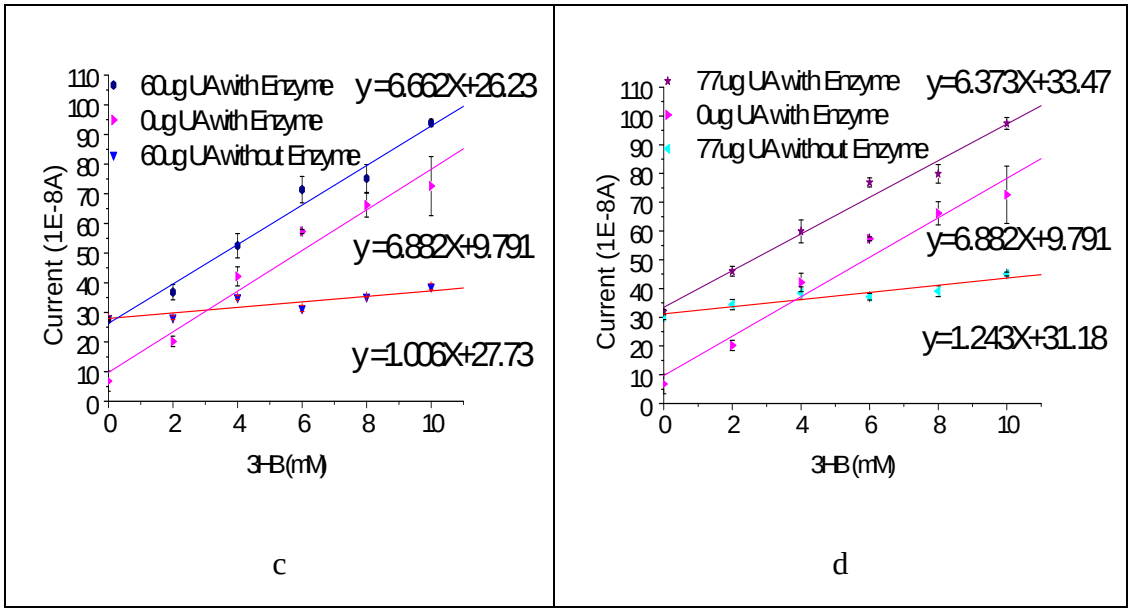

Figure 2. 8 Amperometry of 3HB with different concentrations of uric acid under 37.5 ºC, a)20 ug/ mL uric acid, b) 40 ug/ mL uric acid, c) 60 ug/ mL uric acid, d) 77 ug/ mL uric acid.

Figure 2. 8 shows the amperometry of 3HB in the presence of different concentrations of uric acid in the test medium. In **Figure 2. 8**, the two approximately parallel lines in each plot were the amperometric currents from the micro-biosensor in the presence and the absence of the corresponding concentration of uric acid. The fixed difference in amperometric currents from the two parallel lines, proved that the interference from a fixed concentration of uric acid was identical under different concentrations of 3HB. This interference was linearly related to the amperometric currents on the sensors without enzyme tested in the same concentration of the uric acid (the red line). Thus in the presence of both 3HB and uric acid, the amperometric current (upper line of the two parallel lines) could be regarded as the combination of two currents. One was the amperometric current resulting from the enzymatic reaction (2.1) (lower line of the two parallel lines), the other was the amperometric current from direct oxidation of uric acid (the red line in **Figure 2. 8**). Therefore, in the

detection of 3HB in the presence of a maximum uric acid concentration of 77 ug/ ml, the interference current from uric acid accounted for up to 45% of the total amperometric current, but this interference could be quantified, and the level of 3HB could still be measured accurately.

2.3.5 Evaluation of the interference from NAD^+

In addition to the interference study of the uric acid described above, other potential chemical species were also selected for the assessment of their potential interference effect, *i.e.*, NAD^+. NAD^+ was present in most physiological systems and could be a potential source of interference in the detection of NADH. $NAD^+$was also a reactant in reaction (2.1) and the quantity of NAD^+ presented could become the rate limiting factor in this amperometric detection, which was not desirable. **Figure 2. 9** shows the amperometry results when $NAD^+$was added in the PBS with 0.03 M KCl supporting electrolyte and 3HB over a concentration range of 0 to 10mM. The concentration of $NAD^+$was 2.5g/L, which was comparable to the level used in **Figure 2. 4**.

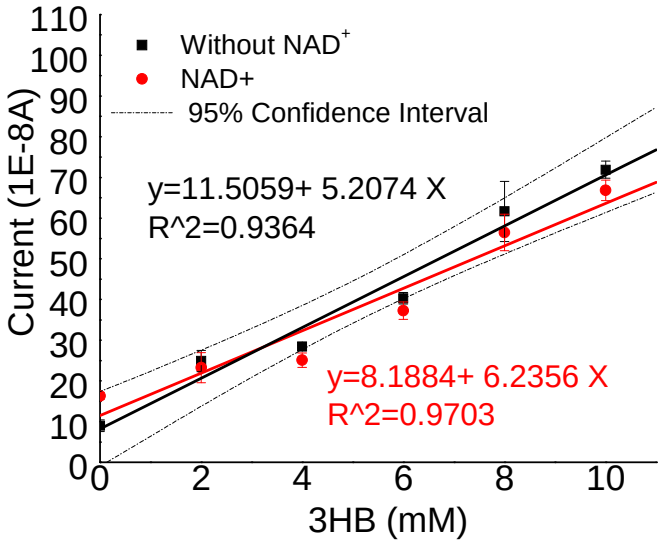

Figure 2. 9 Interference from 2.5g/L NAD^+ under 37.5 ºC.

Figure 2. 9 shows the amperometry of the micro-biosensor which was tested in the test medium together with 3HB and a fixed NAD^+ concentration of 2.5g/L. The experiment results for the identical condition in the absence of NAD^+ (the black line) were also compared in **Figure 2. 9**. The dotted lines show the 95% confidence interval of the obtained amperometric currents in the absence of NAD^+. In the presence of 2.5g/L NAD^+, the amperometric currents from 3HB over a concentration range of 0 to 10mM (the red line) were within this 95% confidence interval. This result showed that adding NAD^+ would not contribute a significant interference in the 3HB detection. Two Sample Independent t-Test analysis also confirmed this conclusion. This could be because sufficient quantity of NAD^+ was immobilized on the working electrode of this sensor during the fabrication. Therefore, the quantity of

NAD^+ present in the test medium did not increase the reaction kinetics for the reaction (2.1) in this amperometric detection.

2.3.6 Test 3HB in bovine serum

In the test medium of the supporting electrolyte of 0.03 M KCl dissolved in PBS solution, 3HB detection was carried out to study the effect of NAD^+ concentration, temperature, and with the enzyme 3HBDH immobilized on the working electrode or dissolved in this test medium. The interference effects from uric acid and NAD^+ were also investigated. It should be recognized that in practical applications, this micro-biosensor should be used in a test medium of physiological fluids, *e.g.*, whole blood, serum or urine. Therefore, this micro-biosensor was evaluated in bovine serum. **Figure 2. 10** shows the amperometry of 3HB dissolved in 100% serum at 37.5 ºC. Sensors without enzyme were also tested under the same experimental condition for comparison purpose.

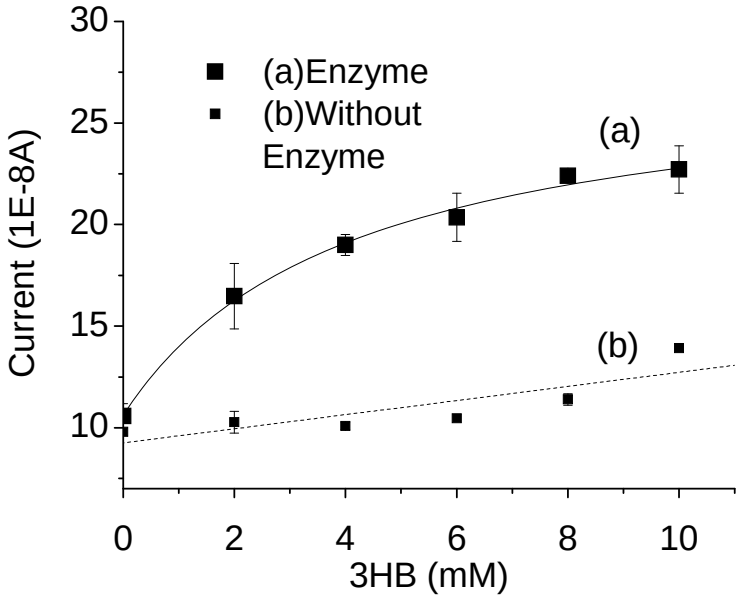

Figure 2. 10 Amperometry of 3HB in serum under 37.5 ºC.

Figure 2. 10 shows that the amperometric currents increased with respect to the concentration of 3HB when 3HBDH was immobilized on the biosensor compared with the biosensor without enzyme. The background (when 3HB was 0mM) for this biosensor in bovine serum and PBS test medium were approximately identical, which could be due to the detection of electrochemical active species in bovine serum, *e.g.*, ascorbic acid. The sensitivity of this biosensor in bovine serum decreased to 20% of the sensitivity of this biosensor in PBS test medium, which was studied and discussed later. Despite the decreased sensitivity, 3HB could still be quantified by this biosensor in 100% bovine serum at 37.5^{o} C.

2.3.7 Spectrometric measurement of NADH and 3HB

The electrochemical measurement of NADH and 3HB by this biosensor was demonstrated. In order to further validate the performance of this biosensor, spectrometric measurement of 3HB was carried out and this spectrometric measurement of 3HB was a standard method to quantify 3HB in an aqueous media. The spectrometric measurements assessed the spectrometric absorbance of the enzymatic produced NADH from 3HB. The absorbance values were directly proportional to the levels of NADH presented, and could be further used to determine the levels of 3HB. In this study, the spectrometric measurements of different concentrations of both NADH and 3HB were carried out and the results were compared to the electrochemical measurement results of NADH and 3HB by the biosensor.

2.3.7.1 Spectrometric measurement of NADH

NADH was added to DI water or 100/% bovine serum in disposable cuvettes to obtain a final NADH concentration in the range of 0 to 0.6 mM. Spectrometric measurements were carried out at 340 nm for the NADH solutions [6]. Calibration curves for different concentrations of NADH were established based on the absorbance value at 340 nm for NADH in both DI water and bovine serum. The temperature in these experiments was fixed at 37.5 °C in order to be consistent with previous electrochemical measurements.

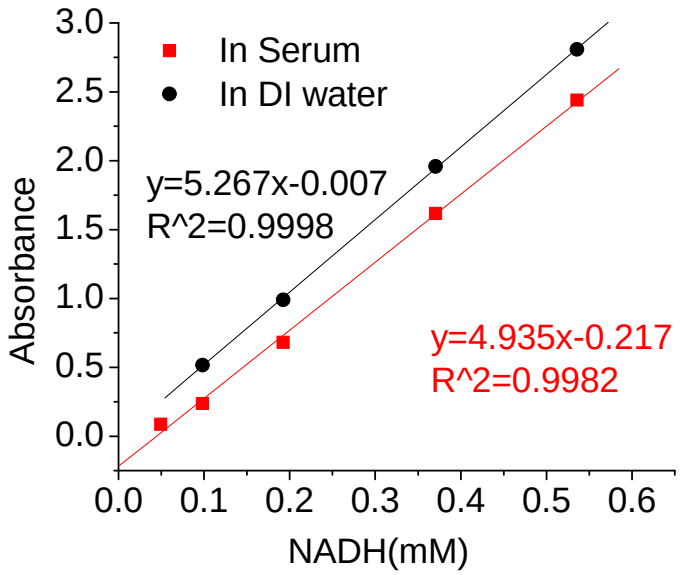

Figure 2. 11 Absorbance of NADH in bovine serum and DI water at 37.5°C

Figure 2. 11 shows that the concentration of NADH could be quantified by the spectrometric measurement in both the bovine serum and the DI water with excellent linearity. Thus, it was meaningful to compare the spectrometric and electrochemical measurements result.

2.3.7.2 Spectrometric measurement of 3HB

The spectrometric measurement of NADH was demonstrated to be feasible. Following the measurement of NADH, experiments were carried out to explore if the level of 3HB could be quantified by the spectrometric measurement at wavelength 340nm. Enzymatic solutions with 4.6 mM NAD^+ and 10 units/mL enzyme 3HBDH were prepared to react with 3HB samples to produce NADH. 3HB samples in the range of 0 to 10mM were prepared and added into the enzymatic solution immediately before measurement. Experiments were carried out in both the buffer

solutions and the bovine serum. The pH of the buffer solution was adjusted to 7.4 to be similar to the pH value of the bovine serum. The temperature was fixed at 37.5°C in all of the tests.

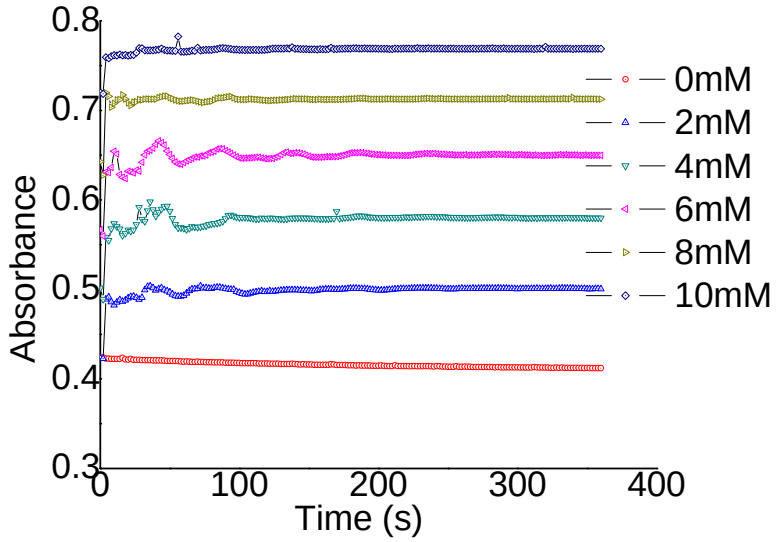

Figure 2. 12 Spectrometric measurement of 3HB in buffer solution

Figure 2. 12 shows that the levels of 3HB can be quantified by spectrometric measurement of the enzymatic produced NADH in buffer solution. The absorbance value remained constant after 3 minutes for all the different levels of 3HB, indicating the reaction reached equilibrium. The same experiments were carried out in the bovine serum.

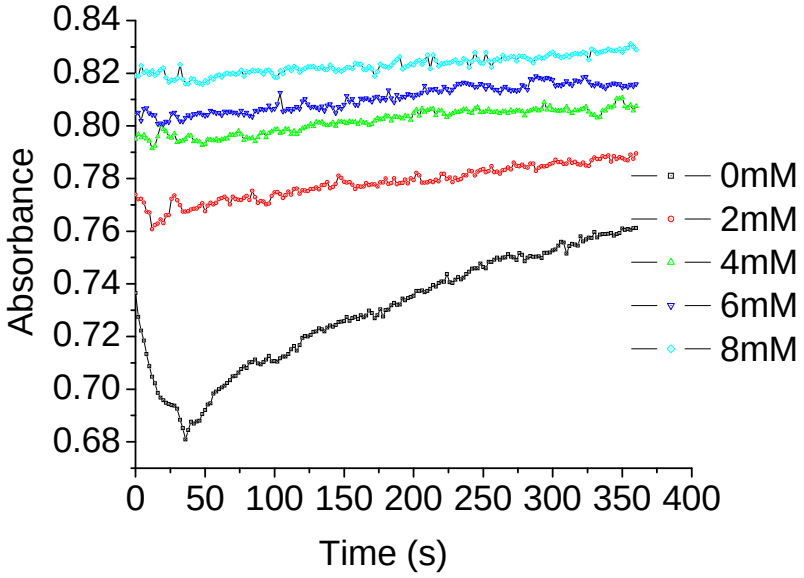

Figure 2. 13 Spectrometric measurement of 3HB in bovine serum

Figure 2. 13 shows that the levels of 3HB could be quantified by spectrometric measurement of the enzymatic produced NADH in the bovine serum. The absorbance value still increased after 3 minutes for all the different levels of 3HB, which could be due to the bovine serum as suggested in **Figure 2. 13**. In order to compare the spectrometric measurement result obtained in the buffer solution and the bovine serum, 3 minutes was selected as the time period for the spectrometric measurement in the bovine serum as well.

The electrochemical measurement and spectrometric measurement of 3HB were compared and analyzed statistically, in both the buffer solution and the bovine serum.

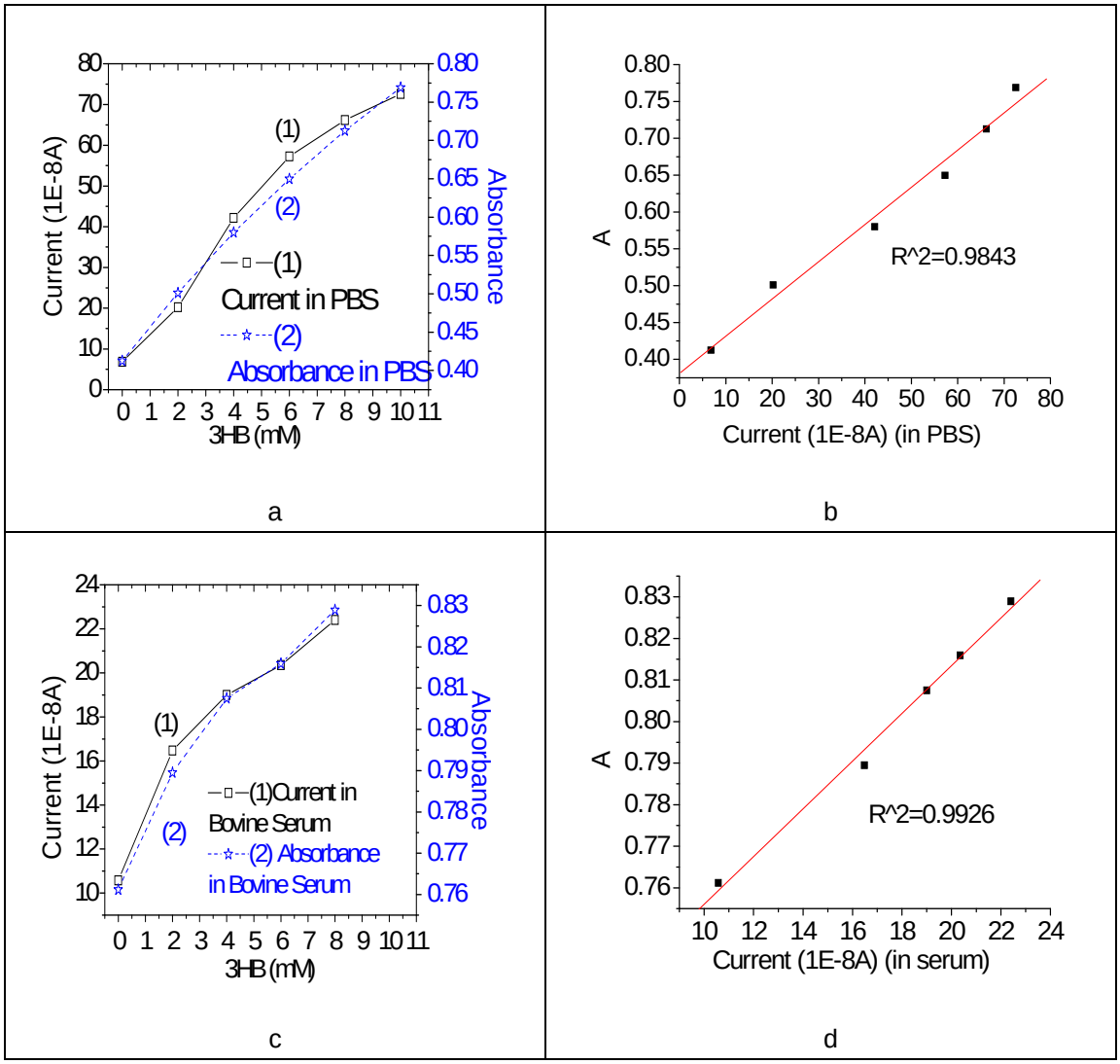

Figure 2. 14 Spectrometric measurement of 3HB at 37.5ºC, compared with the electrochemical measurements. a) In PBS, (1) Current, (2) Absorbance. b) Correlation between different measurement in PBS. c) In undiluted bovine serum, (1) Current, (2) Absorbance. d) Correlation between different measurement in bovine serum.

Figure 2. 14 shows that this biosensor performed well for the 3HB detection using the spectrometric measurements as the basis for comparison. It appeared that the electrochemical outputs of this biosensor and the spectrometric measurements in bovine serum were lower compared to those in PBS. This decrease in the sensor sensitivity in bovine serum could be a result from the binding between enzyme 3HBDH and the serum which may decrease the activity of 3HBDH [20]. However,

the outputs of this electrochemical biosensor and the spectrometric measurements in **Figure 2. 14** (a) and (c) clearly showed that the electrochemical biosensor can be reliable for the quantification of 3HB.

2.4 Conclusions

The importance to develop an amperometric biosensor to detect 3HB for diabetic patient management was discussed. It was demonstrated that 3HB can be quantified by either dissolved 3HBDH in the PBS solution or by immobilized 3HBDH on the sensor prototype surface in the PBS solution and the bovine serum. The temperature for the sensors to operate was optimized to be 37.5ºC. The interferences from uric acid, NAD^+, and serum were tested. The interference from NAD^+ was insignificant. The serum decreased the overall sensitivity of this biosensor by possibly binding to the enzyme 3HBDH. The interferences from uric acid existed but the interference could be quantified by a separate sensor. As a result, the level of 3HB could still be quantified in the presence of these interfering species. Spectrometric measurements of NADH and 3HB were performed in both the PBS and the bovine serum. The spectrometric measurements results of 3HB were compared with the electrochemical measurements of 3HB and these two measurements correlated very well. The data were fitted into either a linear model or a Michaelis- Menten equation successfully, which would be the typical models for enzymatic biosensors. These model fitting confirmed the sensing mechanism of this biosensor through the postulated reaction (2.1).

Reference List

1. Goldstein DE, Little RR, Lorenz RA, Malone JI, Nathan D, Peterson CM, Sacks DB. Tests of glycemia in diabetes. Diabetes Care 2004; 27 (7):1761-1773

2. Laffel L. Ketone bodies: a review of physiology, pathophysiology and application of monitoring to diabetes. Diabetes/Metabolism Research and Reviews 1999; 15 (6):412-426

3. Umpierrez GE, Murphy MB, Kitabchi AE. Diabetic Ketoacidosis and Hyperglycemic Hyperosmolar Syndrome. Diabetes Spectr 2002; 15 (1):28-36

4. Charfen MA, Fernandez-Frackelton M. Diabetic Ketoacidosis. Emergency Medicine Clinics of North America 2005; 23 (3):609-628

5. Csako G. Causes, Consequences, and Recognition of False-Positive Reactions for Ketones. Clin Chem 1990; 36 (7):1388-1389

6. Williamson DH. Enzymic Determination of D(-)-Beta-Hydroxybutyric Acid and Acetoacetic Acid in Blood. Current Contents/Life Sciences 1983; (22):19

7. Kiba N, Inoue Y, Tachibana M, Tani K, Koizumi H. Simultaneous determination of D-glucose and 3-hydroxybutyrate by chemiluminescence detection with immobilized enzymes in a flow injection system. Analytical Sciences 2003; 19 (8):1203-1206

8. Kimura M, Kobayashi K, Matsuoka A, Hayashi K, Kimura Y. Head-space gas-chromatographic determination of 3-hydroxybutyrate in plasma after enzymic reactions, and the relationship among the three ketone bodies. Clin Chem 1985; 31 (4):596-598

9. Forrow NJ, Sanghera GS, Walters SJ, Watkin JL. Development of a commercial amperometric biosensor electrode for the ketone D-3-hydroxybutyrate. Biosensors & Bioelectronics 2005; 20 (8):1617-1625

10. Li G, Ma NZ, Wang Y. A new handheld biosensor for monitoring blood ketones. Sensors and Actuators B-Chemical 2005; 109 (2):285-290

11. Kwan RCH, Hon PYT, Mak WC, Law LY, Hu J, Renneberg R. Biosensor for rapid determination of 3-hydroxybutyrate using bienzyme system. Biosensors & Bioelectronics 2006; 21 (7):1101-1106

12. Byrne HA, Tieszen KL, Hollis S, Dornan TL, New JP. Evaluation of an electrochemical sensor for measuring blood ketones. Diabetes Care 2000; 23 (4):500-503

13. Chiu RW, Ho CS, Tong SF, Ng KF, Lam CW. Evaluation of a new handheld biosensor for point-of-care testing of whole blood beta-hydroxybutyrate concentration. Hong Kong medical journal = Xianggang yi xue za zhi / Hong Kong Academy of Medicine 2002; 8 (3):172

14. Khan ASA, Talbot JA, Tieszen KL, Gardener EA, Gibson JM, New JP. Evaluation of a bedside blood ketone sensor: the effects of acidosis, hyperglycaemia and acetoacetate on sensor performance. Diabetic Medicine 2004; 21 (7):782-785

15. Fang L, Wang SH, Liu CC. An electrochemical biosensor of the ketone 3-[beta]-hydroxybutyrate for potential diabetic patient management. Sensors and Actuators B: Chemical 2008; 129 (2):818-825

16. Krebs HA, Mellanby J, Williamson DH. The equilibrium constant of the beta-hydroxybutyric-dehydrogenase system. Biochem.J. 1962; 82:96-98

17. Wallace TM, Meston NM, Gardner SG, Matthews DR. The hospital and home use of a 30-second hand-held blood ketone meter: guidelines for clinical practice. Diabetic Medicine 2001; 18 (8):640-645

18. Wu F. Animal tissue-based chemiluminescence sensing of uric acid. Analytica Chimica Acta 2005; 536 (1-2):107

19. Bais R. Clinical Chemistry: Principles, Procedures, Correlations, 5th ed. Michael L. Bishop, Edward P. Fody, and Larry Schoeff. Baltimore, MD: Lippincott Williams & Wilkins, 2005, 756 pp., $76.95, hardcover. ISBN 0-7817-4611-6. Clin Chem 2005; 51 (8):1567

20. Vicario C, Arizmendi C, Malloch G, Clark JB, Medina JM. Lactate Utilization by Isolated Cells from Early Neonatal Rat Brain. Journal of Neurochemistry 1991; 57 (5):1700-1707

Chapter 3 Process Parameters Optimization for the Ink Jet Printing of the 3HB Biosensor

3.1 Introduction

Biosensor prototypes had been demonstrated successfully to quantify the level of 3-hydroxybutyrate (3HB) in the previous studies reported in Chapter 2. In order to meet the requirements of a mass-production, a fully-automated technique would have to be employed in both the biosensor prototype preparation and the enzymatic ink addition. In the previous studies, the thick film printing processes were used successfully for the biosensor prototype fabrication. Thus, in this study, it would emphasize on the application of the automated technique for the enzymatic ink addition to the working electrode of the sensor prototype. Ink jet printing was proven to be ideal for biosensor fabrication [1-3]. It facilitated the rapid, reproducible and economically viable production of biosensors [4]. Due to the nature of this process, it also had the potential of integrating the screen printing of a biosensor of its working electrode and adding enzymatic ink together [5]. Therefore, the ink jet printing technique was used in this study to add the enzymatic ink onto the screen- printed working electrode of the biosensor prototype. In addition, both the biosensor preparation and the characterization would be optimized before the application of this ink jet printing technique, in terms of the composition, stability, the optimum volume of the enzymatic ink, the measurement time and the testing sample volume, and others.

In this study, experiments had been carried out to optimize the operation of this biosensor and to assess the feasibility of large quantity production of this biosensor prototype. It was recognized that the essential properties of the biosensor manufacturing process would affect the performance of the fabricated biosensor prototype. Therefore, the essential properties, *e.g.*, the enzyme ink composition, the enzyme ink stability, the quantity of enzymatic ink on each biosensor, the measurement time and the sample volume, were studied in this investigation in order to optimize the performance of the biosensor. The performance of the biosensor was then evaluated by assessing the sensitivity, the background and the repeatability of the electrochemical output of the biosensor. Finally, the inkjet printing technique was applied for the enzyme ink deposition and the printed biosensors were then characterized. The potential interference from acetoacetate (AcAc) was also evaluated.

3.2 Experiment

The biosensor prototypes were fabricated, with enzyme ink of different concentrations manually-spotting and ink jet printing onto the the surface of the working electrode. Electrochemical measurements, *e.g.*, amperometry, were then undertaken of the biosensor in different testing media, including 3HB in buffer solution, and in bovine serum. Potential interference by other species in the physiological sample was also assessed.

3.2.1 Materials

Enzyme 3HBDH (EC 1.1.1.30) was purchased from Wako Chemicals USA. Ir-Carbon particles (5% Ir,) were purchased from E-TEK^{SM}. Phosphate buffer (PBS) and potassium chloride were purchased from Fisher Chemicals. Polyethylenimine, 2-hydroxyethyl cellulose, NAD^+, bovine serum albumin (BSA), NADH, NAD^+, 3HB and acetoacetate (AcAc) were purchased from Sigma-Aldrich. Bovine serum was obtained from Invitrogen. All other chemical were of analytical grade and used as received. All solutions were prepared using de-ionized water.

3.2.2 Fabrication of the enzyme biosensor

This biosensor consisted of an Ir-Carbon modified working electrode with immobilized enzyme 3HBDH, a Ag/AgCl reference electrode, and an Ir-Carbon modified counter electrode. The surface area of the working electrode was approximately 7.85 $*10^{-3}$ cm^2. These electrodes were thick-film screen printed on a polyester substrate. The detailed procedures of the fabrication of this three-electrode configuration enzyme biosensor were described in section 2.2.1 in Chapter 2.

3.2.3 Electrochemical measurements of the biosensor

The performance of the fabricated biosensor prototypes was evaluated using the electrochemical measuring technique, *e.g.*, amperometry. Amperometric measurement was conducted using a CH Instrument 660B electrochemical workstation (CH Instrument, Inc, Austin, TX, USA). These experiments were performed using a 4ml test medium, which was prepared by mixing PBS, supporting electrolyte potassium chloride (KCl, Fisher, Cat. No. P217-500), and 3HB (Sigma-Aldrich, Cat.

No.H6501-5G). This test medium was adjusted to a pH value of 7.2 by adding potassium hydroxide (KOH, Fisher, Cat. No. P251-500). The amperometric measurement was also performed in undiluted bovine serum (Invitrogen, Cat. No.16170-086). The temperature of the solution was well-controlled during the measurement using a water bath (Fisher Scientific ISOTEMP 202). All potentials were referenced to the Ag/Ag Cl electrode. The working potential for all the amperometric experiments was fixed at +0.2 V versus the reference electrode, and the time of recording was 120s in order to reach a steady-state.

3.3 Result and discussion

The performance of this biosensor with different elemental properties in the fabrication and the parameters in the electrochemical characterization were evaluated and compared. These elemental properties in the fabrication included the composition of the enzyme ink, the time interval between the enzyme ink preparation and the biosensor fabrication, the quantity of ink deposited on the working electrode. The characterization parameters included the quantity of sample being evaluated and the duration of the electrochemical measurement. The biosensor prototypes prepared with ink jet printing technique had also been evaluated and the potential interference from AcAc had been assessed.

3.3.1 Comparison between the different enzyme concentrations in ink

Enzyme would often be the most expensive component in a biosensor. Therefore, the quantity of enzyme in a biosensor should be limited in order to be cost-effective. On

the other hand, the quantity of active enzyme present on the working electrode of a biosensor would greatly affect the biosensor's sensitivity and linear range [6, 7]. Therefore, in order to obtain a cost-effective biosensor with acceptable sensitivity and suitable linear range, the enzyme concentration of the ink for a thick film screen printing or ink-jet printing process would need to be optimized. In this study, different quantities of enzyme 3HBDH were added in the ink preparation, resulting in enzyme inks with three levels of enzyme concentration, namely, 30units/ml, 770 units/ml, and 1430 units/ml. Other active ingredients such as NAD^+ and BSA remained the same for these enzyme inks as in the previous chapter. A quantity of 0.6 µl of enzyme ink was dipped onto the working electrode of the biosensor immediately after the enzyme ink was prepared. The biosensors were stored at 4°C overnight before the electrochemical characterization. The experimental results were obtained under +0.2V after 120s.

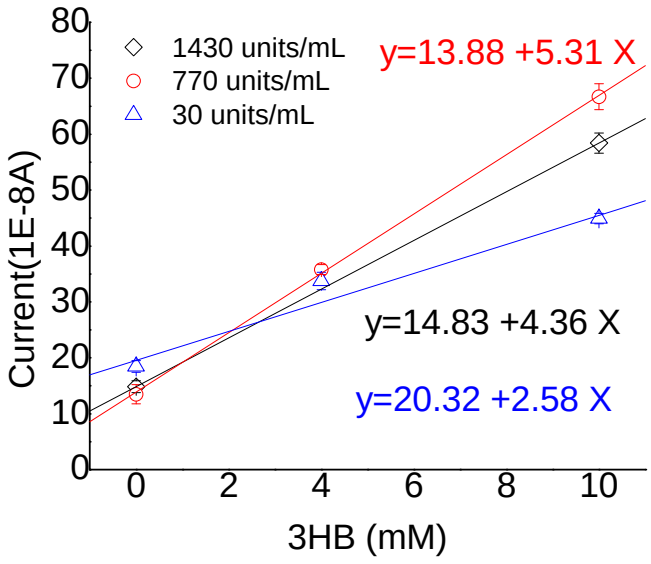

Figure 3. 1 Comparison between enzyme inks with different enzyme concentrations

Figure 3. 1 shows that the sensitivity of this biosensor was the highest when the enzyme concentration was 770 units/ml, changing the concentration to 30 units/ml and 1430 units/ml both decreased the sensitivity. The sensitivity increased from $2.58*10^{-8}$ A/mM to $5.31*10^{-8}$ A/mM as the enzyme ink concentration increased from 30 to 770 units/ml, due to the higher concentration of NADH produced and detected by the working electrode. The sensitivity then reached saturation and decreased to $4.36*10^{-8}$ A/mM when the enzyme ink concentration increased to 1430 units/ml. This was probably due to the reduced charge transport diffusion coefficient at the high enzyme loading [8], and the decreased access of enzyme to substrate in average by adding enzyme loading. The decreased access of enzyme to substrate at high enzyme loading affected the catalytic efficiency of enzyme. Therefore, it was concluded that the sensitivity did not increase proportional to the enzyme ink concentration. Even though the enzymatic ink concentration 30 units/ml was much lower than 770 units/ml, the sensitivity was in the same order of magnitude in both cases. Thus, in large scale manufacturing, low enzyme ink concentration, *e.g.*, 30 units/ml would be selected for the economical reason.

3.3.2 Comparison between the different time delay between enzyme ink preparation and biosensor fabrication

In real applications, the enzyme ink may not be used immediately for the printing or biosensor manufacturing. The delay could be hours and even up to days. The enzyme may lose activity [9] and other electrochemical active substances may be produced during this delay. This effect was studied for enzyme ink of three levels of enzyme

concentration, 30units/ml, 770 units/ml, and 1430 units/ml, to assess the stability of the enzyme ink and the feasibility of using this enzyme ink in the mass-scale production. A quantity of 0.6 µl of the enzyme ink was dipped onto the working electrode of the biosensor immediately after the enzyme ink was prepared or delayed for a selected time period. The biosensors were stored in 4°C overnight before electrochemical characterization. The data were obtained at +0.2V versus the Ag/AgCl reference electrode after 120s.

3.3.2.1 Biosensor using 30 units/ml ink

Enzyme ink of 30units/ml enzyme concentration was prepared, and the performances of two types of biosensor were evaluated in PBS and the results were compared. The first type of the biosensor was prepared immediately after the enzyme ink was formed, while the second type of the biosensor was prepared after exposing the enzyme ink in air for 9 hours at room temperature.

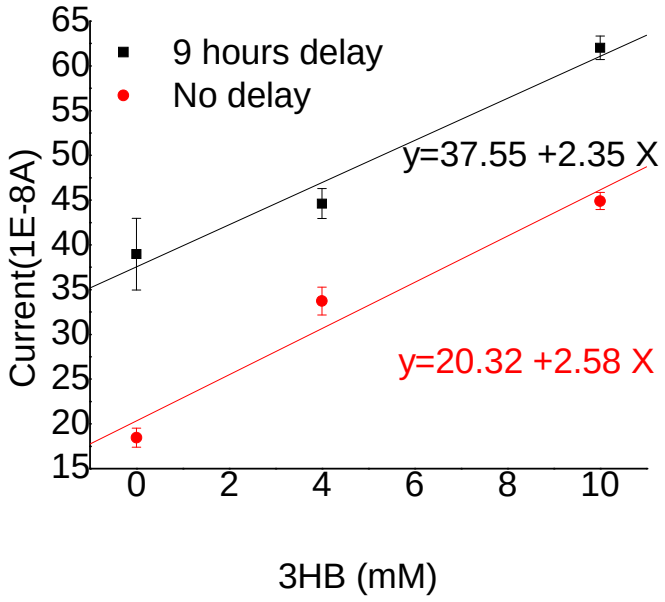

Figure 3. 2 Comparison between biosensors prepared immediately after the ink formation and prepared 9 hours after the ink formation, for enzyme ink of 30 units/ml

Figure 3. 2 shows that when the biosensors were prepared 9 hours after the ink was formed, the biosensors sensitivity did not change significantly, but the background current (the current when 3HB was 0mM) increased from $20*10^{-8}$ A to $37 *10^{-8}$ A This could be due to generation of electrochemical active substances in the enzyme ink during the 9 hours delay . These electrochemical substances were then detected by the working electrode and a larger background current was produced as a result.

3.3.2.2 Biosensor using 770 units/ml ink

Enzyme ink of 70units/ml enzyme concentration was prepared, and the performances of three kinds of biosensors were evaluated in PBS and the results were compared. The first kind of biosensors was prepared immediately after the enzyme ink was formed, while the second kind and third kind of biosensors were prepared after

exposing the enzyme ink in air for 8 hours and 23 hours under ambient temperature, respectively.

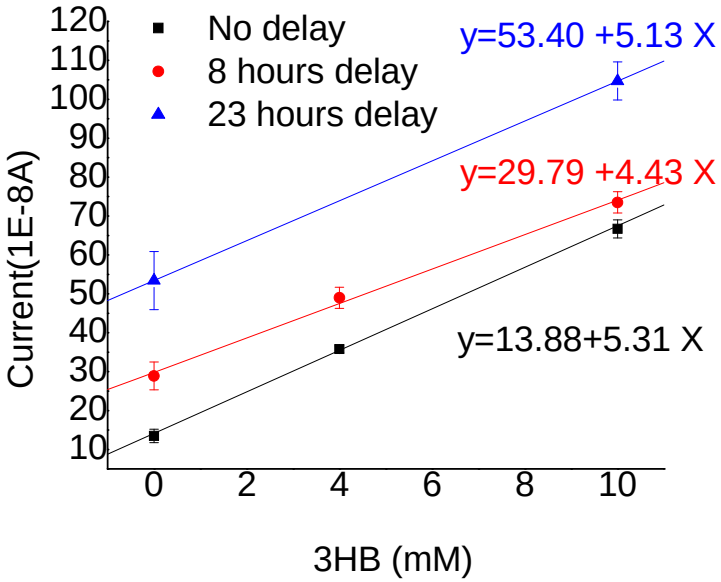

Figure 3. 3 Comparison between biosensors prepared immediately after the ink formation and prepared 8 hours and 23 hours after the ink formation, for enzyme ink of 770 units/ml

Figure 3. 3 shows that when the biosensors were prepared 8 hours and 23 hours after the ink was formed, the biosensors sensitivity did not change significantly, but the background current increased to $29*10^{-8}$ A and then to $53*10^{-8}$ A, respectively. This result showed that the background current increase was slightly less severe when the enzyme concentration was higher in the enzyme ink as compared to low enzyme concentration. It was also noted that the background current increased higher in the early 8 hours period of the delay between the biosensor preparation and the enzyme ink formation.

3.3.2.3 Biosensor of 1430 units/ml ink

Enzyme ink of 1430units/ml enzyme concentration was prepared, and the performances of three types of this biosensor were evaluated in PBS and the results were compared. The first type of the biosensors was prepared immediately after the enzyme ink was formed, while the second type and third type of the biosensors were prepared after exposing the enzyme ink in air for 7 hours and 71 hours in room temperature, respectively.

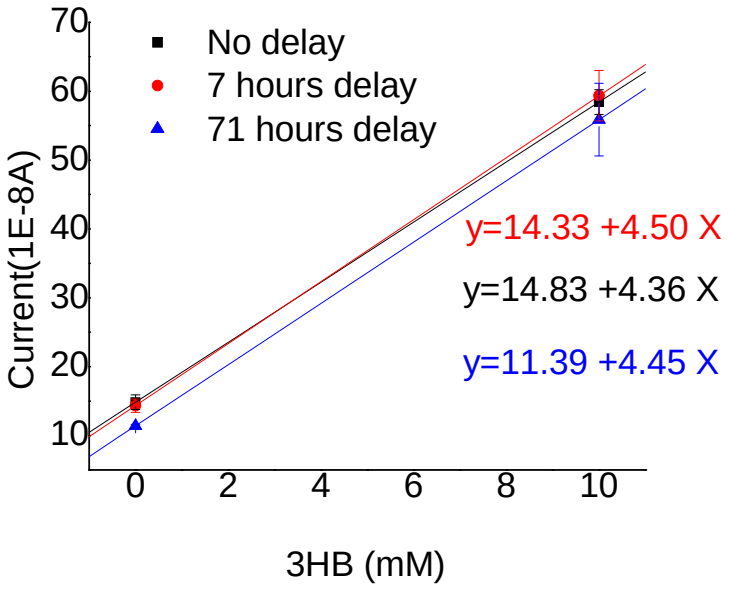

Figure 3. 4 Comparison between biosensors prepared immediately after the ink formation and prepared 7 hours and 71 hours after the ink formation, for enzyme ink of 1430 units/ml

Figure 3. 4 shows that when the biosensors were prepared 7 hours and 71 hours after the ink was produced, the biosensors sensitivity did not change significantly, and the background currents were around $11*10^{-8}$ A to $15*10^{-8}$ A, which showed great

improvement compared to the previous biosensors with lower enzyme ink concentrations.

A possible explanation of this result was that NAD^+ in the enzyme ink degraded to electrochemically active substances, *i.e.*, α-NADH and α-$O^{2'}$-6B-1,4,5,6-tetrahydronicotinamide adenine dinucleotide (cTHNAD) [10] during the time period when the enzyme ink was stored at room temperature. The α-NADH and cTHNAD were then detected by the Ir-modified working electrode at +0.2V vs Ag/AgCl and produced the background current. The detection of the enzymatic produced NADH competed with α-NADH and cTHNAD on the working electrode. It was noted that the enzyme 3HBDH had two effects in the biosensor responses: 1) it catalyzed the enzymatic production of NADH in the presence of 3HB; 2) it reduced the charge transport diffusion coefficient at high enzyme loading [8] and thus reduced the background current in both the presence and the absence of 3HB. Therefore, when enzyme 3HBDH existed in excessive quantity, *e.g.*, 1430 units/ml, the electrochemical response was mostly from the enzymatic produced NADH in the presence of 3HB, while the background current in the absence of 3HB was small due to the reduced charge transport diffusion coefficient at high enzyme loading [8]. On the other hand, when enzyme 3HBDH had a lower quantity in the enzyme ink, *e.g.*, 30 units/ml or 770 units/ml, the electrochemical response which was due to both the enzymatic produced NADH and the electrochemical interference substance α-NADH and cTHNAD, and the charge transport diffusion coefficient was relatively high. As a result, the background current increased at the low enzyme ink loading.

In a brief summary, the high enzyme loading greatly reduced the interference from the delay between enzymatic ink formation and biosensor fabrication, and provided more flexibility in mass-production. However, high enzyme loading also increased the cost. Therefore, from the economical perspective, low enzyme loadings 30 units/ml might still be preferred.

3.3.3 Comparison between the different volumes of ink on biosensor working electrode

The quantity of active enzyme presented on the working electrode of this biosensor prototype greatly affected the biosensor's sensitivity [6, 7]. The quantity of the enzyme on the working electrode was controlled by both the enzyme concentration of the ink and the volume of ink applied. The effect of different enzyme ink concentration was studied and summarized for 30units/ml, 770 units/ml, and 1430 units/ml previously. In this study, the effect of different volumes was assessed for the enzyme ink with concentration of 1430 units/ml. The other ingredients such as NAD^+ and BSA were the same for these enzyme inks. A quantity of 0.6 µl or 1.2 µl of enzyme ink was dipped on the working electrode of the biosensor immediately after the enzyme ink was prepared. The biosensors were stored in 4°C overnight before electrochemical characterization. The data were obtained under +0.2V versus Ag/AgCl reference electrode after 120s.

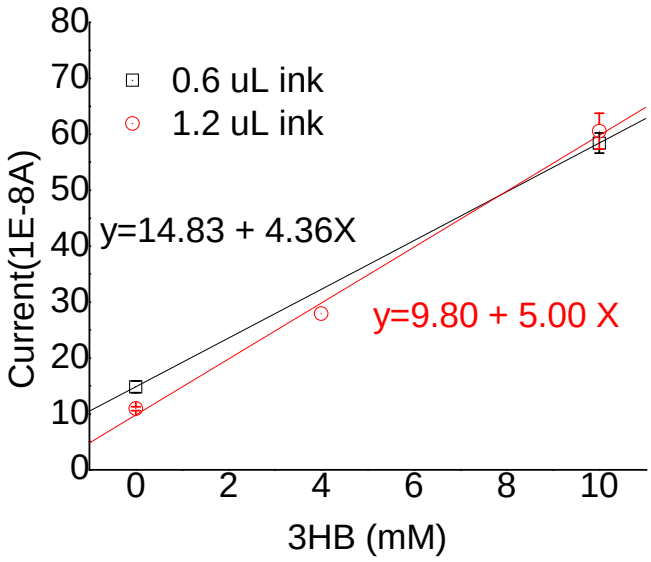

Figure 3. 5 Comparison between biosensors prepared with 0.6 µl of enzyme ink and 1.2 µl of enzyme ink, for enzyme ink of 1430 units/ml

Figure 3. 5 shows that the sensitivity was slightly higher and background was slightly lower for biosensor with more enzyme ink, though not significantly different from the biosensor with less enzyme ink. Since enzyme would be expensive, in large scale manufacturing, low enzyme ink volume should be selected due to the economical reason.

3.3.4 Comparison between the different sample volumes

The elemental properties in the fabrication of the biosensor greatly affected the performance of the biosensor and the effects were summarized. On the other hand, the characterization parameters, such as the sample volume and the measurement time, also affected the performance of the biosensor. The physiological sample volume required for the measurement from end users, *i.e.*, patients greatly affected the users' willingness to use this biosensor. A large volume of physiological fluid such as blood

drawn from a patient resulted in increasing pain and inconvenience. It appeared that smaller sample volumes could pose a challenge for the electrochemical measurement in both accuracy and repeatability. Therefore, experiments were carried out to demonstrate the effect of testing sample volume on the electrochemical response. The two sample volumes chosen were 2ml and 5uL, a typical volume in the order of laboratory experiment and a typical volume in the order of sample required in a commercial biosensor device, respectively. The biosensors were prepared by the enzyme ink of 30 units/ml enzyme. The data were obtained under +0.2V after 120s.

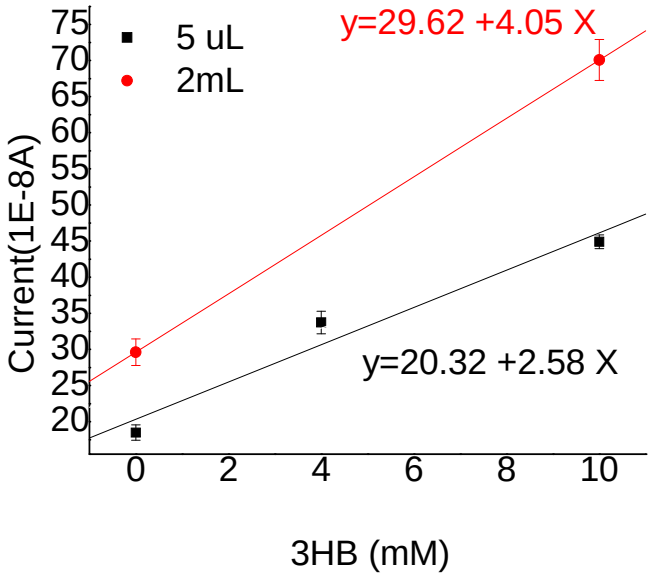

Figure 3. 6 Comparison between 2ml and 5µl testing sample volume, for enzyme ink of 30 units/ml

Figure 3. 6 shows that the electrochemical responses were different when the biosensors prepared in the same manner were tested in testing medium with different volume. Biosensors measured in a 2ml testing medium showed a larger background current and a higher sensitivity than those measured in a 5µl testing medium. The

biosensor's performance in a larger volume of the testing medium was better than in a small volume of the testing medium, but in real application, small volumes, such as 5µl or lower, could still be selected as the volume required due to the preference of the end users.

3.3.5 Comparison between different electrochemical measurement time periods

Measurement time was another characterization parameter that might affect the biosensors' performance as well as the patients' compliance to use such biosensor. Longer measurement times allowed the reaction and electrochemical signal to reach a steady-state, producing a more accurate and repeatable electrochemical result. However, long measurement time also increased the inconvenience for the application of this biosensor. Therefore, experiment was carried out to demonstrate the effect of measurement time on the electrochemical response. Two values of the measurement time were selected as 60 seconds and 120 seconds. The biosensors were prepared by enzyme ink of 30 units/ml enzyme. The data were obtained under +0.2V vs Ag/AgCl reference electrode.

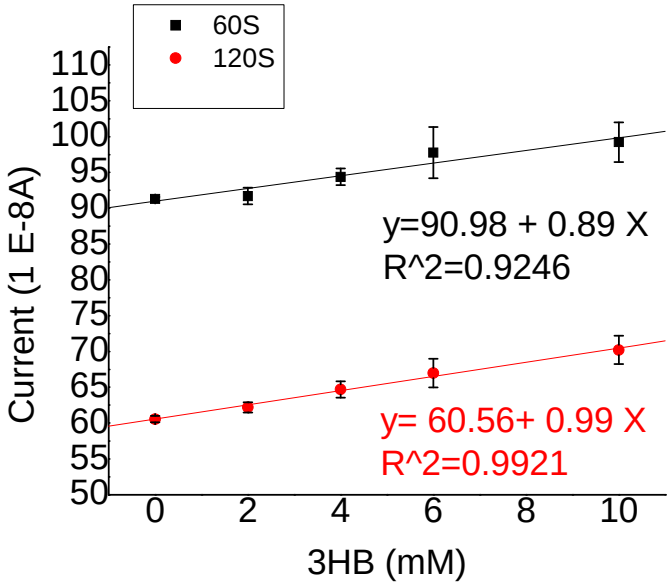

Figure 3. 7 Comparison between 60 and 120 in measurement time in 5µl sample, for enzyme ink of 30 units/ml

Figure 3. 7 shows that when the measurement time was 120s, the electrochemical response presented a lower background, a slightly higher sensitivity and better correlation than the measurement time was 60 seconds. However, in real application shorter measurement time could still be preferred due to the needs of the end user to save time in the measurement.

In summery, in order to have the improve sensing performance from a biosensor, the biosensor should be prepared with a high enzyme loading ink, immediately after enzymatic ink formation ,and characterized in a large volume of sample for a relatively long period of time. However, in practical application these desirable parameters had to be compromised for economical reasons as well as patients' preference.

3.3.6 Assessment of ink jet printed biosensor

The biosensors were prepared using the Asymtek Inkjet Printer and characterized in both the PBS and 100% bovine serum testing medium and all the effects from fabrication and characterization factors were studied and optimized. The enzyme ink for the printing had a concentration of 30 units/ml enzyme and the delay between biosensor printing and ink formation was approximately 8 hours.

3.3.6.1 Assessment of ink jet printed biosensor in PBS

Biosensors prepared by ink jet printing were characterized in 5µl PBS under +0.2V versus a Ag/AgCl reference electrode for 60s under 37.5° C.

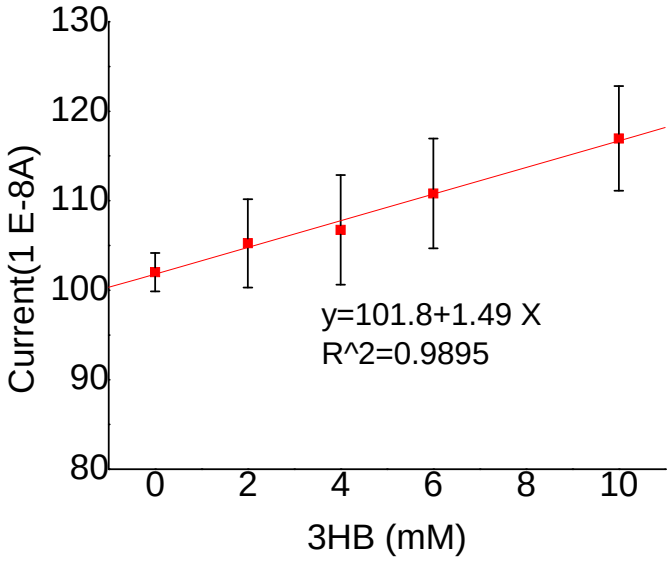

Figure 3. 8 Amperometry of 3HB for biosensors fabricated with ink jet printer in PBS

Figure 3. 8 shows that the electrochemical responses from the large-scale-printed biosensor increased linearly with respect to the level of 3HB in PBS. The correlation was good but the signal had a low sensitivity, a large background and at each level of 3HB, and the signal fluctuated significantly. These could be due to the restrictions required by real application such as usage of enzyme ink with the low enzyme

concentration, the small quantity of enzyme ink printed on working electrode, 8 hours of delay between the enzymatic ink formation and biosensor printing, a relatively short measurement time of 60 seconds and the small quantity of sample in the measurement, *e.g.*, 5µl.

3.3.6.2 Assessment of ink jet printed biosensor in bovine serum

The biosensor prototypes prepared by ink jet printing were characterized in 5µl bovine serum under +0.2V versus a Ag/AgCl reference electrode for 60s under 37.5° C.

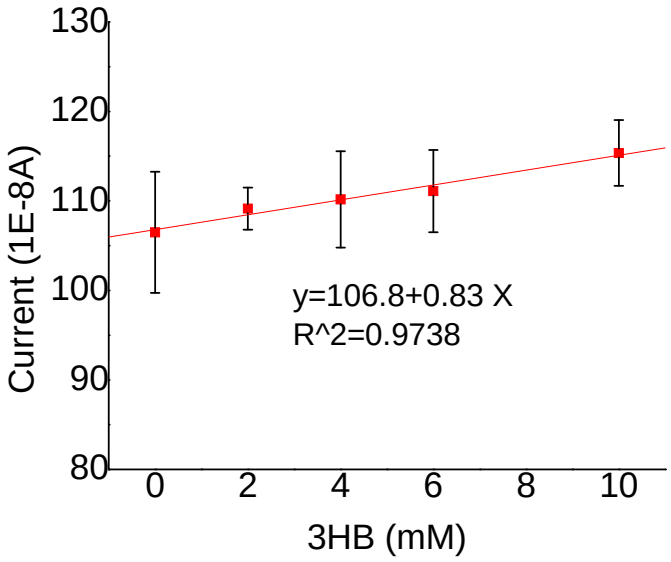

Figure 3. 9 Amperometry of 3HB for biosensors fabricated with ink jet printer in the bovine serum under 37.5° C

Figure 3. 9 shows that the electrochemical responses from the large-scale-printed biosensor increased linearly with respect to the level of 3HB in the bovine serum. The sensitivity was lower than same biosensor assessed in PBS, possibly due to the

binding between enzyme 3HBDH and the serum which may decrease the activity of 3HBDH [11]. The correlation was good, though the signal had a large background, and the signal fluctuated significantly at each level of 3HB.

3.3.7 Assessment of acetoacetate (AcAc) interference on the ink jet printed biosensor

Since AcAc inevitably presented in the blood of diabetic patients, especially for those with a high level of 3HB [12]. It was thus important to assess the potential interference from the AcAc on the 3HB measurement. Therefore, biosensors prepared by ink jet printing were characterized in 5µl bovine serum under +0.2V versus a Ag/AgCl reference electrode for 60s under 37.5° C, with 5mM of AcAc presented in the bovine serum. It should be noted that this value exceeded the physiological concentration of AcAc [12] for evaluation purpose.

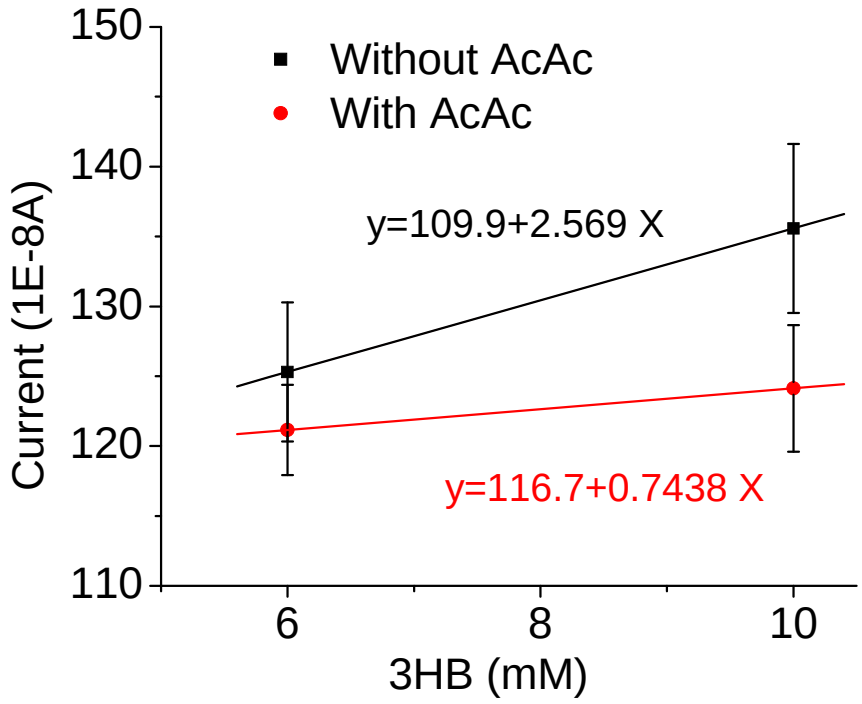

Figure 3. 10 Amperometry of 3HB for biosensors fabricated with ink jet printer, in the presence and absence of 5mM AcAc, in 5µl bovine serum under 37.5° C

Figure 3. 10 shows that the presence of AcAc decreased the signal from amperometric test of 3HB. Both AcAc and NADH were the products of the enzymatic reaction (2.1) to produce NADH from 3HB. Therefore, the presence of AcAc could prevent the production of NADH on the surface of the working electrode of this biosensor, decreasing the signal from the NADH oxidation.

In a brief summary, the interference from AcAc existed in the measurement of 3HB. This interference had been further assessed and the method to quantify the interference from AcAc in 3HB measurement is discussed in the following chapters.

3.4 Conclusions

As a conclusion, the elemental properties in this biosensor fabrication and the parameters in the electrochemical characterization had been assessed. Experiments were carried out to evaluate the relationship between the sensing performance of this biosensor and the elemental properties in the fabrication and the characterization parameters. The biosensor manufacturing process had been evaluated in terms of the enzyme ink composition, the enzyme ink stability and the quantity of ink per biosensor. The biosensor characterization process had been evaluated as well, for the measurement time and the testing sample volume. Consequantly, the value for the elemental properties in the fabrication and the parameters in the characterization were determined based on the experiment results together with the requirements for practical applications. Finally, inkjet printing technique was applied for the enzyme ink deposition to assess the feasibility of mass-production of this biosensor. The biosensors from inkjet printing were characterized in both PBS and bovine serum. The interference from AcAc was also assessed.

Reference List

1. Cho HJ, Parameswaran M, Yu HZ. Fabrication of microsensors using unmodified office in inkjet printers. Sensors and Actuators B-Chemical 2007; 123 (2):749-756

2. Heule M, Vuillemin S, Gauckler LJ. Powder-based ceramic meso- and microscale fabrication processes. Advanced Materials 2003; 15 (15):1237-1245

3. Newman JD, White SF, Tothill IE, Turner APF. Catalytic Materials, Membranes, and Fabrication Technologies Suitable for the Construction of Amperometric Biosensors. Analytical Chemistry 1995; 67 (24):4594-4599

4. Newman JD, Turner APF, Marrazza G. Ink-Jet Printing for the Fabrication of Amperometric Glucose Biosensors. Analytica Chimica Acta 1992; 262 (1):13-17

5. Morrin A, Wilbeer F, Ngamna O, Moulton SE, Killard AJ, Wallace GG, Smyth MR. Novel biosensor fabrication methodology based on processable conducting polyaniline nanoparticles. Electrochemistry Communications 2005; 7 (3):317-322

6. Marzouk SAM, Ashraf SS, Al Tayyari KA. Prototype amperometric biosensor for sialic acid determination. Analytical Chemistry 2007; 79 (4):1668-1674

7. Boujtita M, Hart JP, Pittson R. Development of a disposable ethanol biosensor based on a chemically modified screen-printed electrode coated with alcohol oxidase for the analysis of beer. Biosensors & Bioelectronics 2000; 15 (5-6):257-263

8. Leech D, Daigle F. Optimisation of a reagentless laccase electrode for the detection of the inhibitor azide. Analyst 1998; 123 (10):1971-1974

9. Pandey PC, Upadhyay S, Pathak HC. A new glucose sensor based on encapsulated glucose oxidase within organically modified sol-gel glass. Sensors and Actuators B-Chemical 1999; 60 (2-3):83-89

10. Chenault HK, Whitesides GM. Regeneration of Nicotinamide Cofactors for Use in Organic-Synthesis. Applied Biochemistry and Biotechnology 1987; 14 (2):147-197

11. Vicario C, Arizmendi C, Malloch G, Clark JB, Medina JM. Lactate Utilization by Isolated Cells from Early Neonatal Rat Brain. Journal of Neurochemistry 1991; 57 (5):1700-1707

12. Laffel L. Ketone bodies: a review of physiology, pathophysiology and application of monitoring to diabetes. Diabetes/Metabolism Research and Reviews 1999; 15 (6):412-426

Chapter 4 Electrochemical Biosensor for Nicotinamide Adenine Dinucleotide (NAD^+, Oxidized Form)

4.1 Introduction

Nicotinamide Adenine Dinucleotide (Oxidized Form, NAD^+) is an important co-factor which functions as a substrate or product in several hundred enzymatic reactions, especially in catabolic reactions catalyzed by enzymes. It is also named as beta-nicotinamide adenine dinucleotide, NAD-ox, coenzyme I, diphosphopyridine nucleotide oxidized, DPN^+, DPN-ox, and DPN.

NAD^+ and its phosphorylated derivative, nicotinamide adenine dinucleotide phosphate ($NADP^+$) are two of the most important coenzymes in redox reactions in the cell. Therefore, NAD^+ is related to numerous important biomarkers in early drug development, molecular diagnostics, assay development and bioreactors.

The detection of NAD^+ will be important and meaningful for the biosensor towards various biomarkers and the bioreactor applications [1], and electrochemical detection is a potential means in this development effort. One of the biosensor applications of NAD^+ detection directly related to the research in this study is to quantify the interference of AcAc in the ketone body 3HB detection. The main technical challenge of NAD^+ detection in the reductive mode is the large overpotential, which introduces surface fouling by forming of NAD_2 dimer [2-4]. Consequently, a highly reactive catalyst, *e.g.*, iridium nano-particles supported by carbon, is needed in order to modify the electrode of the biosensor. This catalyst aims to minimize the overpotential and surface fouling, enabling the feasible detection of NAD^+.

4.1.1 Biomarker reaction with NAD^+ as product

Since NAD^+ is related to numerous important biomarkers, the detection of NAD^+ will be important and meaningful for the biosensor towards these biomarkers for biosensor and bioreactor applications. In the reactions with NAD^+ involved, NAD^+ can serve as either the reactant, or the product. This research focuses on the application of the electrochemical detection of NAD^+, which can be further used to quantify the level of the biomarkers of importance. Therefore, only the reactions with NAD^+ as a product are of interest for this research. The most representative biomarkers and the reactions involved are summarized as follows.

1) In the succinate fermentation to butyrate [5]:

The succinate can be fermented by bacterium to butyrate through a series of reactions and the one with NAD^+ involved is shown in reaction (4.1). The detection of NAD^+ can be used to quantify the reaction of succinate fermentation in a bioreactor or to quantify the level of succinate as a biosensor application.

$$\text{NADH + succinate semialdehyde} \xrightarrow[\text{(EC 1.1.1.76)}]{\text{4-hydroxybutyrate dehydrogenase}} \text{NAD}^+ + \text{4-hydroxybutyrate} \qquad (4.1)$$

2) Pyruvate conversion to lactate [6, 7]:

The level of pyruvate is of clinical importance and the level of pyruvate can be quantified through the detection of NAD^+ as shown in the following reaction (4.2).

$$\text{pyruvate + NADH + H}^+ \xrightarrow[\text{EC 1.1.1.28}]{\text{lactate dehydrogenase}} \text{lactate + NAD}^+ \qquad (4.2)$$

3) From salicylate to catechol in the naphthalene degradation [8-10]:

Naphthalene is the simplest fused polycyclic aromatic hydrocarbon, and is abundant in soils. Naphthalene can be catabolized through salicylaldehyde, salicylate, and catechol. The detection of NAD^+ can be used to quantify the level of salicylate or naphthalene as shown in the following reaction.

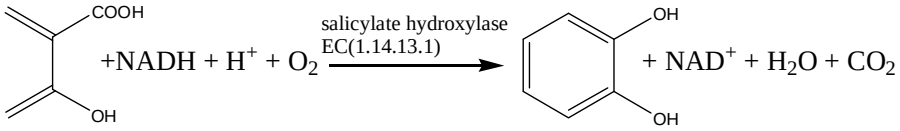

(4.3)

4) In the pathway of lysine biosynthesis [11]:

Lysine is one of the 10 essential amino acids that mammals are unable to synthesize, and must therefore acquire in their diets [11]. Lysine can be produced from aspartate through a series of reactions and one of them is shown as follows.

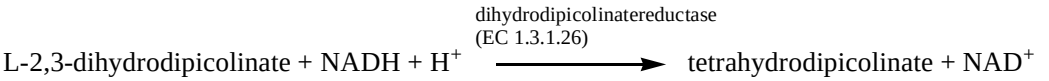

(4.4)

The detection of NAD^+ will be very useful and important in the biosynthesis of lysine for the process control application.

5) Glycine biosynthesis [12]:

Glycine can be biosynthesized by the reverse reactions of the mitochondrial glycine cleavage complex [12]. Glycine biosynthesis has been demonstrated both *in vivo* and *in vitro* as shown in the reaction below.

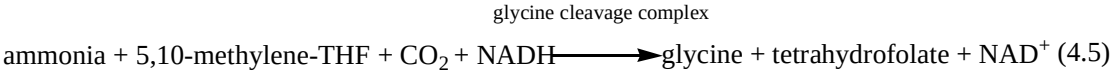

(4.5)

The detection of NAD^+ is very useful and important in the biosynthesis of glycine for the process control application.

6) Glutamate biosynthesis [13]:

The amide group of glutamine is transferred away, generating two molecules of glutamate as shown in the reaction as follow [13]. The detection of NAD^+ can be very useful in the biosynthesis of glutamate as well as the quantification of L-glutamine.

$$\text{NADH + 2-ketoglutarate + L-glutamine} \xrightarrow{\text{glutamate synthase(EC 1.4.1.13)}} \text{NAD}^+ + \text{2 L-glutamate} \quad (4.6)$$

7) Electron transfer (anaerobic):

A series of reactions passes electrons derived from oxidation of one electron carrier to another. The electron carriers are classes of proteins with an unique electron potential. A chain passes from low values to higher, and the highest being the capture of electrons by electron acceptor compounds. The electron carriers often are integral parts of dehydrogenase enzymes. One of the most representative reactions involves the spontaneous electron transfer is shown as follows with NAD^+ as a product.

$$\text{NADH + oxidized flavoprotein (FAD or FMN)} \xrightarrow{\text{spontaneous}} \text{NAD}^+ + \text{reduced flavoprotein } (FADH_2 \text{ or } FMNH_2) \quad (4.7)$$

The detection of NAD^+ can be used to quantify the level of oxidized flavoproteins, *i.e.*, FAD and FMN.

8) In acetylene degradation [14]:

Acetylene can be utilized by both aerobic bacteria and certain anaerobic bacteria for growth [14]. Acetaldehyde has been shown to be an intermediate in all the cases of the pathway for bacteria growth. The acetaldehyde is subsequently converted to other compounds as shown the reaction as follows.

$$\text{NADH + acetaldehyde} \xrightarrow[\text{(EC 1.1.1.1)}]{\text{alcohol dehydrogenase}} \text{NAD}^+ + \text{ethanol} \quad (4.8)$$

Therefore, the detection of NAD^+ can be used to quantify the process of bacteria growth if necessary or monitor the process of acetylene degradation.

In a brief summary, NAD^+ can be found as a common product in these representative reactions involving important biomarkers. Therefore, a convenient and reliable method to monitor the level of NAD^+ will provide a feasible analytical tool for the quantification of these biomarkers in bioreactors and biosensor applications.

4.1.2 Current measurement technique

In order to minimize the overpotential and the surface fouling, various methods had been suggested to modify the electrode, making the electrochemical detection of NAD^+ feasible.

These methods included the application of chemically modified films and transition metal particles. Chemically modified films such as tin hexachlorplatinate [15], poly(3-methylthiophene: poly(phenol red) [16] and azure-chitosan [1] were utilized to modify the electrode for NAD^+ reduction and detection. The transition metal particles supported by carbon activated the electrode and demonstrated unique catalytic effect for the biosensor applications, *e.g*. ruthenium for NAD^+ reduction [2, 3], iridium for H_2O_2 detection [17-19]and NADH oxidation [20]. Our group demonstrated the application of the iridium modified electrode in various biosensor applications effectively [17, 18, 20]. Therefore, the objective of this study was to utilize an iridium-modified electrode to develop a single-use, disposable NAD^+ electrochemical biosensor. This biosensor could be used in the quantification of interference from

AcAc in the 3HB detection, as well as NAD^+ reduction, which could be use for various biomarker sensing.

4.2 Experiment

4.2.1 Materials

Ir-Carbon particles (5% Ir,) were purchased from E-TEK^{SM}. Phosphate buffer (PBS) and potassium chloride were purchased from Fisher Chemicals. Polyethylenimine and 2-hydroxyethyl cellulose were purchased from Sigma-Aldrich. Nicotinamide adenine dinucleotide (Oxidized Form, NAD^+) and nicotinamide adenine dinucleotide (Reduced Form, NADH) were purchased from Sigma-Aldrich. Bovine serum was from Invitrogen. All other chemicals were of analytical grade and used as received. All solutions were prepared using de-ionized water.

4.2.2 Screen-printing of the thick-film biosensor

This biosensor consisted of an Ir-Carbon modified working electrode with immobilized enzyme 3HBDH, a Ag/AgCl reference electrode, and an Ir-Carbon modified counter electrode. The surface area of the working electrode was approximately $7.85 * 10^{-3}$ cm^2. These electrodes were thick-film screen printed on a polyester substrate. The detailed procedures of the fabrication of this three-electrode configuration enzyme biosensor were described in section 2.2.1 in Chapter 2.

4.2.3 Electrochemical characterization

The performance of the fabricated sensor prototype was evaluated using electrochemical measurements such as cyclic voltammetry, multi-potential-steps, and

amperometry with a CH Instrument 660B electrochemical workstation (CH Instrument, Inc, Austin, TX, USA). Cyclic voltammogram was conducted in the presence of 0.2 mM NAD^+, 0.5 mM NAD^+ and the absence of NAD^+ in a 4ml Tris-HCl buffer solution at pH 7.0. The applied potential range of -0.6 V to +0.3V versus the Ag/AgCl reference electrode was used and a linear potential scan rate of 5mV/second was employed. The multi-potential-steps were conducted from -0.4V to -0.1V with 6 steps, and each step lasted for 60s in a 4ml Tris-HCl buffer solution. The cyclic voltammetric study and multi-potential-steps were carried out at an ambient temperature (approximately 25.5 ºC). The amperometric experiments were carried out with a fixed potential of -0.40 V versus the Ag/AgCl reference electrode, and the time of recording was 60s in order to reach a steady-state current. The amperometric study was carried out in either Tris-HCl buffer solution or bovine serum. The temperature of amperometric study was set at ambient temperature (approximately 25.5 ºC), 30.0 ºC and 37.5 ºC in order to determine the optimum sensing temperature. All potentials given in this research were referenced to the printed Ag/AgCl electrode.

4.3 Results and discussion

In this phase of study, we had investigated the feasibility of direct measurement of NAD^+ using the iridium-modified sensor prototype. We also defined an optimal testing condition for this sensor prototype for NAD^+ detection and investigated the potential interference by other biological species. The evaluation of the sensor for the detection of NAD^+ in serum was meaningful in the development of this biosensor prototype; therefore, this evaluation was carried out in this study.

4.3.1 Determination of the reduction voltage

The following sections describe the research that were undertaken in this study. Cyclic voltammogram study of NAD^+ in the Tris-HCl buffer solution was carried out. The cyclic voltammograms for NAD^+ concentrations at 0.2 mM and 0.5 mM, were carried out in a 4mL of the Tris-HCl buffer solution at ambient temperature. Buffer solution without NAD^+ was also characterized under identical conditions as the blank.

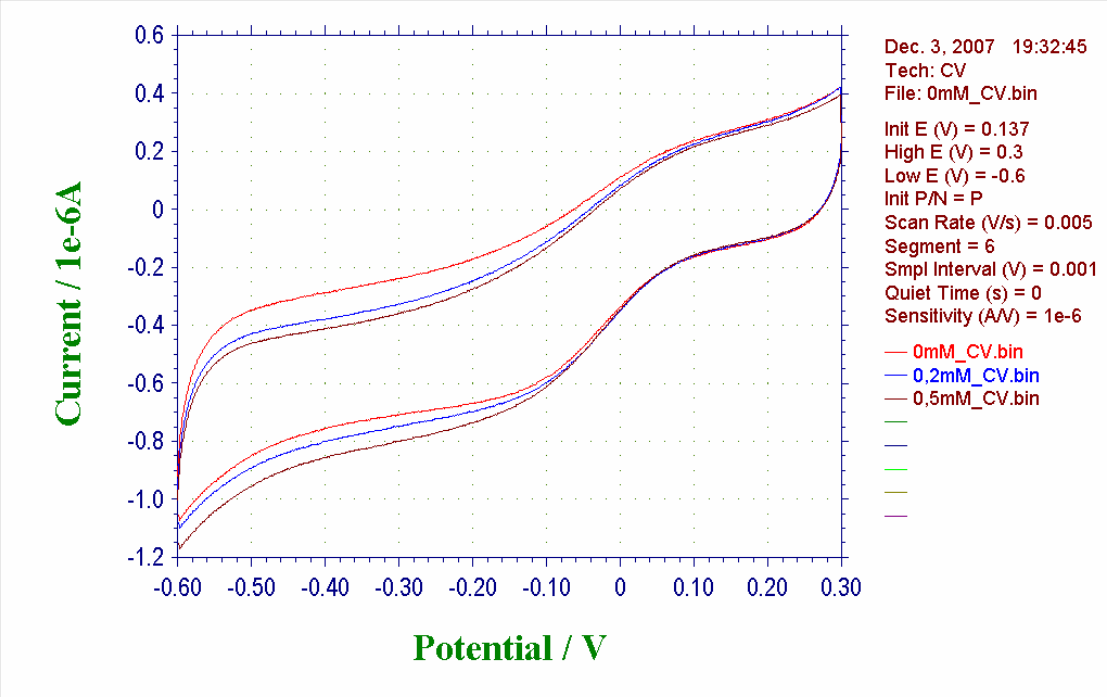

Figure 4. 1 Cyclic voltammogram for background, 0.2mM and 0.5mM NAD^+ under ambient temperature.

Figure 4. 1 shows that the reduction of NAD^+ could be observed at a potential range of -0.10V to -0.60V. Furthermore, the reduction currents for different concentrations of NAD^+ were different as shown in the CV, which demonstrated the feasibility of the electrochemical detection of NAD^+ on this Ir-carbon modified sensor.

The determination of the exact reduction potential was further carried out using the multi-potential-steps technique. The multi-potential-steps were conducted from -0.4V

to -0.1V with 6 steps, and each step lasted for 60s in a 4ml Tris-HCl buffer solution. The result shown in **Figure 4. 2** was the net current after background subtraction.

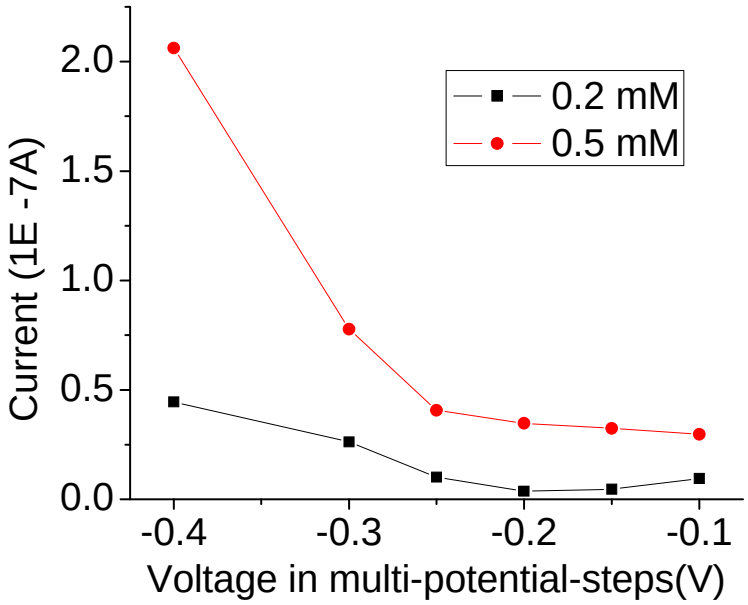

Figure 4. 2 Multi-potential-steps of NAD^+ from -0.4V to -0.1V (with background subtracted)

Figure 4. 2 shows that the reduction currents started to increase significantly at -0.4V. Consequently, the selection of the applied potential to reduce NAD^+ in this sensor development could be based on the results as shown in **Figure 4. 2**. Thus, an applied potential of -0.4 V versus the Ag/AgCl reference electrode for the reduction of NAD^+ was chosen, obtaining a high sensitivity of this sensor and minimizing the potential interference from other electro-active species.

4.3.2 Amperometric measurement of NAD^+ and the temperature effect

Amperometric study of NAD^+ was carried out in Tris-HCl buffer solution. The amperometry for NAD^+ concentration range from 0 mM to 0.5 mM was carried out at

an ambient temperature (approximately 25.5 ºC) and elevated temperatures, *e.g.*, 30.0 ºC and 37.5 ºC, in order to demonstrate the feasibility of NAD^+ sensing under different temperatures and the possible temperature effects on sensing. A potential of -0.4V versus the Ag/AgCl reference electrode was applied based on the results from the cyclic voltammograms and the multi-potential-steps. Our experimental results showed that the system reached a steady state at 60s, and this time was then chosen for our amperometric study.

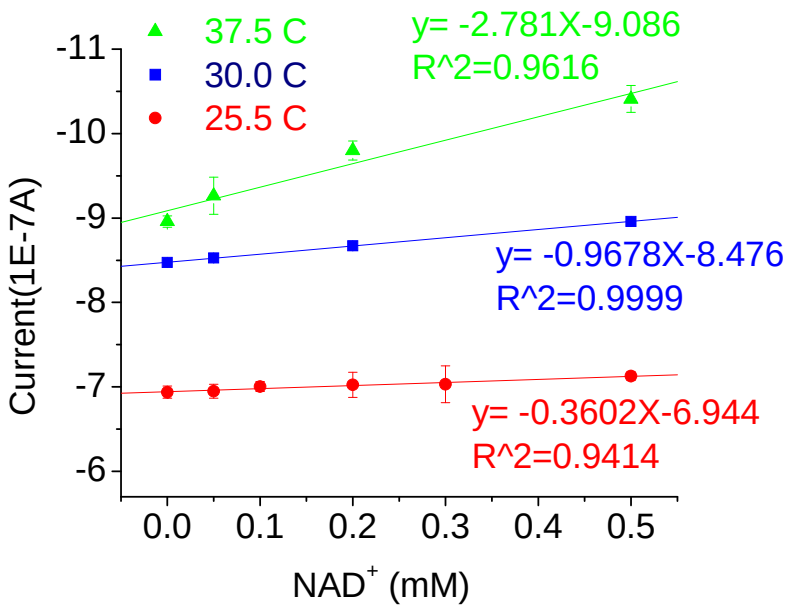

Figure 4. 3 Amperometry of NAD^+ under different temperatures,-0.4V

Figure 4. 3 shows the amperometry of different concentrations of NAD^+ at ambient temperature (approximately 25.5 ºC), 30.0 ºC and 37.5 ºC. The amperometric current increased with the concentration of NAD^+, and a good linearity and good sensitivity of the biosensor at all temperatures existed. At higher temperature, the amperometry showed a large current output, compared to that at lower temperature. The large

current at high temperature could be explained by the electrochemical version of Arrhenius relationship [21]. **Figure 4. 3** shows that the amperometric current could be used to quantify the concentrations of NAD^+ solutions from 0 to 0.5 mM, at an ambient temperatures of approximately 25.5 ºC, elevated temperatures 30.0 ºC and 37.5 ºC. Although the sensitivity and linearity of NAD^+ were better at higher sensing temperature, the ambient temperature was chosen for the convenience of the experiments and practical applications.

4.3.3 Assessment of the possible interference

In the detection of NAD^+, the interference of NADH was a limiting factor for the application of NAD^+ detection since the NADH/ NAD^+ redox couple existed in a significant numbers of enzymatic reactions. In this research, the effect of the different concentrations of NADH on NAD^+ detection was assessed in the presence of 0.5mM NAD^+ under ambient temperature.

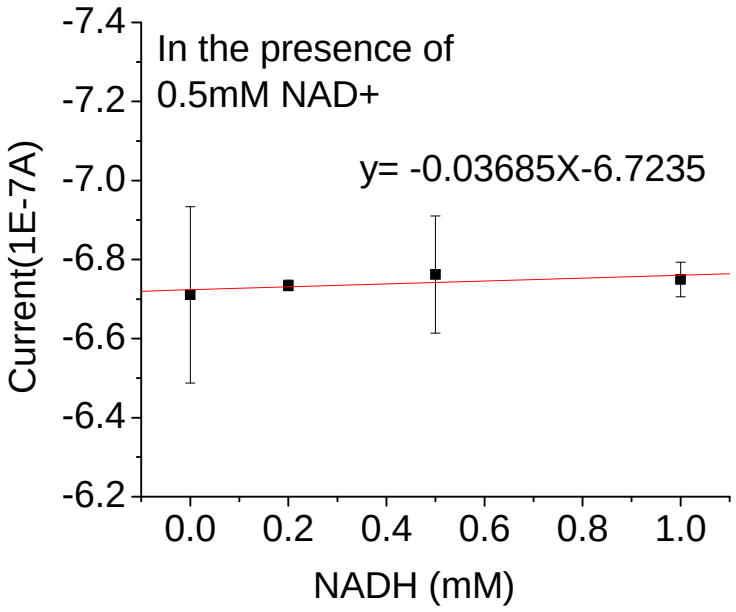

Figure 4. 4 Amperometry of 0.5mM NAD^+ in the presence different concentrations of NADH, at ambient temperature,-0.4V

Figure 4. 4 shows the amperometry of 0.5mM NAD^+ with the different concentrations of NADH. The amperometric responses were similar under different concentrations of NADH. The experimental results suggested that there was minimum or negligible interference by NADH for this NAD^+ biosensor.

4.3.4 Amperometric measurement of NAD^+ in bovine serum

In practical applications, this biosensor will be used in physiological fluids, *e.g.*, whole blood, serum or urine. Therefore, evaluations of this biosensor were carried out in bovine serum which was obtained from Invitrogen. **Figure 4. 5** shows the amperometry of NAD^+ dissolved in 100% bovine serum at ambient temperature.

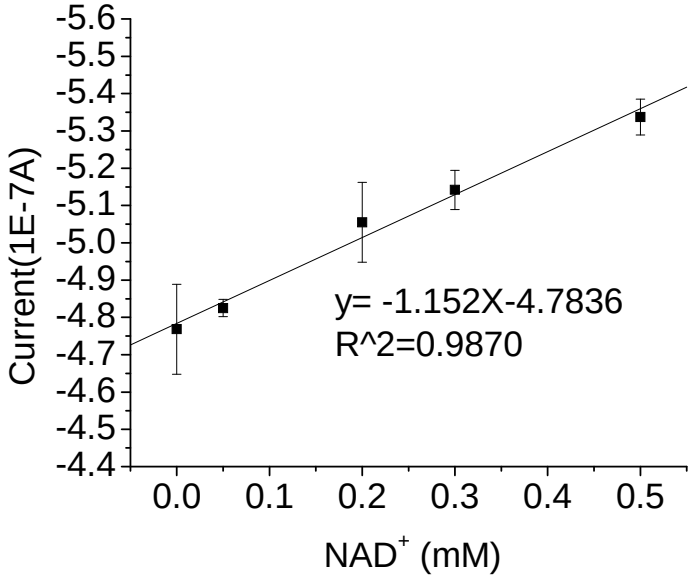

Figure 4. 5 Amperometry of NAD^+ in bovine serum, at ambient temperature,-0.4V

Figure 4. 5 shows that the sensitivity and linearity of NAD^+ detection were very good in the bovine serum. Thus, the performance of this iridium modified biosensor for NAD^+ detection in physiological fluids, *i.e.*, bovine serum appeared to be excellent.

The feasibility of the electrochemical detection of NAD^+ in the bovine serum, together with the high sensitivity under elevated temperature at 37.5 ºC, resulted in the suggestion that this iridium-modified biosensor can be used to quantify the important biomarkers mentioned previously *in vivo*. Due to a larger number of biomarkers related to the NADH/ NAD^+ redox couple, and the high sensitivity and reproducibility, this biosensor may have great potential to serve as a platform technology for various biomarkers based on NAD^+ detection.

4.4. Conclusions

In summary, an iridium-modified biosensor prototype was fabricated using thick film screen printing technique. This single-use disposable biosensor was used for the detection of NAD^+ in the reduction mode in both Tris-HCl buffer solution and 100% bovine serum. This biosensor operated at -0.4 versus the Ag/AgCl reference electrode. The biosensor outputs showed high sensitivity, high linearity, and high reproducibility under ambient temperature (approximately 25.5 ºC), elevated temperatures such as 30.0 ºC and 37.5 ºC. This biosensor was not interfered by the existence of NADH, which demonstrated the feasibility of NAD^+ detection in the enzymatic reactions involving NADH/ NAD^+ redox couple. In most of the enzymatic reactions, a biomarker would be involved. As a result, this biosensor could potentially be applied to quantify a large number of biomarker based on NAD^+ detection, serving as a platform technology. This iridium-modified electrode could potentially be applied to NADH/ NAD^+ regeneration as well with its high catalytic ability. This iridium-modified electrode could also be applied to quantify the interference from AcAc in the 3HB detection for diabetic patient management.

Reference List

1. Tangkuaram T, Wang J, Rodriguez MC, Laocharoensuk R, Veerasai W. Highly stable amplified low-potential electrocatalytic detection of NAD(+) at azure-chitosan modified carbon electrodes. Sensors and Actuators B-Chemical 2007; 121 (1):277-281

2. Azem A, Man F, Omanovic S. Direct regeneration of NADH on a ruthenium modified glassy carbon electrode. Journal of Molecular Catalysis A-Chemical 2004; 219 (2):283-299

3. Man F, Omanovic S. A kinetic study of NAD(+) reduction on a ruthenium modified glassy carbon electrode. Journal of Electroanalytical Chemistry 2004; 568 (1-2):301-313

4. Moiroux J, Deycard S, Malinski T. Electrochemical Reduction of Nad+ and Pyridinium Cations Adsorbed at the Mercury Water Interface - Electrochemical-Behavior of Adsorbed Pyridinyl Radicals. Journal of Electroanalytical Chemistry 1985; 194 (1):99-108

5. Scherf U, Sohling B, Gottschalk G, Linder D, Buckel W. Succinate-Ethanol Fermentation in Clostridium-Kluyveri - Purification and Characterization of 4-Hydroxybutyryl-Coa Dehydratase/Vinylacetyl -Coa Delta(3)-Delta(2) -Isomerase. Archives of Microbiology 1994; 161 (3):239-245

6. Zapatabacri AM, Burstein C. Enzyme Electrode Composed of the Pyruvate Oxidase from Pediococcus Species Coupled to An Oxygen-Electrode for Measurements of Pyruvate in Biological Media. Biosensors 1987; 3 (4):227-237

7. Hetzel M, Brock M, Selmer T, Pierik AJ, Golding BT, Buckel W. Acryloyl-CoA reductase from Clostridium propionicumi - An enzyme complex of propionyl-CoA dehydrogenase and electron-transferring flavoprotein. European Journal of Biochemistry 2003; 270 (5):902-910

8. Connors MA, Barnsley EA. Naphthalene Plasmids in Pseudomonads. Journal of Bacteriology 1982; 149 (3):1096-1101

9. Junior LR, Neto GD, Fernandes JR, Kubota LT. Determination of salicylate in blood serum using an amperometric biosensor based on salicylate hydroxylase immobilized in a polypyrrole-glutaraldehyde matrix. Talanta 2000; 51 (3):547-557

10. Rahni MAN, Guilbault GG, Deoliveira GN. Immobilized Enzyme Electrode for the Determination of Salicylate in Blood-Serum. Analytica Chimica Acta 1986; 181:219-225

11. Bartlett ATM, White PJ. Species of Bacillus That Make A Vegetative Peptidoglycan Containing Lysine Lack Diaminopimelate Epimerase But Have Diaminopimelate Dehydrogenase. Journal of General Microbiology 1985; 131 (SEP):2145-2152

12. Maaheimo H, Fiaux J, Cakar ZP, Bailey JE, Sauer U, Szyperski T. Central carbon metabolism of Saccharomyces cerevisiae explored by biosynthetic fractional C-13 labeling of common amino acids. European Journal of Biochemistry 2001; 268 (8):2464-2479

13. Avendano A, Deluna A, Olivera H, Valenzuela L, Gonzalez A. GDH3 encodes a glutamate dehydrogenase isozyme, a previously unrecognized route for glutamate biosynthesis in Saccharomyces cerevisiae. Journal of Bacteriology 1997; 179 (17):5594-5597

14. Culbertson CW, Zehnder AJB, Oremland RS. Anaerobic Oxidation of Acetylene by Estuarine Sediments and Enrichment Cultures. Applied and Environmental Microbiology 1981; 41 (2):396-403

15. Chen SM, Lin JL. The electrochemical properties of NADH and NAD(+) and their electrocatalytic reactions with tin hexachloroplatinate films. Journal of Electroanalytical Chemistry 2004; 571 (2):223-232

16. Warriner K, Higson S, Vadgama P. A lactate dehydrogenase amperometric pyruvate electrode exploiting direct detection of NAD(+) at a poly(3-methylthiophene): poly(phenol red) modified platinum surface. Materials Science & Engineering C-Biomimetic and Supramolecular Systems 1997; 5 (2):91-99

17. Shen J, Dudik L, Liu CC. An iridium nanoparticles dispersed carbon based thick film electrochemical biosensor and its application for a single use, disposable glucose biosensor. Sensors and Actuators B: Chemical 2007; 125 (1):106-113

18. Shen J, Liu CC. Development of a screen-printed cholesterol biosensor: Comparing the performance of gold and platinum as the working electrode material and fabrication using a self-assembly approach. Sensors and Actuators B: Chemical 2007; 120 (2):417-425

19. Wang J, Rivas G, Chicharro M. Iridium-dispersed carbon paste enzyme electrodes. Electroanalysis 1996; 8 (5):434-437

20. Fang L, Wang SH, Liu CC. An electrochemical biosensor of the ketone 3-[beta]-hydroxybutyrate for potential diabetic patient management. Sensors and Actuators B: Chemical 2008; 129 (2):818-825

21. Tan XC, Tian YX, Cai PX, Zou XY. Glucose biosensor based on glucose oxidase immobilized in sol-gel chitosan/silica hybrid composite film on Prussian

blue modified glass carbon electrode. Analytical and Bioanalytical Chemistry 2005; 381 (2):500-507

Chapter 5. The Development of Fructosyl Valine Biosensor and Glycosylated Hemoglobin Biosensor

5.1 Introduction

Glycosylated hemoglobin (HbA_{1c}) is the stable glucose adduct to the N-terminal group of the β-chain of HbA_0 [1-3]. HbA_{1c} level is defined as the ratio between the glycosylated hemoglobin and the total hemoglobin, which is between 4% to 15% [4]. HbA_{1c} level is considered to be a useful diagnostic marker for diabetic patients in addition to the measurement of the glucose level. Since the life time of hemoglobin in blood is about 2-3 months, the HbA_{1c} level will then indicate the glucose level in the last past 2-3 months. Consequently the measurement of HbA_{1c} is most important for the long-term control of the glycaemic state in diabetic patients [5].

A fast and convenient method for the measurement of HbA_{1c} is important for the point-of-care application, and ideally this method should be integrated with the current glucose meter for diabetes patient management. Enzymatic method is rapid and selective by nature. Therefore, there is great interest in the development of an electrochemical enzyme biosensor for HbA_{1c} detection, particularly if this HbA_{1c} biosensor can be single use and disposable. Enzymatic assay of HbA_{1c} consists of the following steps: firstly HbA_{1c} proteolysis produces glycated hexapeptides; secondly glycated hexapeptides is further decomposed to fructosyl amine such as Fructosyl Valine **(**FV); finally FV is catalyzed by enzyme FAO to produce hydrogen peroxide, which can be detected electrochemically[6].

$$HbA_{1c} \xrightarrow{\text{endoproteinase Glu-C}} \text{glycated hexapeptides Fru-Val-His-Leu-Thr-Pro-Glu} \xrightarrow{\text{proteinase}} FV \xrightarrow{FAO} H_2O_2 \quad (5.1)$$

As shown in reaction (5.1), if a biosensor can detect HbA_{1c} through these three reaction steps, each reaction step will function as expected. Thus, the last reaction step in producing the hydrogen peroxide from FV can be used to produce a FV biosensor. The development of a FV biosensor is relatively simpler and will demonstrate the feasibility of the HbA_{1c} biosensor development. Therefore, the aim of this study is to develop an electrochemical FV biosensor first as the pilot study, then to develop an electrochemical HbA_{1c} biosensor based on the FV biosensor.

5.1.1 Current electrochemical measurement technique

The electrochemical enzymatic assay for FV was applied in this research as well as in other related study carried out by other research groups. Sode *et.al* developed an enzyme fructosyl amine oxidase from marine yeast to detect fructosyl amine (FV) [7-9]. In these studies, an enzyme sensor utilizing a novel fructosyl amine oxidase(FAO) from a marine yeast was developed [7], and the FAO was cultivated in a culture medium and purified. The partially-purified FAO (0.05 units) was casted into a membrane and placed onto a 3mm platinum electrode. This FAO membrane catalyzed FV producing hydrogen peroxide, which was then detected electrochemically at +600mV(vs a Ag/AgCl reference electrode) in a stirred 10ml testing solution. The optimal temperature was chosen to be between 30 ºC and 45 ºC, and the optimal pH value was between 7 and 7.5. The sensitivity for this sensor was 0.4 $uAmM^{-1}$ cm^{-2} between 0.05mM and 1.8mM FV. A flow-injection analysis (FIA)

enzyme sensor for the FV was also developed [8]. All the operation conditions were the same as described in the previous publication [7]. The concentration range of FV that could be quantified was extended to 0.2 to 10mM at a temperature of 25 ºC, and the sensitivity was 4.6 $nAmM^{-1}\,cm^{-2}$. This FIA enzyme biosensor was claimed to be the first sensor towards fructosyl dipeptide, though with insufficient sensitivity. Increasing the quantity of enzyme immobilized might increase the sensitivity. The group of Sode later developed enzyme fructosyl amine oxidase (FAO) from bacterium *Arthrobacter* sp. FV1-1 in order to increase the enzyme quantity and quality. This enzyme FAO was immobilized on a membrane for a FIA sensor and the operating pH and temperature were set to be 7.0ºC and 25.0ºC, respectively. This FIA sensor showed detection limit of 1μM FV with a sensitivity of 7.1 $\mu AmM^{-1}\,cm^{-2}$.

Yonehara et.al [10]developed an enzyme FAO and an enzyme assay for HbA_{1c} based on this enzyme. This assay detected the produced H_2O_2 photometrically and claimed to have a high sensitivity towards H_2O_2 and it would not be interfered from hemoglobin. This assay showed correlation with the HPLC method and the immunoassay when HbA_{1c} was between 4% and 10% [11].

In summary, the current electrochemical measurements of FV needed to improve in terms of the sensitivity and the repeatability of the detection. Ideally a FV biosensor should operate at a lower potential, at ambient temperature and would require a small sample volume in order to minimize the potential interference, improving the operational convenience and the patient's compliance. Furthermore, it would be highly desirable if this FV biosensor could be a single use, disposable devices. Thus,

this phase of our study was carried out to develop a single use, disposable, reagent free, electrochemical FV biosensor, requiring a relatively small sample volume(3 μl) and operating at a relatively low potential (+0.25V vs a Ag/AgCl reference electrode) in ambient temperature.

5.2 Fructosyl Valine Biosensor

Firstly, an electrochemical FV biosensor was developed as the pilot study for the HbA_{1c} biosensor. As shown in reaction (5.2), this FV biosensor would detect the H_2O_2 produced from FV. The amperometric current from the electrochemical detection of H_2O_2 could be used to quantify the level of FV.

$$\text{Fructosyl Valine(FV)} \xrightarrow{\text{FAO}} H_2O_2 \qquad (5.2)$$

In reaction (5.1) shown previously, the FV was from the enzymatic reaction for HbA_{1c}, and this FV biosensor further immobilized with the enzymes to catalyze the first two reaction steps in reaction (5.1), could potentially function as an HbA_{1c} biosensor. Therefore, the development of a FV biosensor would be simpler than the development of an HbA_{1c} biosensor. Consequently, a FV biosensor would firstly be developed in order to demonstrate the feasibility of a HbA_{1c} biosensor development, serving as a pilot study for the electrochemical HbA_{1c} biosensor.

5.2.1 Experiment

5.2.1.1 Materials and Reagents

Enzyme Fructosyl-Amino Acid Oxidase (EC 1.5.3.x, FAO) was purchased from Sigma-Aldrich. Ir-Carbon particles (5% Ir,) were purchased from E-TEK^{SM}. Phosphate buffer (PBS) and potassium chloride were purchased from Fisher

Chemicals. Polyethylenimine and 2-hydroxyethyl cellulose were purchased from Sigma-Aldrich. FV was synthesized and purified in house as previously reported [12, 13]. A mixture of 18.8g L-valine (0.16mol) in 400ml pyridine (both from Sigma-Aldrich) and 400ml acetic acid were mixed and stirred for 30 minutes at ambient temperature. Then 40g (0.22mol) of glucose (Sigma-Aldrich) were added, purged with argon for 5 minutes and stirred for 4 days at ambient temperature. After 4 days the dark mixture was filtered and the solvent was evaporated. A slightly yellowish amorphous product was resulted from re-crystallization in methanol. This product was further purified by semi-preparative HPLC. The collected Fru-Val fractions were combined and lyophilized to a colorless powder. Purity was checked by ^{1}H NMR spectroscopy and evaporative light scattering detection; all analytical data including the mass were in agreement with an earlier report [13]. All other chemical were of analytical grade and used as received. All solutions were prepared using de-ionized water.

5.2.1.2 Screen-printing of the thick-film sensor

This sensor prototype consisted of an Ir-Carbon modified working electrode, a Ag/AgCl reference electrode, and an Ir-Carbon modified counter electrode. The surface area of the working electrode was approximately 7.85×10^{-3} cm^2. These electrodes were printed on a polyester substrate. The detailed procedures of the fabrication of this three-electrode configuration biosensor were described in section 2.2.1 in Chapter 2.

5.2.1.3 Fabrication of the enzyme FAO biosensor

The iridium-modified electrochemical sensor prototype structure described previously was then used as the basis for the construction of the enzymatic FAO biosensor. Enzyme FAO was immobilized onto the surface of the working electrode. The fabrication steps of this biosensor could be described as follows.

a. Preparation of the enzyme FAO ink:

Enzyme FAO ink was prepared in the following manner and applied to the sensor prototype. 1ml of the ink from step (a) described in section 2.2.1 in Chapter 2 was mixed with 100 units of enzyme FAO. Mixing of these components was carried out until a clear solution was obtained.

b. Fabrication of the biosensor:

The enzyme ink from step (a) was then pipetted manually onto the Ir-Carbon working electrode of a sensor prototype, forming the working electrode of this biosensor. This biosensor was stored at 4ºC prior to the electrochemical measurement.

5.2.1.4 Electrochemical characterization

The performance of the fabricated sensor prototypes was evaluated using electrochemical measurement, namely, amperometry. The amperometric experiment was conducted using a CH Instrument 660B electrochemical workstation (CH Instrument, Inc, Austin, TX, USA). The experiment was performed using a test medium, which was prepared by mixing PBS, FV or H_2O_2, and 0.03 M potassium chloride as supporting electrolyte to maintain the conductivity of this test medium. This test medium was adjusted to pH 7.0 by adding potassium hydroxide. The

temperature of the test was at ambient temperature (approximately 26.1 ºC). All potentials given in this research were referenced to the Ag/AgCl electrode. The working potential for the amperometric experiments was fixed at +0.25 V or -0.40 V versus the reference electrode, and the time of recording was 120s in order to reach a steady-state measurement.

5.2.2 Results and discussion

As shown previously, the H_2O_2 is the final product in reaction (5.1). Therefore, the amperometric measurement of H_2O_2 was carried out first to demonstrate the feasibility of detecting FV and HbA_{1c}, through the measurement of H_2O_2. Amperometric study of H_2O_2 in the phosphate buffer solution (PBS) was carried out in the concentration range according to the physiological concentration of HbA_{1c} [8], in a 5ml of the test medium at ambient temperature. The amperometry was obtained at +0.25 V and -0.40V vs a Ag/AgCl reference electrode for 120s in order to minimize any potential interference[14].

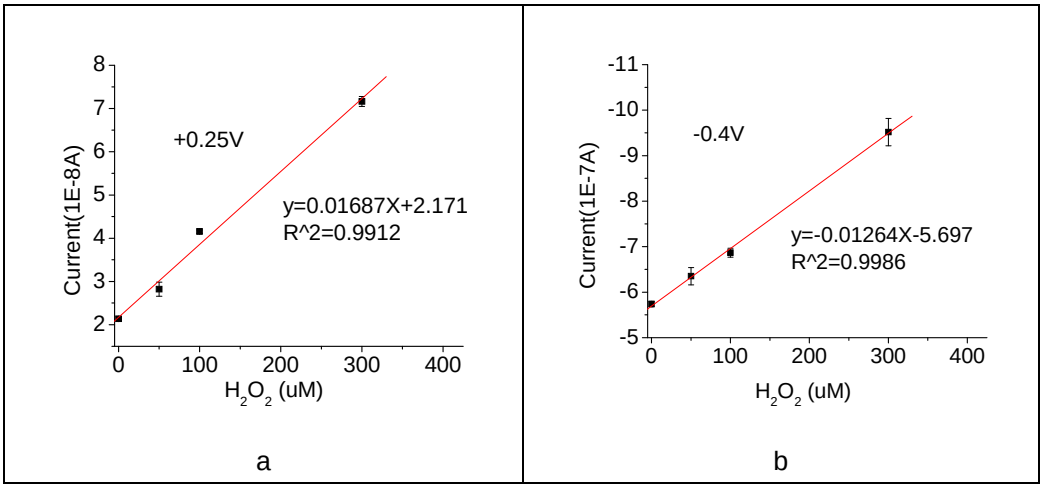

Figure 5. 1 The amperometry for H_2O_2 under ambient temperature, a) under oxidation mode at +0.25V, b) under reduction mode at -0.4V

Figure 5. 1 shows that the level of H_2O_2 could be quantified very well by this biosensor, in both oxidation mode and reduction mode at ambient temperature. This result formed the basis of future study on the development of biosensors for FV and HbA_{1c} detection.

The amperometric study of FV in the phosphate buffer solution (PBS) was carried out in a 3 µl of the test medium with the concentration range from 0 to 2 mM[8]. The amperometry was obtained at +0.25 V vs a Ag/AgCl reference electrode in order to compare the result with the previous study[7-9].

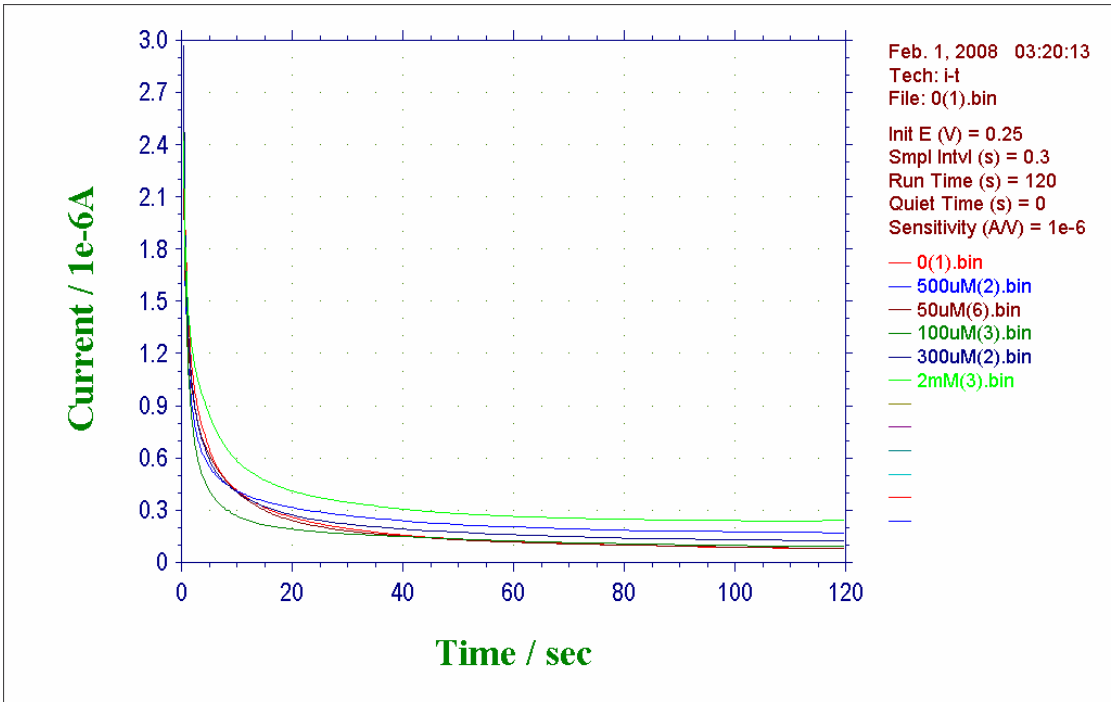

Figure 5. 2 The amperometry for FV

Figure 5. 2 shows the current in amperometry reached steady-state after 120s. This steady-state current increased with the concentration of FV. Consequently, the calibration curve could be established based on this result, as shown in **Figure 5. 3**.

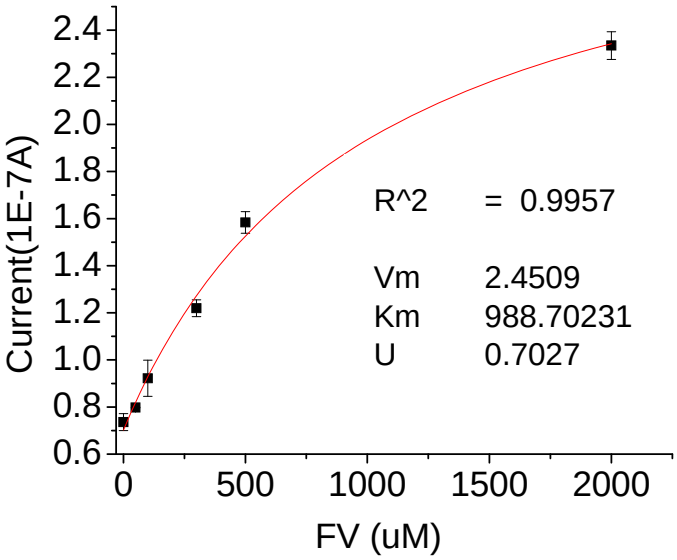

Figure 5. 3 The calibration curve for the FV biosensor

Figure 5. 3 shows the current output at 120s for each concentration of FV in the amperometry. The current values were fitted into the Michaelis-Menten equation since the detection of each FV was based on the enzymatic reaction (1). A factor U was added into the Michaelis-Menten equation to offset the current response at zero FV concentration. The correlation was very good for this model. The current value obtained below 1mM FV was plotted separately in **Figure 5. 4**.

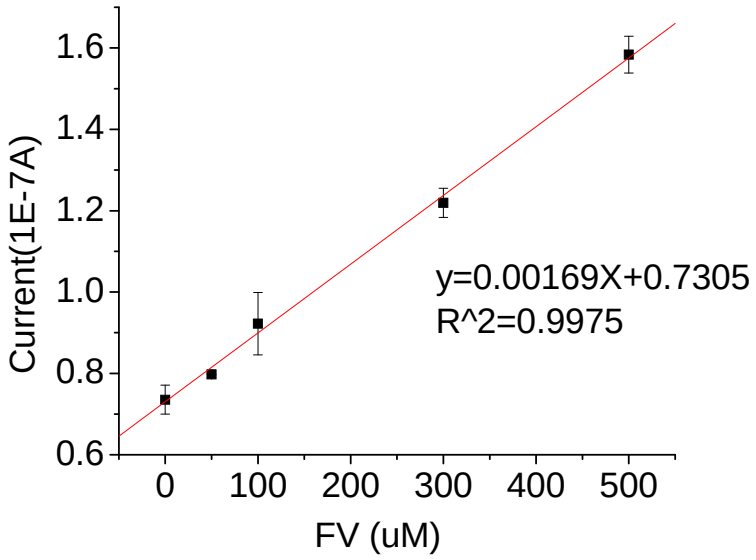

Figure 5. 4 The calibration curve for the FV biosensor at concentration below 1mM FV

Figure 5. 4 shows the amperometric output of this biosensor for the detection of FV in PBS. The current at each concentration of FV was fitted into a linear model. The sensitivity was 21.5 μA $mM^{-1}cm^{-2}$, several magnitudes higher than the value reported in the physiological range [7]. In addition, the operating potential in the study was lower than most of the similar research carried out previously. The linearity, sensitivity and reproducibility of this biosensor were excellent as shown. This biosensor for FV was demonstrated to be suitable for the basis of a practical HbA_{1c} electrochemical biosensor. The potential interference need to be assessed in the future study.

5.2.3 Conclusions

In summary, an iridium-modified biosensor prototype was fabricated using thick film screen printing technique. This single use, disposable biosensor was used for the detection of fructosyl valine, a model compound for the HbA_{1c} detection, using an

immobilized FAO enzyme on the biosensor working electrode. This detection was based on the measurement of H_2O_2 produced from the enzymatic reaction which was then used to quantify the analyte, FV, in the test medium. This biosensor operates at +0.25 V versus a Ag/AgCl reference electrode at an ambient temperature. The biosensor outputs demonstrated a Michaelis-Menten enzymatic mechanism overall, and the outputs of the biosensor were linear to the concentration of FV over the physiological range of importance. The electrochemical measurement showed that this biosensor prototype had a high sensitivity, a high linearity, and a high reproducibility and only required 3 µl of sample volume. This biosensor prototype could be used effectively as the basis for HbA_{1c} detection for diabetic patient management.

5.3 Glycoyslated Hemoglobin Biosensor

This study aimed to develop an electrochemical HbA_{1c} biosensor. In the previous effort, a FV biosensor had been developed and proved to be feasible for the quantification of FV concentration. The FV was the middle product from HbA_{1c} to H_2O_2 as shown in reaction (5.1). Therefore, an HbA_{1c} biosensor could potentially be developed, by combining the developed FV biosensor and the enzymatic reactions to produce FV from HbA_{1c}.

5.3.1 Experiment

5.3.1.1 Materials and Reagents

Enzyme Fructosyl-Amino Acid Oxidase (EC 1.5.3.x, FAO), α-chymotrypsin, and endoproteinase Glu-C were purchased from Sigma-Aldrich. Ir-Carbon particles (5%

Ir,) were purchased from E-TEK[SM]. Phosphate buffer (PBS) and potassium chloride were purchased from Fisher Chemicals. Polyethylenimine and 2-hydroxyethyl cellulose were purchased from Sigma-Aldrich. N-Cyclohexyl-2-aminoethane sulfonic acid (CHES), Triton X100, and Sodium dodecyl sulfate (SDS) were purchased from Sigma-Aldrich. The HbA_{1c} standard calibrators were purchased from Diazyme Laboratories, Poway, CA. The HbA_{1c} in whole blood sample from patients were purchased from ProMedDx, LLC, Norton, MA. All other chemical were of analytical grade and used as received. All solutions were prepared using de-ionized water.

5.3.1.2 Screen-printing of the thick-film sensor

The Ir-Carbon modified sensor prototype had the same configuration and fabrication procedures as described in section 2.2.1 in Chapter 2.

5.3.1.3 Fabrication of the enzyme HbA_{1c} biosensor

The iridium-modified electrochemical sensor structure described previously was then used as the basis for the construction of the enzymatic HbA_{1c} biosensor. The fabrication steps of this biosensor could be described as follows.

(a) Preparation of the ink for the blank sensor:

Blank sensors with working electrode modified by ink without enzymes were prepared and tested for comparison purpose. The ink for these sensors was prepared in the following manner. A 6.6 mg bovine serum albumin, 72.3 mg of α-chymotrypsin (83.9 units/mg) and 50µl 1.0M calcium chloride were added to 1ml of the ink prepared as described in step (a) in section 2.2.1 in Chapter 2. The calcium in the calcium chloride was used to activate the enzyme α-chymotrypsin and maintain the

activity of this enzyme. The mixing was completed when a clear homogeneous solution had been obtained.

(b) Preparation of the enzyme ink:

The enzyme ink was prepared based on the ink for blank sensors described previously. 0.5 ml of the ink from step (a) was mixed with 690 units of endoproteinase Glu-C, and 100 units of fructosyl-amino acid oxidase. Mixing of these components was carried out until a clear solution was obtained.

(c) Fabrication of the biosensor:

The enzyme ink from step (b) was then pipetted manually onto the Ir-Carbon working electrode of a sensor prototype, forming the working electrode of this biosensor. This biosensor was stored at 4ºC prior to electrochemical measurement.

5.3.1.4 Electrochemical characterization

The performance of the fabricated sensor prototypes was evaluated using electrochemical measurements, namely amperometry and chronoamperometry. The amperometric experiment was conducted using a CH Instrument 660B electrochemical workstation (CH Instrument, Inc, Austin, TX, USA). This experiment was performed using a test medium, which was prepared by mixing PBS, HbA_{1c}, and 0.03 M potassium chloride as supporting electrolyte to maintain the conductivity of this test medium. This test medium was adjusted to desired pH by adding potassium hydroxide. The temperature of the test was under ambient temperature. All potentials given in this research were referenced to the Ag/AgCl electrode. The working

potential for the amperometric experiments was fixed at +0.25 V or -0.4 V versus the reference electrode, and the time of recording was 60s or 120s in order to reach a steady-state. The chronoamperometric measurement was conducted using a CH Instrument 660B electrochemical workstation in a test medium also. The chronoamperometric experiment was carried out with two different values of working electrode potentials. First the working electrode potential of +0 V versus the reference electrode was applied for 60 seconds, allowing the reaction to precede and accumulation of the reaction product H_2O_2. Next the working electrode potential of +0.25 V versus the reference electrode was selected as the detection voltage of reaction product H_2O_2, and the time was set to be 60 seconds.

5.3.2 Results and discussion

5.3.2.1 Detection of HbA_{1c} in buffer solution and bovine serum, comparing the sensing voltage and the sample volume

A 1.575 ml test medium was prepared by mixing pH 7.0 PBS, 0.03 M potassium chloride, 0.05M calcium chloride as supporting electrolyte to maintain the conductivity of this test medium. Alternatively, a 1.0 ml test medium of 100% bovine serum was used in this test. No extra calcium chloride was added in the bovine serum, as approximately 1.2mM of calcium chloride already existed in bovine serum. Next, 8 mg of α-chymotrypsin(40 units/mg), 150 units of endoproteinase Glu-C, and 25 units of fructosyl-amino acid oxidase were added into the test medium(either PBS or bovine serum), to cleave HbA_{1c} and release H_2O_2. The PBS test medium was adjusted to the pH value of 8.0 by adding potassium hydroxide. Haemolysed HbA_{1c} (1.0 mg

with concentration of 2mg/mL) was then added into the testing medium gradually. The mixture was incubated at ambient temperature (approximately 24.0°C) for 5 minutes. The final solution was then tested by the Ir-C sensor under +0.25V and -0.4V amperometricly for 120 seconds in a beaker at the ambient temperature. Amperometric test at +0.25V for 60 seconds was also carried out using a 3µl sample volume on the Ir-C sensor surface.

The current responses in PBS and bovine serum under +0.25V and -0.4V vs the reference electrode were collected and presented.

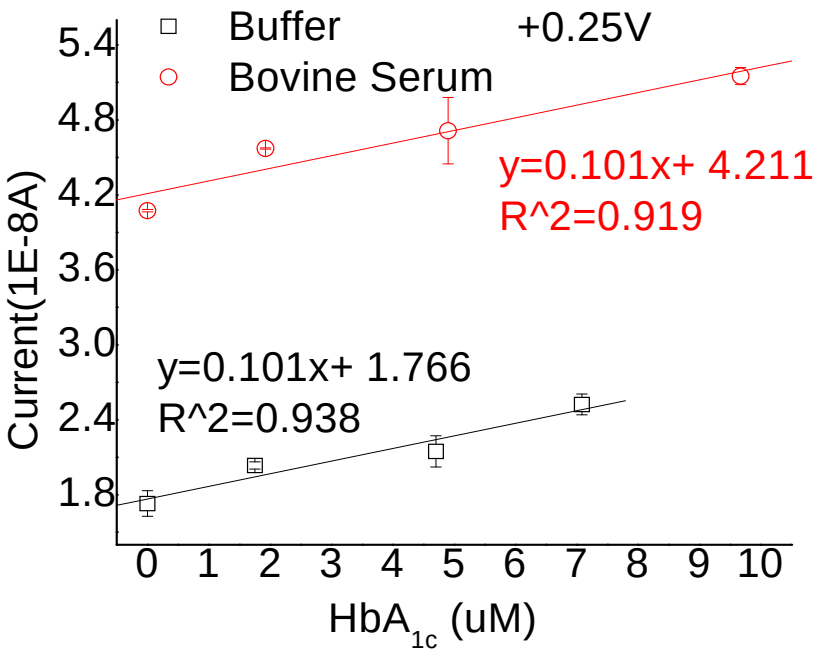

Figure 5. 5 Test of HbA_{1c} at +0.25V in PBS and bovine serum, under ambient temperature

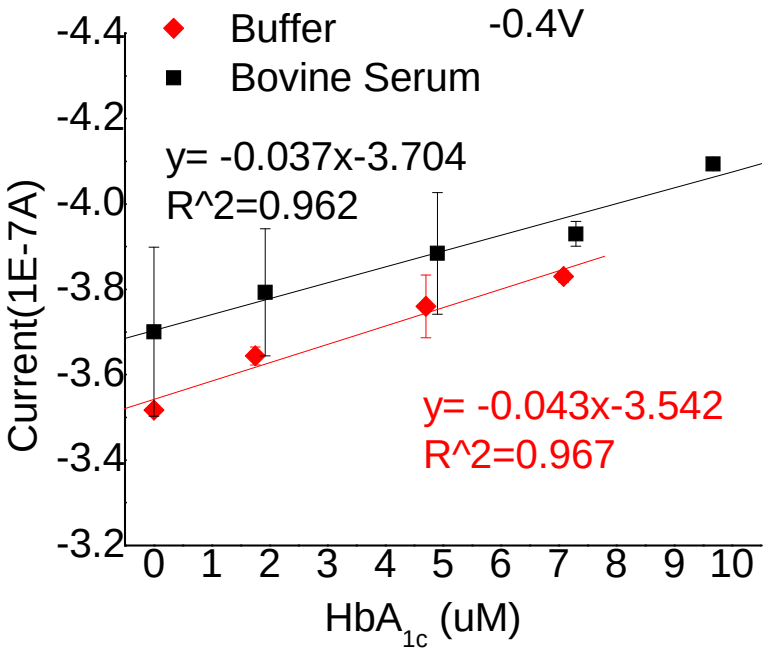

Figure 5. 6 Test of HbA_{1c} at -0.4V in PBS and bovine serum, under ambient temperature

It can be realized from that the results shown in **Figure 5. 5** and **Figure 5. 6** that HbA_{1c} could be quantified in both buffer solution and bovine serum, even at concentration much lower than the physiological range. The test of HbA_{1c} under both oxidation mode (+0.25V) and reduction mode (-0.4V) had good sensitivity and linearity. The quantification of HbA_{1c} in both buffer solution and undiluted bovine serum was feasible with similar sensitivities, in both oxidation mode and reduction mode. Due to the relatively large background current at reduction, oxidation mode (+0.25V) was then chosen for further study.

Furthermore, amperometric test at +0.25V for 60 seconds was carried out when reducing the sample volume to 3µl on the Ir-C sensor surface. The current responses

in the 3µl bovine serum testing sample were collected and assessed, together with the data obtained under similar conditions in PBS for comparison purposes.

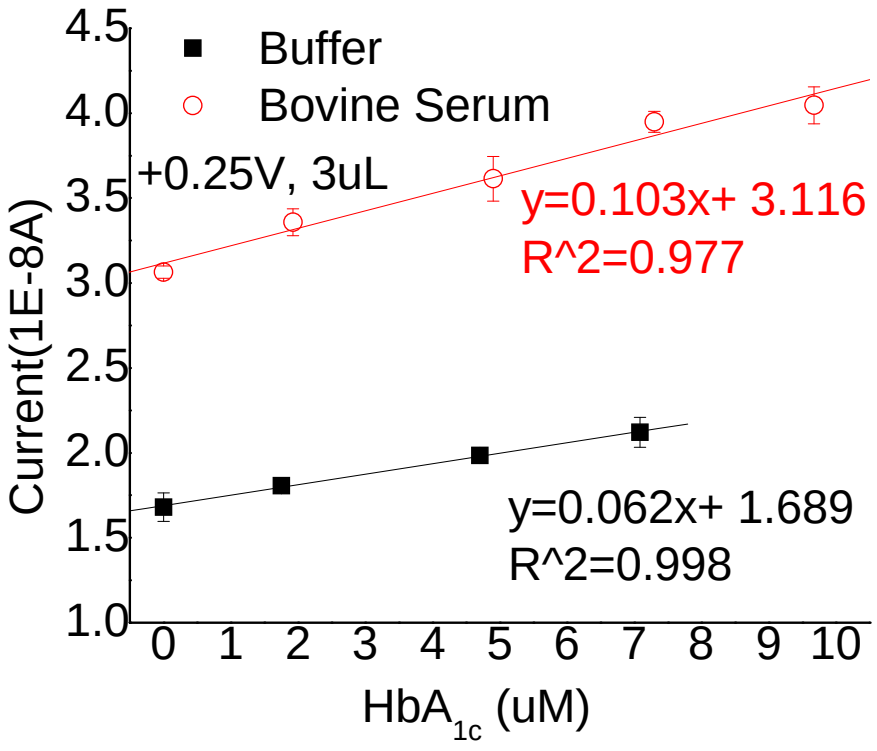

Figure 5. 7 Test of HbA_{1c} at +0.25V, use 3µl sample, under ambient temperature

Figure 5. 7 shows that use of a small sample volume, *i.e.,* 3µl, in the oxidation quantification mode of the amperometry did not decrease the sensitivity and linearity in the detection of HbA_{1c} in the bovine serum. Comparing with **Figure 5. 5**, the background current was smaller for the quantification in the bovine serum with a smaller sample volume. This study demonstrated that the electrochemical quantification of the level of HbA_{1c} in PBS and bovine serum, with a small sample size, *i.e.,* 3µl, would be practical.

5.3.2.2 Detection of HbA_{1c} with enzymes immobilized on sensor

In this research, the feasibility for the quantification of HbA_{1c} had been demonstrated with the enzymes dissolved in PBS and bovine serum, even using a very small sample volume. The HbA_{1c} was enzymatically cleaved resulting in the formation of H_2O_2 as show in reaction (5.1). In order to develop a practical reagent-free biosensor, the three enzymes involved were immobilized together on the surface of the working electrode in this study. This study further aimed to determine the feasibility of this immobilization approach for HbA_{1c} detection, verifying the efficacy of the co-immobilization of the enzymes onto a single electrode surface and providing guidance for the manufacturing feasibility for a single use, disposable HbA_{1c} biosensor.

5.3.2.2.1 Detection of HbA_{1c} with enzymes immobilized on sensor in buffer

This biosensor for HbA_{1c} detection was fabricated as described previously. Chronoamperometric measurement was carried out with this biosensor for HbA_{1c} in buffer solution. For comparison purpose, results from experiment carried out under identical conditions on the blank sensor were shown as well.

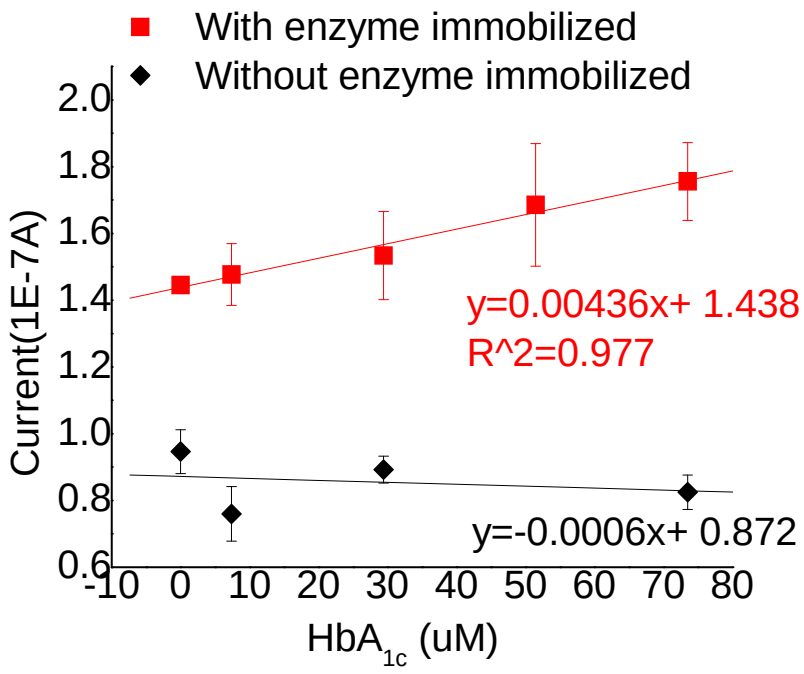

Figure 5. 8 Test of HbA_{1c} in 3µl sample, after 1 minute incubation at 0 V, and 1 minute at +0.25V, at ambient temperature with enzymes immobilized on sensor

Figure 5. 8 shows the calibration curve after a one-minute incubation time at 0V and a one-minute testing at +0.25V verse the Ag/AgCl reference electrode. The linearity of the calibration was very good. The electrochemical signal increased with respect to the concentration of HbA_{1c} on the biosensor with the enzymes immobilized in a manner described previously, while the signal did not increase on the blank sensor. Briefly stated, the results obtained demonstrated that the co-immobilization of the enzymes onto the iridium-modified disposable sensor could be used for HbA_{1c} detection. The tested HbA_{1c} concentration range was much lower than that for a physiological system indicating the actual sensitivity of this sensor for HbA_{1c} detection could be very good and very practical for diabetic management applications.

5.3.2.2.2 Detection of HbA_{1c} from standard calibrator in whole blood cell with enzymes immobilized on sensor

Two standard HbA_{1c} calibrators in the freeze-dried whole blood cell were purchased from Diazyme Laboratories, Poway, CA. These two calibrators were mixed with different ratios, in order to obtain samples with different HbA_{1c} value. These samples were then dissolved in the lysis buffer to release HbA_{1c} from the blood cells. The lysis buffer had 100 mM CHES, 1% Triton X100, and 0.45% SDS in 0.1M Tris-HCl buffer. A 3µl dissolved sample was then placed onto the working electrode with the immobilized enzymes. The chronoamperometric measurement was then carried out. The incubation time in this chronoamperometric measurement was chosen to be 1 minute at 0V, followed by a 1 minute testing at +0.25V for the reaction to reach a steady-state assessment.

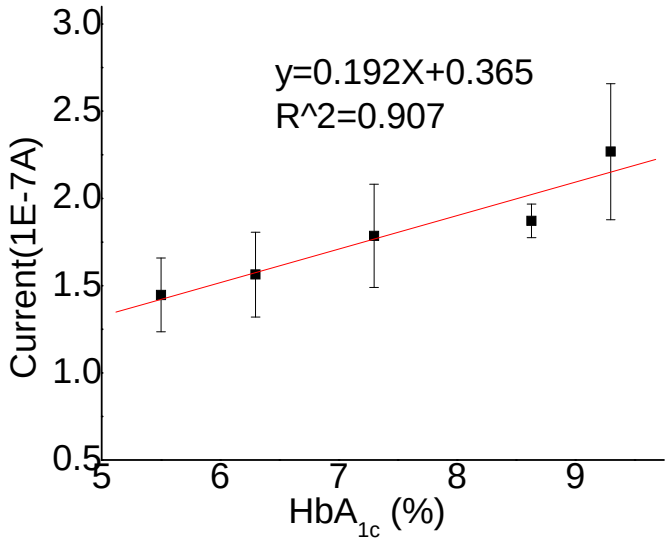

Figure 5. 9 Test of HbA_{1c} in 3µl sample, after 1 minute at 0V and 1 minute testing at +0.25V, under ambient temperature with enzymes immobilized on sensor

The linearity and sensitivity of the calibration for this HbA_{1c} biosensor were good, particularly at the 60 seconds recording time at +0.25V versus the Ag/AgCl reference electrode. The electrochemical measurement results were compared and correlated with the standard spectrometric measurement for identical calibrators[15] used in this electrochemical measurement.

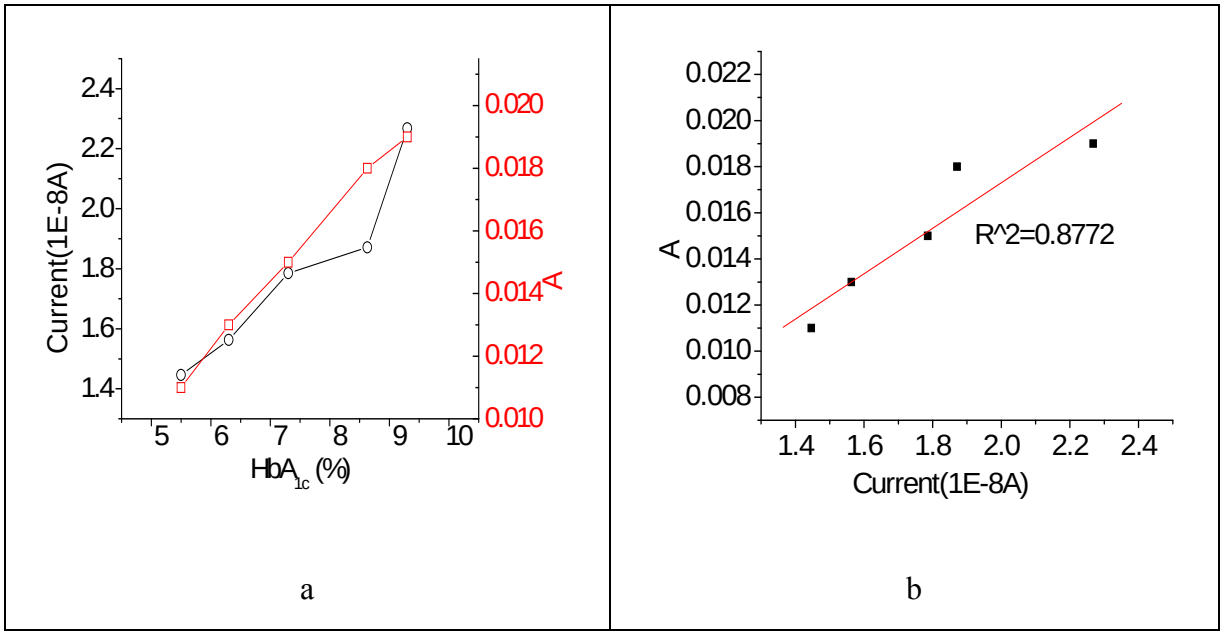

Figure 5. 10 Spectrometric measurement[15] of HbA_{1c} compared with the electrochemical measurements. a)Comparisation. b)Correlation between measurements

Figure 5. 10 shows that this electrochemical biosensor performed well for the HbA_{1c} detection using the spectrometric measurements as the basis for comparison. This result further validated the electrochemical measurement of HbA_{1c} with the immobilized enzymes and the electrochemical detection technique used in this research.

5.3.2.2.3 Detection of HbA_{1c} in whole blood sample from patients with enzymes and lysis agent immobilized on sensor

In order to obtain a practical reagent-free biosensor, the lysing process of HbA_{1c} needed to be integrated with the enzymatic cleavage of $HbA_{1c.}$ Therefore, the enzyme ink described previously was mixed with the lysis buffer. This mixture was then placed onto the Ir-Carbon working electrode of the sensor prototype using a micro-pipette forming the working electrode of this biosensor. This biosensor was stored at 4ºC prior to any electrochemical measurement. The whole blood samples from diabetic patients were purchased from ProMedDX, LLC, Norton, MA, and provided a distribution of HbA_{1c} from 4.9% to 13.6%. It should be noted that the level of HbA_{1c} was defined as the ratio between the glycosylated hemoglobin and the total hemoglobin[4]. Therefore, although the level of in the whole blood increased from 4.9% to 13.6%, the concentration of HbA_{1c} may not increase in the same manner. In order to release HbA_{1c} from the red blood cell and produce H_2O_2 in the presence of the enzymes, 1.5 minutes incubation time was selected in the chronoamperometric measurement.

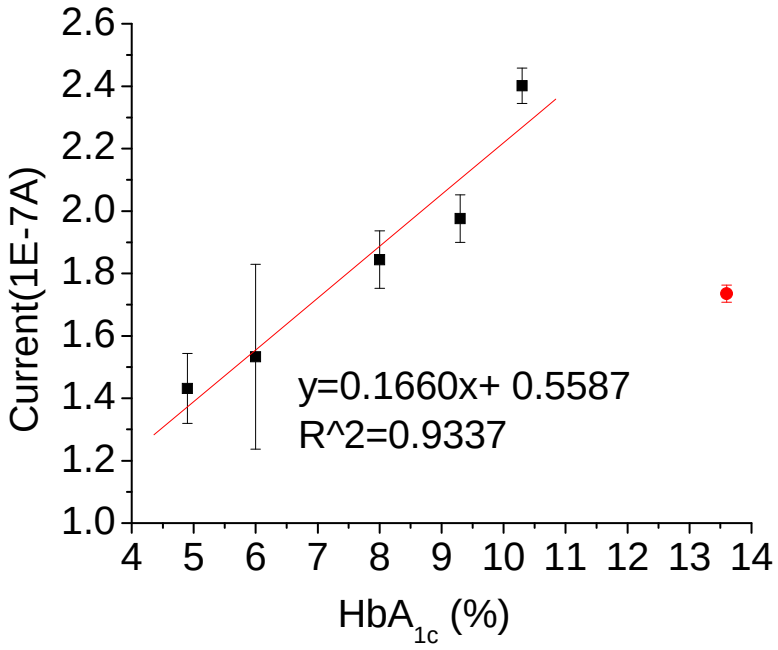

Figure 5. 11 Test of HbA_{1c} in 3µl sample, after 1.5 minutes incubation at 0V, and 1 minute testing at +0.25V, under ambient temperature with enzymes and lysis agent immobilized on sensor

Figure 5. 11 shows that HbA_{1c} in a 3µl sample from the patient's blood could be measured by this biosensor with the combination of the enzymes together with the lysis agent immobilized on the sensor working electrode. The linearity was good at the normal concentration range of HbA_{1c}. However, the electrochemical output decreased at very high concentration of HbA_{1c}. This could be due to the concentration variation of HbA_{1c} resulted from different total hemoglobin concentration from the individual blood sample. This could also be resulted from the dilution of the enzyme concentration after adding the lysis buffer in the enzyme ink, limiting the linear range of this biosensor. We believed that modifications on the enzyme loading could enhance further the performance of this biosensor.

5.3.3 Conclusions

In summary, an electrochemical reagent-free biosensor for the detection of HbA_{1c} was developed. Quantification of HbA_{1c} was carried out in buffer solution and whole blood samples from patient. The results obtained demonstrated that the co-immobilization of the enzymes and the lysis buffer onto the iridium-modified disposable sensor could be used practically for HbA_{1c} detection in whole blood cell from patients. This reagent-free electrochemical biosensor detected HbA_{1c} in the physiological range with practical sensitivity and good linearity. Further study would be carried out to assess the reproducibility, potential interference, to increase the linear range of this biosensor and to offset the variation of hemoglobin concentration.

Reference List

1. Goldstein DE, Little RR, Lorenz RA, Malone JI, Nathan D, Peterson CM, Sacks DB. Tests of glycemia in diabetes. Diabetes Care 2004; 27 (7):1761-1773

2. John WG. Haemoglobin A1c reference method. Scandinavian Journal Of Clinical And Laboratory Investigation 2006; 66 (1):1-4

3. Kilpatrick ES. HbA1c measurement. J Clin Pathol 2004; 57 (4):344-345

4. John WG. Haemoglobin A1c: analysis and standardisation. Clinical Chemistry And Laboratory Medicine: CCLM / FESCC 2003; 41 (9):1199-1212

5. Jeppsson JO. Approved IFCC Reference Method for the Measurement of HbA. Clinical Chemistry and Laboratory Medicine 2002; 40 (1):78

6. Nanjo Y, Hayashi R, Yao T. An enzymatic method for the rapid measurement of the hemoglobin A(1c) by a flow-injection system comprised of an electrochemical detector with a specific enzyme-reactor and a spectrophotometer. Analytica Chimica Acta 2007; 583 (1):45-54

7. Tsugawa W, Ishimura F, Ogawa K, Sode K. Development of an enzyme sensor utilizing a novel fructosyl amine oxidase from a marine yeast. Electrochemistry 2000; 68 (11):869-871

8. Ogawa K, Stollner D, Scheller F, Warsinke A, Ishimura F, Tsugawa W, Ferri S, Sode K. Development of a flow-injection analysis (FIA) enzyme sensor for fructosyl amine monitoring. Analytical and Bioanalytical Chemistry 2002; 373 (4-5):211-214

9. Sakaguchi A, Tsugawa W, Ferri S, Sode K. Development of highly-sensitive fructosyl-valine enzyme sensor employing recombinant fructosyl amine oxidase. Electrochemistry 2003; 71 (6):442-445

10. Sakurabayashi I, Watano T, Yonehara S, Ishimaru K, Hirai K, Komori T, Yagi M. New enzymatic assay for glycohemoglobin. Clin Chem 2003; 49 (2):269-274

11. Yonehara, Satoshi and Yagi, Yuji. Method of quantifying hemoglobin and method of measuring glycation ratio of hemoglobin. 9-14-2004. (GENERIC) US: Patent 6790665

12. Rajkumar R, Warsinke A, Mohwald H, Scheller FW, Katterle M. Development of fructosyl valine binding polymers by covalent imprinting. Biosensors & Bioelectronics 2007; 22 (12):3318-3325

13. Keil P, Mortensen HB, Christophersen C. Fructosylvaline. A simple model of the N-terminal residue of human haemoglobin A1c. Acta chemica Scandinavica.Series B: Organic chemistry and biochemistry 1985; 39 (3):191

14. Shen J, Dudik L, Liu CC. An iridium nanoparticles dispersed carbon based thick film electrochemical biosensor and its application for a single use, disposable glucose biosensor. Sensors and Actuators B: Chemical 2007; 125 (1):106-113

15. Yuan CS, Datta A, and Wang YP. Methods and compositions for determination of glycated proteins. 12-26-2008. (GENERIC)
US Patent 7153666

Chapter 6 Mathematical Modeling of Biosensor in Solution

6.1 Introduction

For an amperometric biosensor, the enzymatic reaction within the vicinity of the working electrode surface is related to the sensitivity and detection limit of a biosensor. Therefore, it will be meaningful and important to quantify the reaction rate in the vicinity of the working electrode surface of the biosensor and correlate the reaction rate with the biosensor performance. It is normally not possible to measure the concentrations of reactants or products in the vicinity of the electrode surface in solution with analytical methods, not to mention within the enzymatic ink layer immobilized onto the electrode surface as in our case. As a result, various mathematical models of amperometric biosensor have been developed [1, 2]. The mathematical models are important to study and optimize the sensing performance of a biosensor.

Therefore, the aim of this study was to develop a mathematical model to assess the reaction kinetics in the vicinity of the electrode surface in a buffer solution, to compare the mathematical model with the experimental results, and finally to apply this mathematical model for the biosensor construction. Specifically, the 3HB reaction in the presence of enzyme 3HBDH described in Chapter 2 and Chapter 3 would be studied.

6.2 Mathematical model, boundary conditions, initial conditions, parameters for the model, and simplified model

Mathematical model together with appropriate boundary conditions and initial conditions were described to simulate the enzymatic reaction, and the electrochemical detection. This model took the experimental arrangement into consideration with reasonable simplification. The parameters for this model were chosen based on the experiment condition and the experiment result.

6.2.1 Mathematical model

First the model was developed for the 3HB enzymatic reaction in the buffer test media containing 0.03M KCl as the supporting electrolyte in a beaker as shown in **Figure 6. 1**.

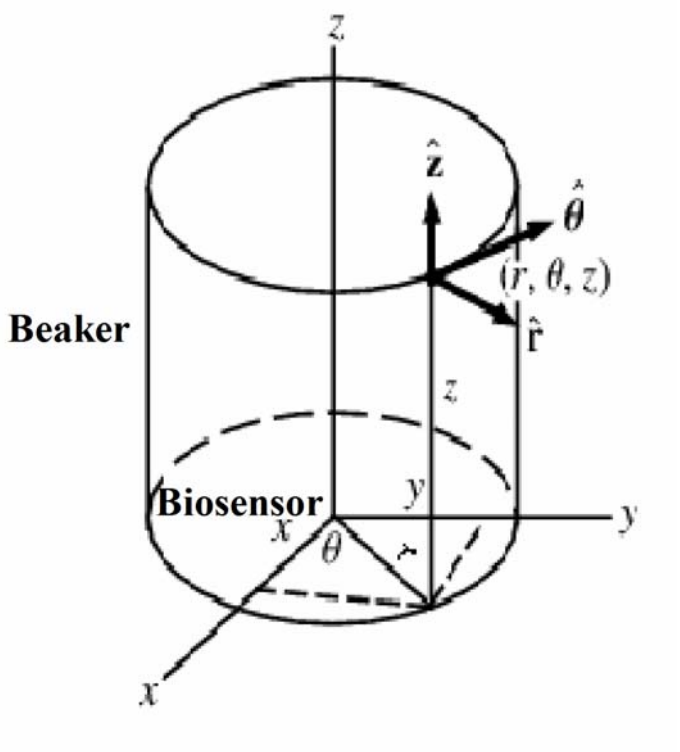

Figure 6. 1 Schematic illustration of the container for enzymatic reaction

The enzymatic reaction (2.1) was simplified to reaction (6.1), representing a single reactant enzymatic reaction. In this simplified reaction (6.1), substrate(S) 3HB reacted

to product (P) NADH in the presence of enzyme 3HBDH. The produced NADH was further quantified electrochemically by the iridium modified biosensor.

$$\text{3-hydroxybutyrate} + NAD^{+} \xrightarrow{\text{3HBDH}} AcAc + NADH + H^{+} \quad (2.1)$$

$$\text{Substract} \xrightarrow{\text{Enzyme}} \text{Product} \quad (6.1)$$

The enzymatic reaction (6.1) followed the Michaelis-Menten relationship as shown in equation (6.2), where the kinetics of substrate was determined by the Michaelis-Menten constants Vm(with unit mM/s) and Km(with unit mM).

$$\text{Michaelis-Menten: } ds/dt = -Vm * s/(Km + s) \quad (6.2)$$

Since one mole of substrate would produce one mole of product as shown in the stoichmetry in reaction (2.1), the kinetics of the product would just be the same as the substrate with opposite sign as shown in equation (6.3).

$$\text{Michaelis-Menten: } dp/dt = Vm * s/(Km + s) \quad (6.3)$$

Equation (6.2) and (6.3) described the enzymatic reaction of 3HB, producing NADH without spatial change. On the other hand, in a real electrochemical measurement of 3HB, the produced NADH would be detected and consumed on the surface of the working electrode with concentration change in space. Therefore, a reaction-diffusion model [3, 4]would be necessary to accurately simulate and predict this reaction followed by the electrochemical detection.

Cylindrical coordinates were selected based on the shape of the reaction container in **Figure 6. 1**. In a cylindrical coordination, both S and P were factors of t (time), z (height), r (radius), and θ (angular element). In this particular beaker and biosensor system, the biosensor was regarded as being positioned in the center of the beaker bottom and faced up in order to simplify the mathematics involved. As a result, when

setting position of the biosensor to be zero in both z and r, S and P should be symmetric with respect to z axis and not a function of θ anymore. Thus, the reaction-diffusion model was described mathematically in equation (6.4) and (6.5), two coupled partial differential equations. The D in equation (6.4) and (6.5) was diffusion coefficient (with unit cm^2/s).

$$\frac{\partial s}{\partial t} - D[\frac{\partial^2 s}{\partial z^2} + \frac{\partial^2 s}{\partial r^2} + \frac{1}{r}\frac{\partial s}{\partial r}] = -\frac{Vm * s}{Km + s} \tag{6.4}$$

$$\frac{\partial p}{\partial t} - D[\frac{\partial^2 p}{\partial z^2} + \frac{\partial^2 p}{\partial r^2} + \frac{1}{r}\frac{\partial p}{\partial r}] = +\frac{Vm * s}{Km + s} \tag{6.5}$$

6.2.2 Boundary conditions and initial conditions

The values of S and P before the reaction started were taken as the initial conditions (IC). In the IC shown in (6.6), the S had a fixed value and the P was zero before reaction took place.

$$IC : s(0, r, z) = s_0,\ p(0, r, z) = 0 \tag{6.6}$$

The boundary conditions (BC) at the upper surface (z1) and the outer radius (r1)of the solution containing S and P were easily defined since there were not material exchanges between the solution and the beaker, and evaporation was ignored in the relatively short time frame of the experiment.

At the bottom of the beaker (z=0), there was no material loss and gain for 3HB(S) but the produced NADH (P) would be detected and consumed on the surface of the working electrode. In fact, as suggested in **Figure 2.2**, the P would be zero at the detection voltage, +0.2 V vs Ag/AgCl reference electrode, constituting the BC.

In order to avoid singularity in equations (6.4) and (6.5), the inner radius was not set at zero but a very small number (r0), which was approximately zero. Since the concentration profile of S and P were both symmetric and continuous with respect to z axis(r=0), the flux of both S and P would be zero at the z axis and approximately zero at the inner radius(r=r0).

The BC was summarized and listed mathematically in equation (6.7).

$$
\begin{aligned}
&BC: \frac{\partial s}{\partial r} = 0(r = r0), \frac{\partial p}{\partial r} = 0(r = r0), \\
&\frac{\partial s}{\partial r} = 0(r = r1), \frac{\partial p}{\partial r} = 0(r = r1), \\
&\frac{\partial s}{\partial z} = 0(z = 0),\ p = 0(z = 0), \\
&\frac{\partial s}{\partial z} = 0(z = z1), \frac{\partial p}{\partial z} = 0(z = z1),
\end{aligned}
\tag{6.7}
$$

6.2.3 Parameters for this model

The values of the parameters for this model were decided based on the experimental arrangement and the experiment result. The Michaelis-Menten constants Km and Vm were chosen to be 1.853 mM and 0.4167 mM/s for equations (6.4) and (6.5). The value of Km was obtained from **Figure 2.5(C)** under the temperature of 37.5 ºC, which was in agreement with reported value [5, 6]. The Vm was calculated from the enzyme units presented in the reaction. The typical radius (r1) and height (z1) of 4ml solution in a cylindrical beaker were selected to be both at 1 centimeter. The diffusion coefficient was set at $1x10^{-5}$ cm^2/s, a typical value in aqueous solution. The initial concentration of S was between 0 to 10mM according to experiments carried out, and S was assumed to be uniform within the beaker after mixing.

6.2.4 Simplified model

After setting up all the mathematic equations, the boundary conditions, and the initial conditions, it was realized that the model could be further simplified from the two coupled partial differential equations. Especially for equation (6.4), it was further simplified to an ordinary differential equation due to the zero flux boundary conditions everywhere and the uniform concentration at the beginning. The reaction and concentration of S was exactly the same as the reaction in bulk reactor, which was normally described by an ordinary differential equation. Therefore, equation (6.4) was simplified to be equation (6.8), listed as follows together with the same IC and slightly modified BC.

$$\frac{\partial s}{\partial t} = -\frac{Vm * s}{Km + s} \tag{6.8}$$

$$\frac{\partial p}{\partial t} - D[\frac{\partial^2 p}{\partial z^2} + \frac{\partial^2 p}{\partial r^2} + \frac{1}{r}\frac{\partial p}{\partial r}] = +\frac{Vm * s}{Km + s} \tag{6.5}$$

$$IC : s(0, r, z) = s_0,\ p(0, r, z) = 0 \tag{6.6}$$

$$BC : \frac{\partial p}{\partial r} = 0(r = r0),$$
$$\frac{\partial p}{\partial r} = 0(r = r1),$$
$$p = 0(z = 0),$$
$$\frac{\partial p}{\partial z} = 0(z = z1), \tag{6.9}$$

The BC for the simplified model did not have terms related to S, since the ordinary differential equation could be solved with the IC alone.

6.3 Results and discussion

The reaction-diffusion model was solved in Mathematica 6®. The graphical results were generated to illustrate the concentration profile of the reaction substrate and product.

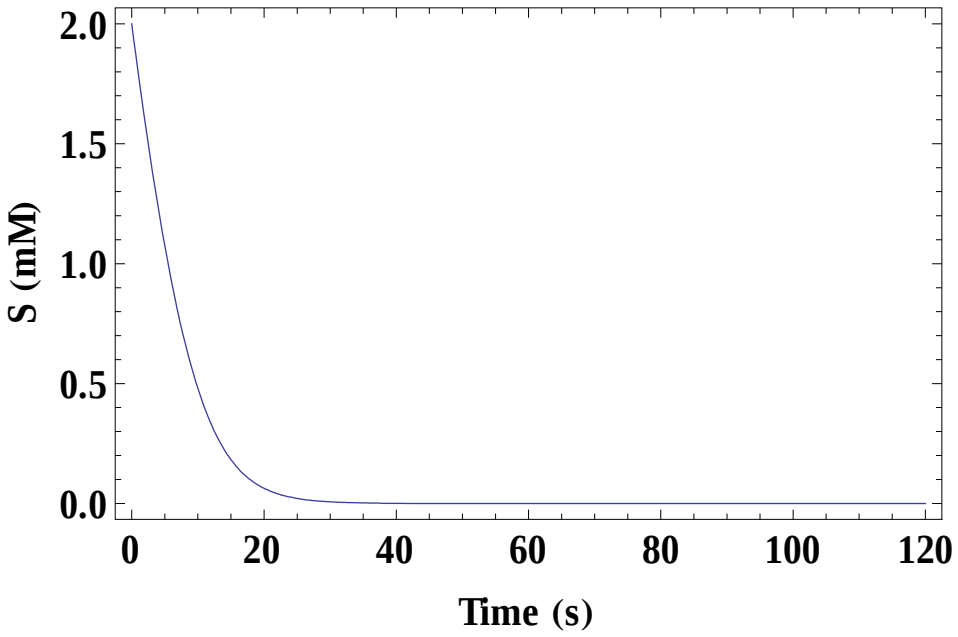

Figure 6. 2 Concentration of S versus time

Figure 6. 2 shows the concentration change of S with respect to time during the reaction. For a starting concentration of 2mM, the S decreased with time, representing the consumption of S during this reaction as shown in equation (6.8). Since S was the result of an ordinary differential equation, there was not any concentration change in space. Therefore, the concentration of S was uniform in the reaction beaker throughout the reaction, consistent with the assumption in classical reaction model in bulk reactor [7].

The concentration of P with respect to both time and space was also simulated. Since only the concentration change in the vicinity of biosensor surface affected the

electrical current measured, this simulation focused on the concentration profile within the radius of the biosensor working electrode.

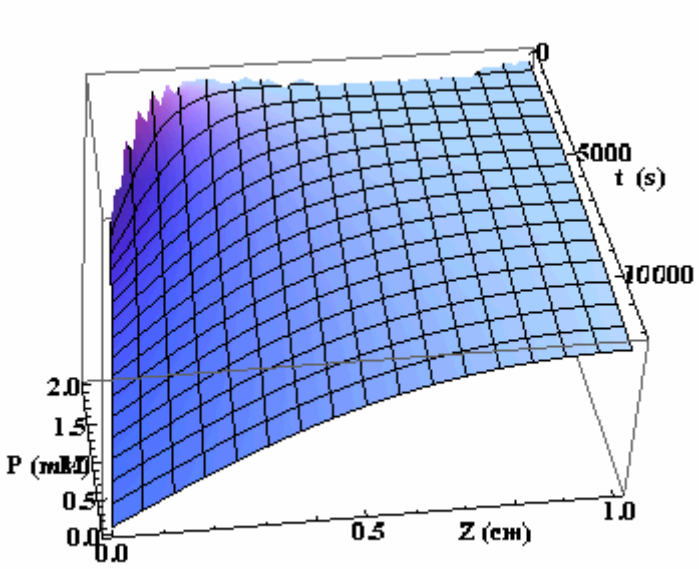

Figure 6. 3 The concentration of P versus height(z) and time(t), when r is at fixed value of 0.01cm

Figure 6. 3 shows that the concentration of P changed with both time and z as suggested in equation (6.5). At a fixed value of time, the P increased with the height, which could be explained since P was electrochemically measured and consumed at the bottom where the working electrode was placed. This concentration change of P gradually affected the top of the solution in reaction beaker with the time increased.

The concentration profiles for both S and P were simulated and demonstrated. The aim of this study was to associate the electrochemical measurement result with the simulation. Therefore, it was necessary to derive the electrochemical current from the concentration profile as shown in equation (6.10).

$$i = -nFDA\frac{dc}{dz} \qquad (6.10)$$

On the right side of the equation (6.10), the derivative of concentration profile was

multiplied by the diffusion coefficient (D) to produce the flux of material, the electrochemical current was derived by the material flux multiplied by the Faraday constant (F, 96500 coulomb/mol), the number of electron carried by one molecular of electrochemical active species (n, n=2 for NADH), and the surface area of the working electrode (A=0.007854 cm^2).

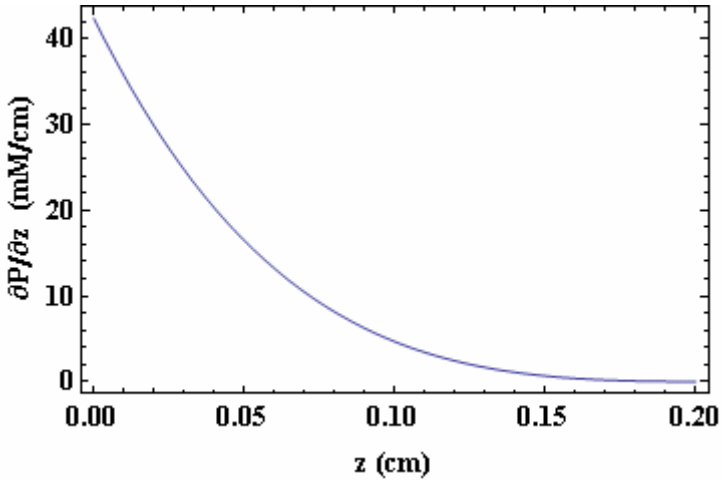

Figure 6. 4 Derivative of concentration profile for P versus height (z) after120 seconds

Figure 6. 4 shows the derivative of the simulated concentration profile for P versus height at the reaction time 120 seconds. The corresponding current was calculated by equation (6.10) based on the derivative at zero height (the surface of the working electrode of this biosensor) and the exact simulation and calculation procedure were repeated for other 3HB concentrations, *e.g*, from 0 to 10mM. The value of the derivative of concentration profile for P versus height after 120 seconds reaction and the calculated currents were listed as follows.

Table 6. 1 The calculated derivative of the concentration profile of P versus height (z) at z=0, and the corresponding currents for different concentration of 3HB

3HB(mM)	Current (μA)	dP/dz (mM/cm)
0	0	0
2	0.637	42
4	1.273	84
6	1.959	129
8	2.633	174
10	3.320	219

The calculated currents were further plotted as the follows based on the value in

Table 6. 1.

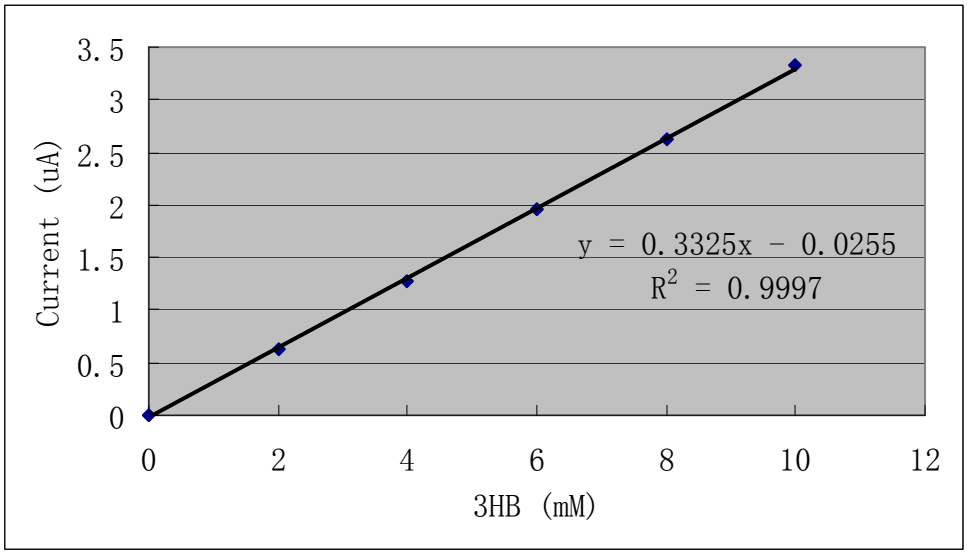

Figure 6. 5 The calculated currents versus the different concentrations of 3HB

Figure 6. 5 shows that the calculated currents for 3HB detection increased linearly with the concentration of 3HB. This linear increase model was inconsistent with the Michaelis-Menten model from experiment shown in **Figure 2.5**, and the calculated value was approximately 10 times bigger than the experiment result.

The difference between the experiment and simulation results could be due to that the concentration of S decreased to approximately 0 in this model as shown in **Figure 6. 2**.

On the other hand, a reversible chemical reaction should always reach an equilibrium [8] and the final concentration of S would be a value related to the initial concentration of the reactants and the equilibrium constant. Hence equation (6.3) and (6.4) were modified in order to consider the reaction equilibrium. The reaction equilibrium constant [8] could be shown in the following equation (6.11).

$$K_{equ}=[H^+]\,[AcAc]\,[NADH]/\,[3HB]\,[NAD^+] = 1.42 \times 10^{-9}\ M \qquad (6.11)$$

For each starting 3HB (S) concentration, the equilibrium concentration of NADH (P) could be calculated based on equation (6.11), the starting concentration of NAD^+ (7.6g/L = 11.46mM) and the value of pH(7.2). The calculated P and the ratio between S and P at equilibrium were listed in **Table 6. 2**.

Table 6. 2 The calculated value of P and the ratio between S and P at equilibrium

S(mM)	P(mM)	S/P
0	0	N/A
2	0.588	3.40
4	0.865	4.63
6	1.073	5.59
8	1.246	6.42
10	1.396	7.16

This ratio between S and P at equilibrium were used to modify the equation (6.2) and (6.3), ensuring that the reaction reached equilibrium finally.

$$\text{Modified Michaelis-Menten: } ds/dt = -\frac{Vm*(s - s/p \times p)}{Km + s} \qquad (6.12)$$

$$\text{Modified Michaelis-Menten: } dp/dt = +\frac{Vm*(s - s/p \times p)}{Km + s} \qquad (6.13)$$

As a result of equation (6.12) and (6.13), the reaction-diffusion model became the equations as follows.

$$\frac{\partial s}{\partial t} - D[\frac{\partial^2 s}{\partial z^2} + \frac{\partial^2 s}{\partial r^2} + \frac{1}{r}\frac{\partial s}{\partial r}] = -\frac{Vm*(s - s/p \times p)}{Km + s} \quad (6.14)$$

$$\frac{\partial p}{\partial t} - D[\frac{\partial^2 p}{\partial z^2} + \frac{\partial^2 p}{\partial r^2} + \frac{1}{r}\frac{\partial p}{\partial r}] = +\frac{Vm*(s - s/p \times p)}{Km + s} \quad (6.15)$$

The S/P shown in equation (6.14) and (6.15) was the ration between S and P from **Table 6. 2**. The amperometric currents for different S (3HB) could be simulated and derived in the exactly same manner based on equation (6.14) and (6.15), with the IC and BC shown in equation (6.6) and (6.7). The calculated derivative of concentration profile of P versus height and the electrochemical currents were listed a follows.

Table 6.3 The calculated derivative of the concentration profile of P versus height (z) at z=0, and the corresponding currents for different concentration of 3HB, after modify the model

3HB(mM)	Current(uA)	dP/dz(mM/cm)
0	0	0
2	0.197	13
4	0.318	21
6	0.409	27
8	0.485	32
10	0.553	37

The current shown in **Table 6.3** was plotted and compared with the model before modification and the experiment result.

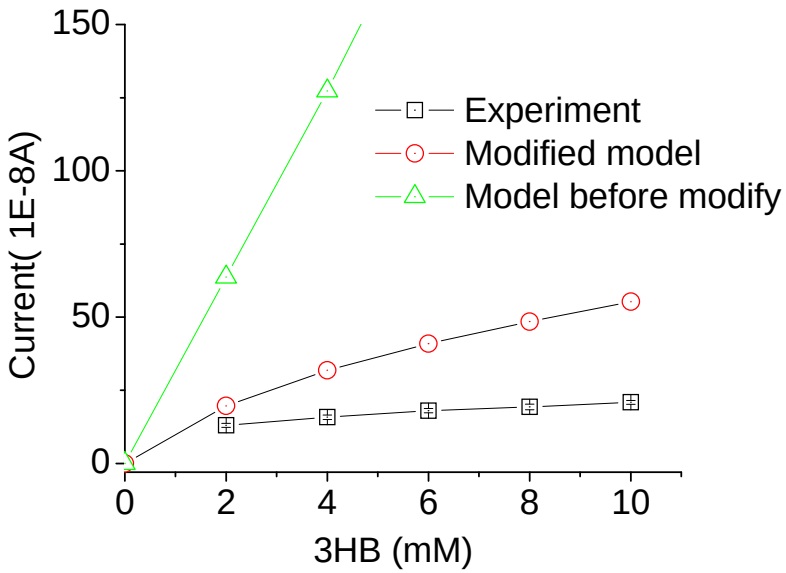

Figure 6. 6 Comparison between the model results before and after modification, and the experiment result

Figure 6. 6 shows that after modification, the model showed improved consistency with the experiment results. The amperometric currents in the model were in the same order of the currents from experiment. Further more, the amperometric currents in this modified model deviated from linear pattern and could be explained by the Michaelis-Menten relationship.

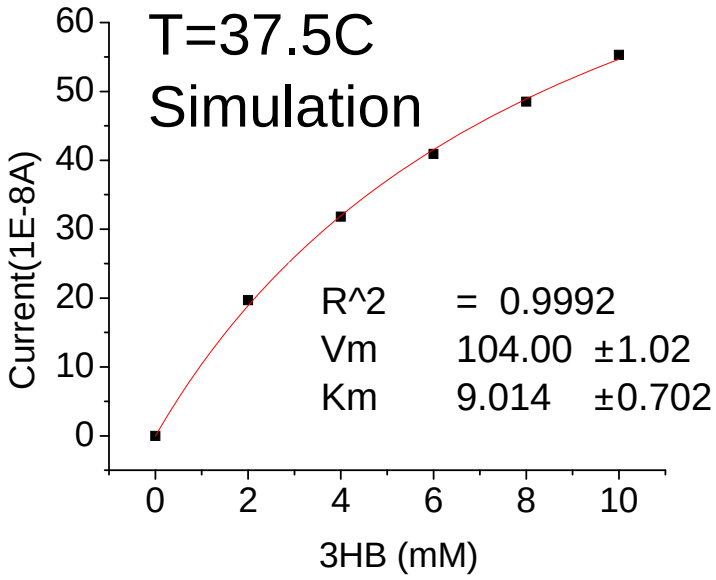

Figure 6. 7 Result from the modified model showing the current outputs followed the Michaelis-Menten relationship for different concentrations of 3HB

Figure 6. 7 shows that the currents from the modified model excellently followed the Michaelis-Menten relationship, a characteristic result for enzymatic reaction.

6.4 Conclusions

In summary, a diffusion-reaction model was developed for the electrochemical detection of 3HB in solution. After taking the reaction equilibrium into consideration, the model achieved good agreement with the experiment results. The result from the model could be explained by the Michaelis-Menten relationship, a typical relationship for an enzymatic reaction. This diffusion-reaction model could be easily applied in enzymatic reactions in addition to the 3HB reaction. Further effort would emphasize the modification of the model in order to offset the difference between the mathematical simulation and the experiment, as well as on the development of a

model for immobilized enzyme biosensor, and on the application of this model to optimize the biosensor composition and performance.

Reference List

1. Kukla AL, Shirshov YM. Computer simulation of transport processes in biosensor microreactors. Sensors and Actuators B-Chemical 1998; 48 (1-3):461-466

2. Neykov A, Georgiev T. Mathematical modelling of amperometric biosensor systems with non-linear enzyme kinetics. Chemical and Biochemical Engineering Quarterly 1998; 12 (2):73-79

3. Baronas R, Ivanauskas F, Ivanauskas F, Kulys J. The effect of diffusion limitations on the response of amperometric biosensors with substrate cyclic conversion. Journal of Mathematical Chemistry 2004; 35 (3):199-213

4. Vijayendran RA, Ligler FS, Leckband DE. A computational reaction-diffusion model for the analysis of transport-limited kinetics. Analytical Chemistry 1999; 71 (23):5405-5412

5. Feller C, Gunther R, Hofmann HJ, Grunow M. Molecular Basis of Substrate Recognition in D-3-Hydroxybutyrate Dehydrogenase from *Pseudomonas putida*. ChemBioChem 2006; 7 (9):1410-1418

6. Gjedde A, Crone C. Induction processes in blood-brain transfer of ketone bodies during starvation. American Journal of Physiology 1975; 229 (5):1165

7. Fogler H.S. Elements of Chemical Reaction Engineering, 4th Edition, 2005

8. Krebs HA, Mellanby J, Williamson DH. The equilibrium constant of the beta-hydroxybutyric-dehydrogenase system. Biochem.J. 1962; 82:96-98

Chapter 7 Conclusions and Recommendations for Future Work

The goal of this research was to apply thick-film screen printing technology to produce a single-use, disposable, cost-effective electrochemical biosensor prototype in large scale. Iridium nanoparticles supported by carbon were selected to modify the electrode of the biosensor for its excellent catalytic effect towards the commonly detected electrochemical active species, *i.e.*, hydrogen peroxide, nicotinamide adenine dinucleotide (Reduced Form, NADH), and nicotinamide adenine dinucleotide (Oxidized Form, NAD^+). Various analytes of clinical importance could then be quantified based on the detection of the hydrogen peroxide, NADH, or NAD^+, by selecting one or more enzymatic reactions to produce these detectable species from the analytes of interest. Therefore, the development of this electrochemical biosensor prototype could establish a platform technology for various analytes of biomedical or biological importance. This study focused on biosensing of the following analytes related to diabetes, *i.e.*, 3-hydroxybutyrate (3HB), fructosyl valine, HbA_{1c}. Therefore, by using this biosensor prototype to measure these analytes successfully, this platform technology could be applied in one of the most important area of biosensors, namely, diabetic patient management.

The first part of this study discussed the importance to develop an amperometric biosensor to detect 3HB for diabetic patient management. It was demonstrated that 3HB could be quantified by either dissolved 3HBDH in the PBS solution or by immobilized 3HBDH on the sensor prototype surface detecting 3HB in the PBS

solution and the bovine serum. The operating temperature for this biosensor was optimized to be 37.5ºC. The interferences from uric acid, NAD^+, and serum were tested. The interference from NAD^+ was insignificant. The serum decreased the overall sensitivity of this biosensor by possibly binding to the enzyme 3HBDH. The interferences from uric acid existed but the interference could be quantified by a separate sensor. As a result, the level of 3HB could be quantified in the presence of these potentially interferential species. Spectrometric measurements of NADH and 3HB were performed in both PBS and bovine serum test medium. The spectrometric measurement results of 3HB were compared with the electrochemical measurements of 3HB and these two measurements correlated very well. All the data were fitted into either linear model or Michaelis- Menten equation successfully, which was the typical model for an enzymatic biosensor.

After the detection of 3HB was proven to be feasible based on this platform technology, the element properties in this 3HB biosensor fabrication and the parameters in the electrochemical characterization had been assessed. Experiments had been carried out to evaluate the relationship between the biosensor's sensing performance and the element properties in the fabrication and the characterization parameters. The biosensor manufacturing process had been evaluated in terms of the enzyme ink composition, the enzyme ink stability and the quantity of ink for the biosensor. The biosensor characterization process had been evaluated as well, in terms of the measurement time and the testing sample volume. Consequently, the value for

the element properties in fabrication and the parameters in the characterization of the biosensor were determined based on the experiment results together with the requirements for practical applications. Finally, inkjet printing technique was applied for the enzyme ink deposition in order to assess the feasibility of mass-production of this biosensor. The biosensors from inkjet printing were characterized in both PBS and bovine serum. The interference from AcAc was also assessed to be significant, which would be addressed in the next part of this study.

In order to quantify the interference from AcAc on the 3HB detection, and to quantify the numerous analytes related to NAD^+, this biosensor prototype was used for the detection of NAD^+ in the reduction mode in both Tris-HCl buffer solution and 100% bovine serum. This biosensor operated at -0.4 versus the Ag/AgCl reference electrode. The biosensor outputs showed high sensitivity, high linearity, and high reproducibility at ambient temperature (approximately 25.5 ºC), elevated temperatures, namely, 30.0 ºC and 37.5 ºC. This biosensor was free from the potential interference of NADH, which demonstrated the feasibility of NAD^+ detection in the enzymatic reactions involving NADH/ NAD^+ redox couple.

In most of these NADH/ NAD^+ redox couple related enzymatic reactions, a biomarker would be involved. Consequently, this biosensor could potentially be applied to quantify a large number of biomarker based on NAD^+ detection, serving as a platform technology. This iridium-modified electrode could potentially be applied to NADH/ NAD^+ regeneration as well with its high catalytic ability. This iridium-modified

electrode could also be applied to quantify the interference from AcAc in the 3HB detection for diabetic patient management.

The measurement of HbA_{1c} was most important for the long-term control of the glycaemic state in diabetic patients as the HbA_{1c} level indicated the last 2-3 months glucose level. This biosensor prototype was used for the detection of both HbA_{1c}, and fructosyl valine(FV), a model compound for the HbA_{1c} detection.

In the development of the FV sensor, the FAO enzyme was immobilized on the biosensor working electrode. This detection was based on the measurement of H_2O_2 produced from the enzymatic reaction which was then used to quantify the analyte, FV, in the test medium. This biosensor operates at +0.25 V versus Ag/Ag Cl reference electrode at an ambient temperature. The biosensor outputs demonstrated a Michaelis-Menten enzymatic mechanism overall, and the outputs were linear over the physiological range of importance. The electrochemical measurement showed this biosensor prototype had a high sensitivity, a high linearity, and a high reproducibility and only required 3 µl of sample volume. This biosensor prototype could be used effectively as the basis for HbA_{1c} detection for diabetic patient management.

In this study, an electrochemical regent-free biosensor for the detection of HbA_{1c} was developed based on the FV biosensor. Quantification of HbA_{1c} was carried out in buffer solution at pH 7.0 and whole blood samples from patient. The results obtained demonstrated that the co-immobilization of the enzymes and the lysis buffer onto the

iridium-modified disposable sensor could be used for HbA_{1c} detection in whole blood cells from patients. This regent-free electrochemical biosensor detected HbA_{1c} in the physiological range with practical sensitivity and good linearity.

A diffusion-reaction model was developed for the electrochemical detection of 3HB in solution. Taking the reaction equilibrium into consideration, the model achieved good agreement with the experiment results. The result from the model could be explained by the Michaelis-Menten relationship, a typical relationship for an enzymatic reaction. This diffusion-reaction model could be easily applied in enzymatic reactions in addition to the 3HB reaction.

Based on the conclusion summarized above, we believed that additional and future studies should focus on the followings. For the 3HB biosensor, the long-term stability would be assessed. For the NAD^+ biosensor, future study would be carried out to demonstrate the application of NAD^+ detection for quantification of biomarkers of interest in bioreactor and biosensor applications. As of the HbA1c biosensor, future work would be needed to assess the reproducibility, potential interference, to increase the linear range of this biosensor and to offset the variation of hemoglobin concentration. For the mathematical modeling, future effort would emphasize on the modification of the model to offset the difference between simulation and experiment, as well as on the development of a model for immobilized enzyme biosensor, and apply this model to optimize the biosensor composition and performance.

Appendix A1

This appendix shows Mathematica 6 code for the simplified model discussed in Section 6.2.4.

```
Reaction diffusion in cylindrical coordinates
Parameters
km=1.853(*mM from experiment and reference*);
vm=0.4167(*m M/s from unit of enzyme 25units/ml*);
diff=.00001(*cm2/s*);
s0=2(*mM*);
r0=.0001(*cm,inner radius*);
r1=z1=1(*cm,outer radius*);
ODE for s
sx=NDSolve[{s'[t]==-vm*s[t]/(km+s[t]),s[0]    s0},s,{t,0,12000}]
Plot[Evaluate[s[t]/.sx],{t,0,50}]
{{s    InterpolatingFunction[{{0.,12000.}},<>]}}
```

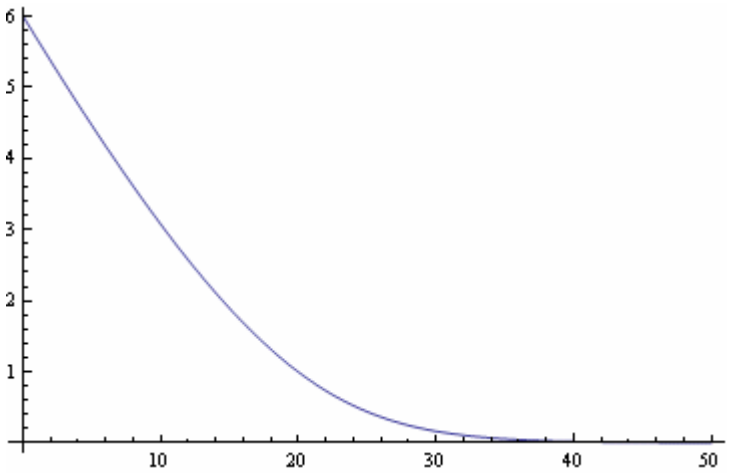


```
PDE for s
(*ODE for s*)
tf=12000;
sx=NDSolve[{s'[t]==-vm*s[t]/(km+s[t]),s[0]    s0},s,{t,0,tf}];
(*Solution function s[t]*)sf=s[t]/.sx[[1]];
Plot[sf,{t,0,tf/100},PlotRange All,Frame True, FrameLabel {"Time (s)","S (mM)"},BaseStyle {FontFamily "Times",FontSize 14,FontWeight Bold}]
```

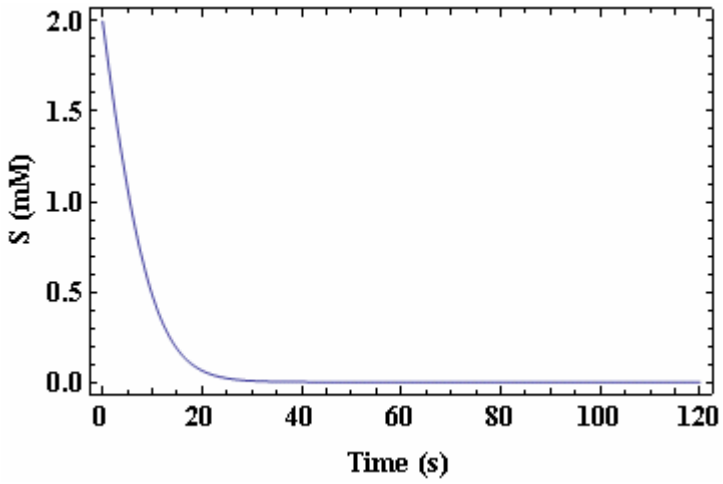

(*PDE for p*)pds:={D[p[t,r,z],t] diff*($\partial_{z,z}p[t, r, z]$ + $\partial_{r,r}p[t, r, z]$ +1/r $\partial_{r}p[t, r, z]$) +(vm*sf)/(km+sf)};

(*IC*)ICs:={p[0,r,z] 0}
(*BC*)BCs={Derivative[0,1,0][p][t,r0,z] Derivative[0,1,0][p][t,r1,z] 0,
p[t,r,0] 0,Derivative[0,0,1][p][t,r,z1] 0};
tf1=12000;
sos=NDSolve[Join[pds,ICs,BCs],p,{t,0,tf1},{r,r0,r1},{z,0,z1}];//Timing
{0.351,Null}
Plot3D[Evaluate[p[t,0.01,z]/.sos],{t,0,tf1},{z,0,z1},AxesLabel {" t (s)","
Z (cm)" , " P
(mM)"},BaseStyle {FontFamily "Times",FontSize 13,FontWeight Bold}]

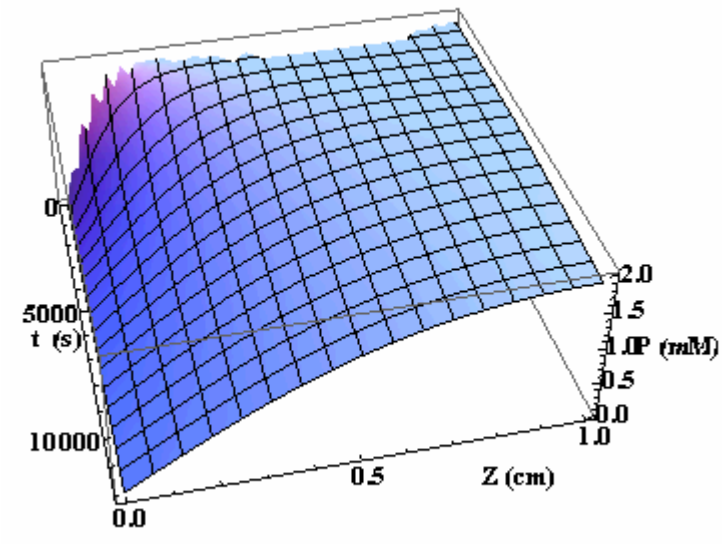

Plot3D[p[tf1,r,z]/.sos,{r,r0,r1},{z,0,z1},AxesLabel Automatic]

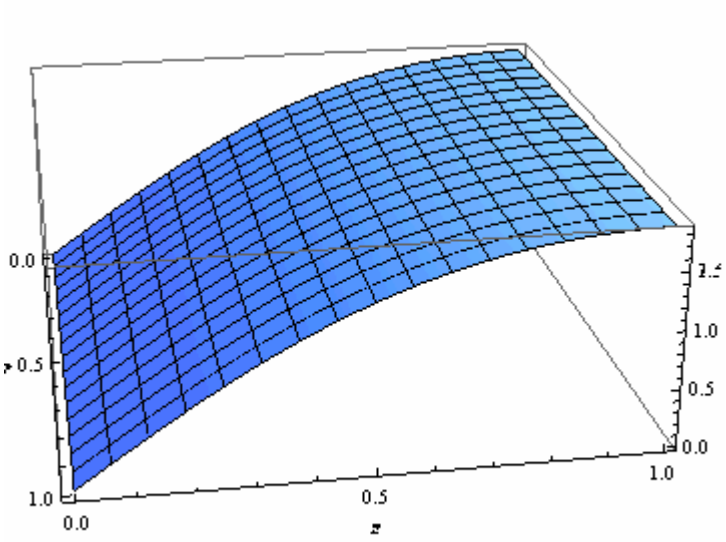

Plot[Evaluate[∂_t p[t, 0.05, 0.01] /.sos],{t,0,120},PlotRange All, Frame True, FrameLabel {"Time (s)","P (mM)"},BaseStyle {FontFamily "Times",FontSize 14,FontWeight Bold}]

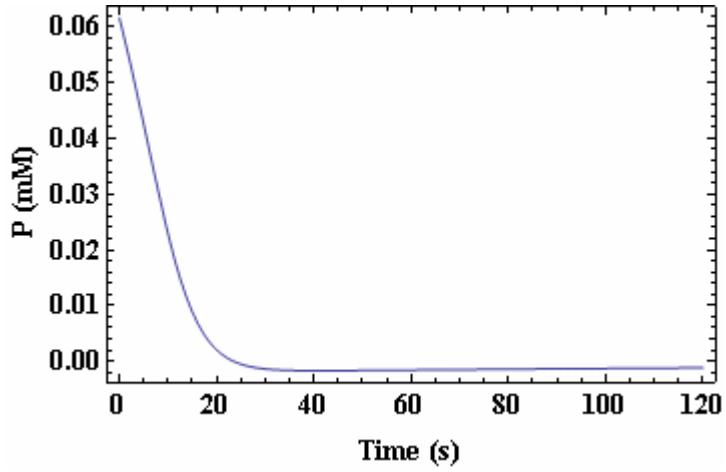

Plot[Evaluate[∂_z p[120, 0.05, z] /.sos],{z,0,0.2},PlotRange All,Frame True, FrameLabel {"z (cm)"," P/ z (mM/cm)"},BaseStyle {FontFamily "Times",FontSize 14,FontWeight Bold}]

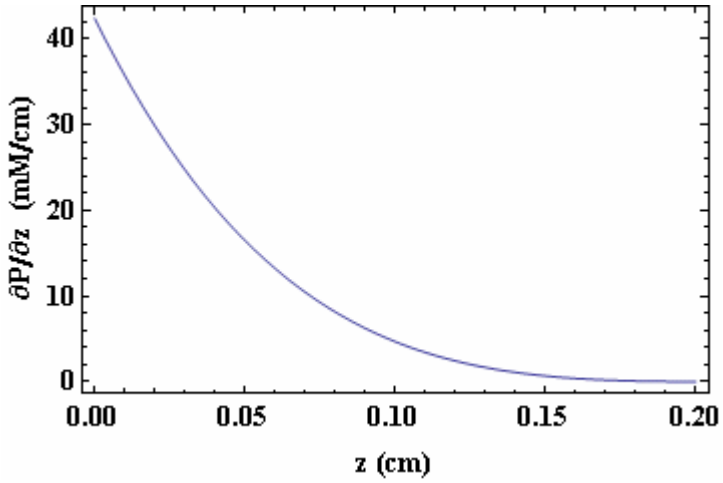
40
30
20
10
0
∂Pf/∂z (mM/cm)
0.00
0.05
0.10
0.15
0.20
z (cm)

Appendix A2

This appendix shows Mathematica 6 code for the modified model discussed in Section 6.3.

Reaction diffusion in cylindrical coordinates
Parameters
km=1.853(*mM from experiment and reference*);
vm=0.4167(*m M/s from unit of enzyme 25units/ml*);
diff=.00001(*cm2/s*);
s0=10(*mM*);
r0=.0001(*cm,inner radius*);
r1=z1=1(*cm,outer radius*);
Coupled PDE

(*PDE*)pde={D[s[t,r,z],t] diff ($\partial_{z,z}$s[t, r, z] + $\partial_{r,r}$s[t, r, z] +1/r ∂_{r}s[t, r, z])
-vm*(s[t,r,z]-7.163405949*p[t,r,z])/(km+s[t,r,z]),D[p[t,r,z],t] diff
($\partial_{z,z}$p[t, r, z] + $\partial_{r,r}$p[t, r, z] +1/r ∂_{r}p[t, r, z])
+vm*(s[t,r,z]-7.163405949*p[t,r,z])/(km+s[t,r,z])};
(*IC*)IC={s[0,r,z] s0,p[0,r,z] 0};
(*BC*)BC={Derivative[0,1,0][s][t,r0,z] 0,Derivative[0,1,0][p][t,r0,z] 0,
Derivative[0,1,0][s][t,r1,z] 0,Derivative[0,1,0][p][t,r1,z] 0,
Derivative[0,0,1][s][t,r,0] 0,p[t,r,0] 0,
Derivative[0,0,1][s][t,r,z1] 0,Derivative[0,0,1][p][t,r,z1] 0};
sol=NDSolve[Join[pde,IC,BC],{s,p},{t,0,120},{r,r0,r1},{z,0,z1}]
{{s InterpolatingFunction[{{0.,120.},{0.0001,1.},{0.,1.}},<>],p InterpolatingFun
ction[{{0.,120.},{0.0001,1.},{0.,1.}},<>]}}
Plot3D[Evaluate[p[120,r,z]/.sol],{r,r0,r1},{z,0,z1}]

Plot3D[Evaluate[s[t,0.01,z]/.sol],{t,0,20},{z,0,z1},AxesLabel {" t (s)","
Z (cm)" , " S
(mM)"},BaseStyle {FontFamily "Times",FontSize 13,FontWeight Bold}]

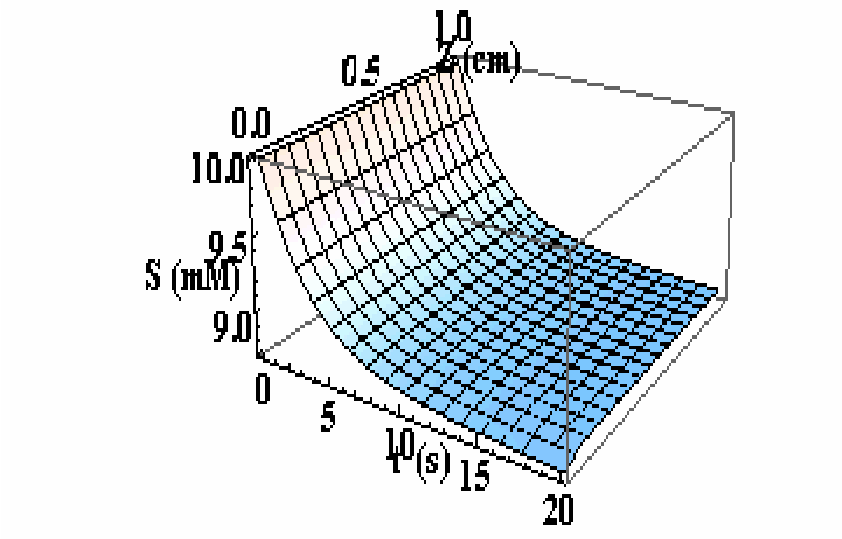

Plot[Evaluate[$\partial_z p[120, 0.05, z]$ /.sol],{z,0,0.1},PlotRange All, Frame True, FrameLabel {"Time (s)","P (mM)"},BaseStyle {FontFamily "Times",FontSize 14,FontWeight Bold}]

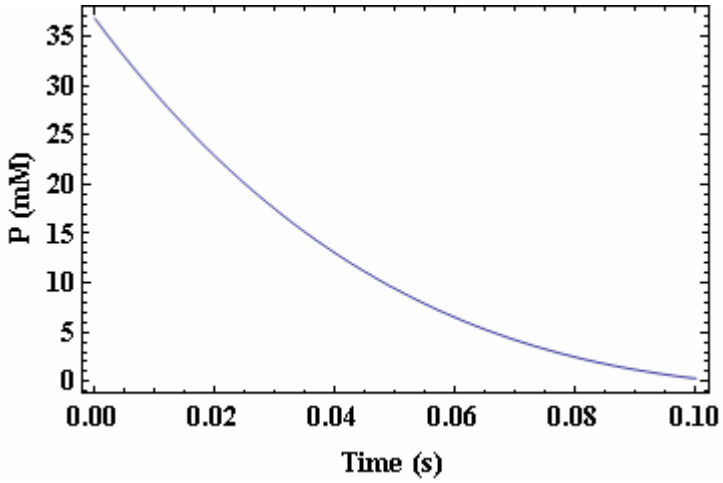

Bibliography

Avendano A, Deluna A, Olivera H, Valenzuela L, Gonzalez A. GDH3 encodes a glutamate dehydrogenase isozyme, a previously unrecognized route for glutamate biosynthesis in Saccharomyces cerevisiae. Journal of Bacteriology 1997; 179 (17):5594-5597

Azem A, Man F, Omanovic S. Direct regeneration of NADH on a ruthenium modified glassy carbon electrode. Journal of Molecular Catalysis A-Chemical 2004; 219 (2):283-299

Bais R. Clinical Chemistry: Principles, Procedures, Correlations, 5th ed. Michael L. Bishop, Edward P. Fody, and Larry Schoeff. Baltimore, MD: Lippincott Williams & Wilkins, 2005, 756 pp., $76.95, hardcover. ISBN 0-7817-4611-6. Clin Chem 2005; 51 (8):1567

Baronas R, Ivanauskas F, Ivanauskas F, Kulys J. The effect of diffusion limitations on the response of amperometric biosensors with substrate cyclic conversion. Journal of Mathematical Chemistry 2004; 35 (3):199-213

Bartlett ATM, White PJ. Species of Bacillus That Make A Vegetative Peptidoglycan Containing Lysine Lack Diaminopimelate Epimerase But Have Diaminopimelate Dehydrogenase. Journal of General Microbiology 1985; 131 (SEP):2145-2152

Boujtita M, Hart JP, Pittson R. Development of a disposable ethanol biosensor based on a chemically modified screen-printed electrode coated with alcohol oxidase for the analysis of beer. Biosensors & Bioelectronics 2000; 15 (5-6):257-263

Boujtita M, Hart JP, Pittson R. Development of a disposable ethanol biosensor based on a chemically modified screen-printed electrode coated with alcohol oxidase for the analysis of beer. Biosensors & Bioelectronics 2000; 15 (5-6):257-263

Byrne HA, Tieszen KL, Hollis S, Dornan TL, New JP. Evaluation of an electrochemical sensor for measuring blood ketones. Diabetes Care 2000; 23 (4):500-503

Charfen MA, Fernandez-Frackelton M. Diabetic Ketoacidosis. Emergency Medicine Clinics of North America 2005; 23 (3):609-628

Chen SM, Lin JL. The electrochemical properties of NADH and NAD(+) and their electrocatalytic reactions with tin hexachloroplatinate films. Journal of Electroanalytical Chemistry 2004; 571 (2):223-232

Chenault HK, Whitesides GM. Regeneration of Nicotinamide Cofactors for Use in Organic-Synthesis. Applied Biochemistry and Biotechnology 1987; 14 (2):147-197

Chiu RW, Ho CS, Tong SF, Ng KF, Lam CW. Evaluation of a new handheld biosensor for point-of-care testing of whole blood beta-hydroxybutyrate concentration. Hong Kong medical journal = Xianggang yi xue za zhi / Hong Kong Academy of Medicine 2002; 8 (3):172

Cho HJ, Parameswaran M, Yu HZ. Fabrication of microsensors using unmodified office in inkjet printers. Sensors and Actuators B-Chemical 2007; 123 (2):749-756

Clark LC, Lyons C. Electrode systems for continuous monitoring in cardiovascular surgery. Annals of the New York Academy of Sciences 1962; 102 (1):29-45

Connors MA, Barnsley EA. Naphthalene Plasmids in Pseudomonads. Journal of Bacteriology 1982; 149 (3):1096-1101

Coursin DB, Connery LE, Ketzler JT. Perioperative diabetic and hyperglycemic management issues. Critical Care Medicine 2004; 32 (4):S116-S125

Csako G. Causes, Consequences, and Recognition of False-Positive Reactions for Ketones. Clin Chem 1990; 36 (7):1388-1389

Culbertson CW, Zehnder AJB, Oremland RS. Anaerobic Oxidation of Acetylene by Estuarine Sediments and Enrichment Cultures. Applied and Environmental Microbiology 1981; 41 (2):396-403

D'Orazio P. Biosensors in clinical chemistry. Clinica Chimica Acta 2003; 334 (1-2):41-69

Diamond D. Progress in Sensor Array Research. Electroanalysis 1993; 5 (9-10):795-802

Fang L, Wang SH, Liu CC. An electrochemical biosensor of the ketone 3-[beta]-hydroxybutyrate for potential diabetic patient management. Sensors and Actuators B: Chemical 2008; 129 (2):818-825

Feller C, Gunther R, Hofmann HJ, Grunow M. Molecular Basis of Substrate Recognition in D-3-Hydroxybutyrate Dehydrogenase from *Pseudomonas putida*. ChemBioChem 2006; 7 (9):1410-1418

Filonov AE, Akhmetov LI, Puntus IF, Esikova TZ, Gafarov AB, Izmalkova TY, Sokolov SL, Kosheleva IA, Boronin AM. The construction and monitoring of genetically tagged, plasmid-containing, naphthalene-degrading strains in soil. Microbiology 2005; 74 (4):453-458

Fogler H.S. Elements of Chemical Reaction Engineering, 4th Edition, 2005

Forrow NJ, Sanghera GS, Walters SJ, Watkin JL. Development of a commercial amperometric biosensor electrode for the ketone D-3-hydroxybutyrate. Biosensors & Bioelectronics 2005; 20 (8):1617-1625

Gjedde A, Crone C. Induction processes in blood-brain transfer of ketone bodies during starvation. American Journal of Physiology 1975; 229 (5):1165

Goldstein DE, Little RR, Lorenz RA, Malone JI, Nathan D, Peterson CM, Sacks DB. Tests of glycemia in diabetes. Diabetes Care 2004; 27 (7):1761-1773

Hahn CEW. Electrochemical analysis of clinical blood-gases, gases and vapours. Analyst 1998; 123 (6):57R-86R

He PA, Xu Y, Fang YZ. A review: Electrochemical DNA biosensors for sequence recognition. Analytical Letters 2005; 38 (15):2597-2623

Hetzel M, Brock M, Selmer T, Pierik AJ, Golding BT, Buckel W. Acryloyl-CoA reductase from Clostridium propionicumi - An enzyme complex of propionyl-CoA dehydrogenase and electron-transferring flavoprotein. European Journal of Biochemistry 2003; 270 (5):902-910

Heule M, Vuillemin S, Gauckler LJ. Powder-based ceramic meso- and microscale fabrication processes. Advanced Materials 2003; 15 (15):1237-1245

Jeppsson. Approved IFCC Reference Method for the Measurement of HbA. Clinical Chemistry and Laboratory Medicine 2002; 40 (1):78

John WG. Haemoglobin A1c reference method. Scandinavian Journal Of Clinical And Laboratory Investigation 2006; 66 (1):1-4

John WG. Haemoglobin A1c: analysis and standardisation. Clinical Chemistry And Laboratory Medicine: CCLM / FESCC 2003; 41 (9):1199-1212

Junior LR, Neto GD, Fernandes JR, Kubota LT. Determination of salicylate in blood serum using an amperometric biosensor based on salicylate hydroxylase immobilized in a polypyrrole-glutaraldehyde matrix. Talanta 2000; 51 (3):547-557

Keil P, Mortensen HB, Christophersen C. Fructosylvaline. A simple model of the N-terminal residue of human haemoglobin A1c. Acta chemica Scandinavica.Series B: Organic chemistry and biochemistry 1985; 39 (3):191

Khan ASA, Talbot JA, Tieszen KL, Gardener EA, Gibson JM, New JP. Evaluation of a bedside blood ketone sensor: the effects of acidosis, hyperglycaemia and acetoacetate on sensor performance. Diabetic Medicine 2004; 21 (7):782-785

Kiba N, Inoue Y, Tachibana M, Tani K, Koizumi H. Simultaneous determination of D-glucose and 3-hydroxybutyrate by chemiluminescence detection with immobilized enzymes in a flow injection system. Analytical Sciences 2003; 19 (8):1203-1206

Kilpatrick ES. HbA1c measurement. J Clin Pathol 2004; 57 (4):344-345

Kimura M, Kobayashi K, Matsuoka A, Hayashi K, Kimura Y. Head-space gas-chromatographic determination of 3-hydroxybutyrate in plasma after enzymic reactions, and the relationship among the three ketone bodies. Clin Chem 1985; 31 (4):596-598

Koschinsky T, Heinemann L. Sensors for glucose monitoring: technical and clinical aspects. Diabetes-Metabolism Research and Reviews 2001; 17 (2):113-123

Krebs HA, Mellanby J, Williamson DH. The equilibrium constant of the beta-hydroxybutyric-dehydrogenase system. Biochem.J. 1962; 82:96-98

Kukla AL, Shirshov YM. Computer simulation of transport processes in biosensor microreactors. Sensors and Actuators B-Chemical 1998; 48 (1-3):461-466

Kwan RCH, Hon PYT, Mak WC, Law LY, Hu J, Renneberg R. Biosensor for rapid determination of 3-hydroxybutyrate using bienzyme system. Biosensors & Bioelectronics 2006; 21 (7):1101-1106

Laffel L. Ketone bodies: a review of physiology, pathophysiology and application of monitoring to diabetes. Diabetes/Metabolism Research and Reviews 1999; 15 (6):412-426

Leech D, Daigle F. Optimisation of a reagentless laccase electrode for the detection of the inhibitor azide. Analyst 1998; 123 (10):1971-1974

Levitt NS, Bradshaw D, Zwarenstein MF, Bawa AA, Maphumolo S. Audit of public sector primary diabetes care in Cape Town, South Africa: High prevalence of complications, uncontrolled hyperglycaemia, and hypertension. Diabetic Medicine 1997; 14 (12):1073-1077

Li CM, Dong H, Cao XD, Luong JHT, Zhang XJ. Implantable electrochemical sensors for biomedical and clinical applications: Progress, problems, and future possibilities. Current Medicinal Chemistry 2007; 14 (8):937-951

Li G, Ma NZ, Wang Y. A new handheld biosensor for monitoring blood ketones. Sensors and Actuators B-Chemical 2005; 109 (2):285-290

Lim DV, Simpson JM, Kearns EA, Kramer MF. Current and developing technologies for monitoring agents of bioterrorism and biowarfare. Clinical Microbiology Reviews 2005; 18 (4):583-+

Lin JH, Ju HX. Electrochemical and chemiluminescent immunosensors for tumor markers. Biosensors & Bioelectronics 2005; 20 (8):1461-1470

Maaheimo H, Fiaux J, Cakar ZP, Bailey JE, Sauer U, Szyperski T. Central carbon metabolism of Saccharomyces cerevisiae explored by biosynthetic fractional C-13 labeling of common amino acids. European Journal of Biochemistry 2001; 268 (8):2464-2479

Macleod KM, Gold AE, Frier BM. Frequency, Severity and Symptomatology of Hypoglycemia - A Comparative Trial of Human and Porcine Insulins in Type-1 Diabetic-Patients. Diabetic Medicine 1995; 12 (2):134-141

Malhotra BD, Chaubey A. Biosensors for clinical diagnostics industry. Sensors and Actuators B-Chemical 2003; 91 (1-3):117-127

Man F, Omanovic S. A kinetic study of NAD(+) reduction on a ruthenium modified glassy carbon electrode. Journal of Electroanalytical Chemistry 2004; 568 (1-2):301-313

Marc J.Madou. Fundamentals of Microfabrication: The Science of Miniaturization, 2002

Marzouk SAM, Ashraf SS, Al Tayyari KA. Prototype amperometric biosensor for sialic acid determination. Analytical Chemistry 2007; 79 (4):1668-1674

Mehrvar M, Abdi M. Recent developments, characteristics, and potential applications of electrochemical biosensors. Analytical Sciences 2004; 20 (8):1113-1126

Moiroux J, Deycard S, Malinski T. Electrochemical Reduction of Nad+ and Pyridinium Cations Adsorbed at the Mercury Water Interface - Electrochemical-Behavior of Adsorbed Pyridinyl Radicals. Journal of Electroanalytical Chemistry 1985; 194 (1):99-108

Morrin A, Wilbeer F, Ngamna O, Moulton SE, Killard AJ, Wallace GG, Smyth MR. Novel biosensor fabrication methodology based on processable conducting polyaniline nanoparticles. Electrochemistry Communications 2005; 7 (3):317-322

Murphy L. Biosensors and bioelectrochemistry. Current Opinion in Chemical Biology 2006; 10 (2):177-184

Nanjo Y, Hayashi R, Yao T. An enzymatic method for the rapid measurement of the hemoglobin A(1c) by a flow-injection system comprised of an electrochemical detector with a specific enzyme-reactor and a spectrophotometer. Analytica Chimica Acta 2007; 583 (1):45-54

Newman JD, Turner APF, Marrazza G. Ink-Jet Printing for the Fabrication of Amperometric Glucose Biosensors. Analytica Chimica Acta 1992; 262 (1):13-17

Newman JD, White SF, Tothill IE, Turner APF. Catalytic Materials, Membranes, and Fabrication Technologies Suitable for the Construction of Amperometric Biosensors. Analytical Chemistry 1995; 67 (24):4594-4599

Neykov A, Georgiev T. Mathematical modelling of amperometric biosensor systems with non-linear enzyme kinetics. Chemical and Biochemical Engineering Quarterly 1998; 12 (2):73-79

Odenthal KJ, Gooding JJ. An introduction to electrochemical DNA biosensors. Analyst 2007; 132 (7):603-610

Ogawa K, Stollner D, Scheller F, Warsinke A, Ishimura F, Tsugawa W, Ferri S, Sode K. Development of a flow-injection analysis (FIA) enzyme sensor for fructosyl amine monitoring. Analytical and Bioanalytical Chemistry 2002; 373 (4-5):211-214

Pandey PC, Upadhyay S, Pathak HC. A new glucose sensor based on encapsulated glucose oxidase within organically modified sol-gel glass. Sensors and Actuators B-Chemical 1999; 60 (2-3):83-89

Plegge V, Slama M, Suselbeck B, Wienke D, Spener F, Knoll M, Zaborosch C. Analysis of ternary mixtures with a single dynamic microbial sensor and chemometrics using a nonlinear multivariate calibration. Analytical Chemistry 2000; 72 (13):2937-2942

Rahni MAN, Guilbault GG, Deoliveira GN. Immobilized Enzyme Electrode for the Determination of Salicylate in Blood-Serum. Analytica Chimica Acta 1986; 181:219-225

Rajkumar R, Warsinke A, Mohwald H, Scheller FW, Katterle M. Development of fructosyl valine binding polymers by covalent imprinting. Biosensors & Bioelectronics 2007; 22 (12):3318-3325

Rivas GA, Pedano ML, Ferreyra NF. Electrochemical biosensors for sequence-specific DNA detection. Analytical Letters 2005; 38 (15):2653-2703

Sakaguchi A, Tsugawa W, Ferri S, Sode K. Development of highly-sensitive fructosyl-valine enzyme sensor employing recombinant fructosyl amine oxidase. Electrochemistry 2003; 71 (6):442-445

Sakurabayashi I, Watano T, Yonehara S, Ishimaru K, Hirai K, Komori T, Yagi M. New enzymatic assay for glycohemoglobin. Clin Chem 2003; 49 (2):269-274

Scherf U, Sohling B, Gottschalk G, Linder D, Buckel W. Succinate-Ethanol Fermentation in Clostridium-Kluyveri - Purification and Characterization of 4-Hydroxybutyryl-Coa Dehydratase/Vinylacetyl-Coa Delta(3)-Delta(2)-Isomerase. Archives of Microbiology 1994; 161 (3):239-245

Shah J, Wilkins E. Electrochemical biosensors for detection of biological warfare agents. Electroanalysis 2003; 15 (3):157-167

Shen J, Dudik L, Liu CC. An iridium nanoparticles dispersed carbon based thick film electrochemical biosensor and its application for a single use, disposable glucose biosensor. Sensors and Actuators B: Chemical 2007; 125 (1):106-113

Shen J, Liu CC. Development of a screen-printed cholesterol biosensor: Comparing the performance of gold and platinum as the working electrode material and fabrication using a self-assembly approach. Sensors and Actuators B: Chemical 2007; 120 (2):417-425

Suzuki H. Advances in the microfabrication of electrochemical sensors and systems. Electroanalysis 2000; 12 (9):703-715

Tan XC, Tian YX, Cai PX, Zou XY. Glucose biosensor based on glucose oxidase immobilized in sol-gel chitosan/silica hybrid composite film on Prussian blue modified glass carbon electrode. Analytical and Bioanalytical Chemistry 2005; 381 (2):500-507

Tangkuaram T, Wang J, Rodriguez MC, Laocharoensuk R, Veerasai W. Highly stable amplified low-potential electrocatalytic detection of NAD(+) at azure-chitosan modified carbon electrodes. Sensors and Actuators B-Chemical 2007; 121 (1):277-281

Thevenot DR, Toth K, Durst RA, Wilson GS. Electrochemical biosensors: recommended definitions and classification. Biosensors & Bioelectronics 2001; 16 (1-2):121-131

Tsugawa W, Ishimura F, Ogawa K, Sode K. Development of an enzyme sensor utilizing a novel fructosyl amine oxidase from a marine yeast. Electrochemistry 2000; 68 (11):869-871

Umpierrez GE, Murphy MB, Kitabchi AE. Diabetic Ketoacidosis and Hyperglycemic Hyperosmolar Syndrome. Diabetes Spectr 2002; 15 (1):28-36

Vicario C, Arizmendi C, Malloch G, Clark JB, Medina JM. Lactate Utilization by Isolated Cells from Early Neonatal Rat Brain. Journal of Neurochemistry 1991; 57 (5):1700-1707

Vijayendran RA, Ligler FS, Leckband DE. A computational reaction-diffusion model for the analysis of transport-limited kinetics. Analytical Chemistry 1999; 71 (23):5405-5412

Wallace TM, Meston NM, Gardner SG, Matthews DR. The hospital and home use of a 30-second hand-held blood ketone meter: guidelines for clinical practice. Diabetic Medicine 2001; 18 (8):640-645

Wang J. Glucose biosensors: 40 years of advances and challenges. Electroanalysis 2001; 13 (12):983-988

Wang J, Rivas G, Chicharro M. Iridium-dispersed carbon paste enzyme electrodes. Electroanalysis 1996; 8 (5):434-437

Wang K, Jiang DC, Liu BH, Zhang S, Lu TP, Kong JL. Label-free immunosensors-principles and applications. Chinese Journal of Analytical Chemistry 2005; 33 (3):411-416

Wang P, Xu GX, Qin LF, Xu Y, Li Y, Li R. Cell-based biosensors and its application in biomedicine. Sensors and Actuators B-Chemical 2005; 108 (1-2):576-584

Warriner K, Higson S, Vadgama P. A lactate dehydrogenase amperometric pyruvate electrode exploiting direct detection of NAD(+) at a poly(3-methylthiophene): poly(phenol red) modified platinum surface. Materials Science & Engineering C-Biomimetic and Supramolecular Systems 1997; 5 (2):91-99

Wild S, Roglic G, Green A, Sicree R, King H. Global prevalence of diabetes - Estimates for the year 2000 and projections for 2030. Diabetes Care 2004; 27 (5):1047-1053

Williamson DH. Enzymic Determination of D(-)-Beta-Hydroxybutyric Acid and Acetoacetic Acid in Blood. Current Contents/Life Sciences 1983; (22):19

Wolf B, Kraus M, Brischwein M, Ehret R, Baumann W, Lehmann M. Biofunctional hybrid structures - cell-silicon hybrids for applications in biomedicine and bioinformatics. Bioelectrochemistry and Bioenergetics 1998; 46 (2):215-225

Wu F. Animal tissue-based chemiluminescence sensing of uric acid. Analytica Chimica Acta 2005; 536 (1-2):107

Yonehara, Satoshi and Yagi, Yuji. Method of quantifying hemoglobin and method of measuring glycation ratio of hemoglobin. 9-14-2004. (GENERIC)
US: Patent 6790665

Yuan CS, Datta A, and Wang YP. Methods and compositions for determination of glycated proteins. 12-26-2008. (GENERIC)
US Patent 7153666

Zapatabacri AM, Burstein C. Enzyme Electrode Composed of the Pyruvate Oxidase from Pediococcus Species Coupled to An Oxygen-Electrode for Measurements of Pyruvate in Biological Media. Biosensors 1987; 3 (4):227-237